Multiple Track Signatures of Long-lived Particles

Sandbox Studio/Symmetry Magazine

SFU
SIMON FRASER UNIVERSITY

Jackson Burzynski

Roadmap of Dark Matter Models for Run 3 Workshop

13 May 2024

ATLAS EXPERIMENT

Overview

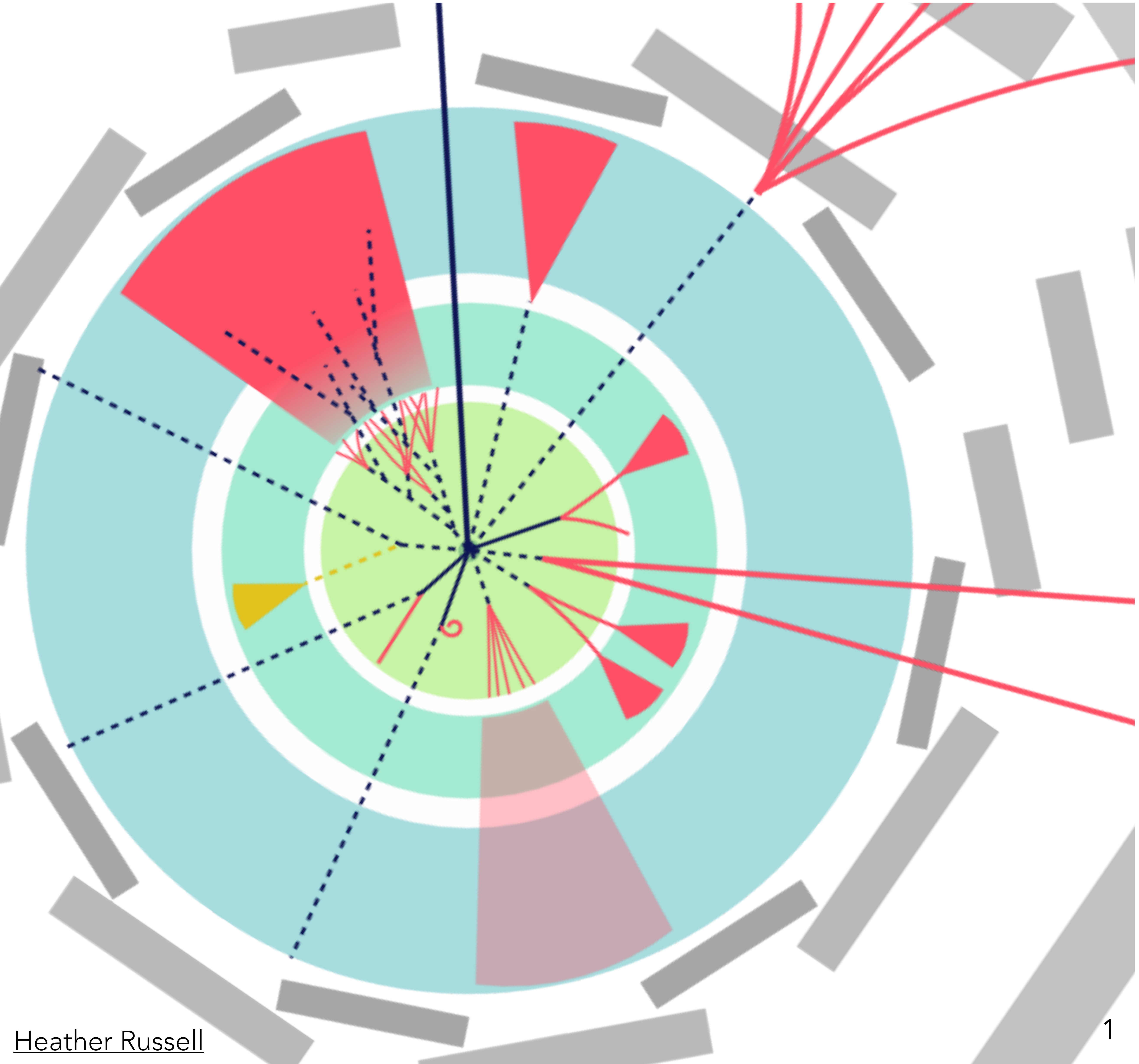

Long-lived particles give rise to a wide range of exotic signatures

Overview

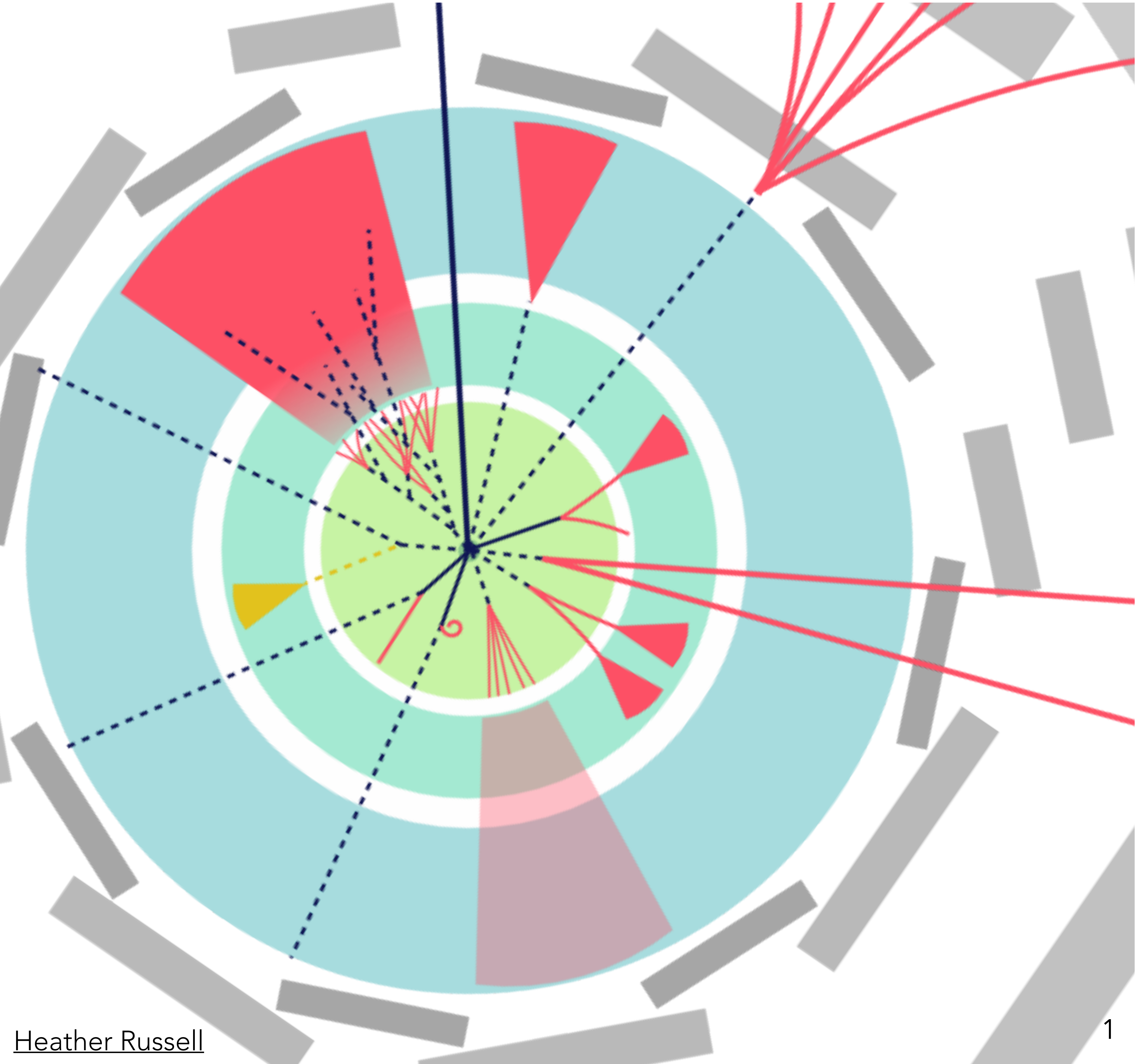

Long-lived particles give rise to a wide range of exotic signatures

I will be focusing on Inner Detector *track-based signatures*

Overview

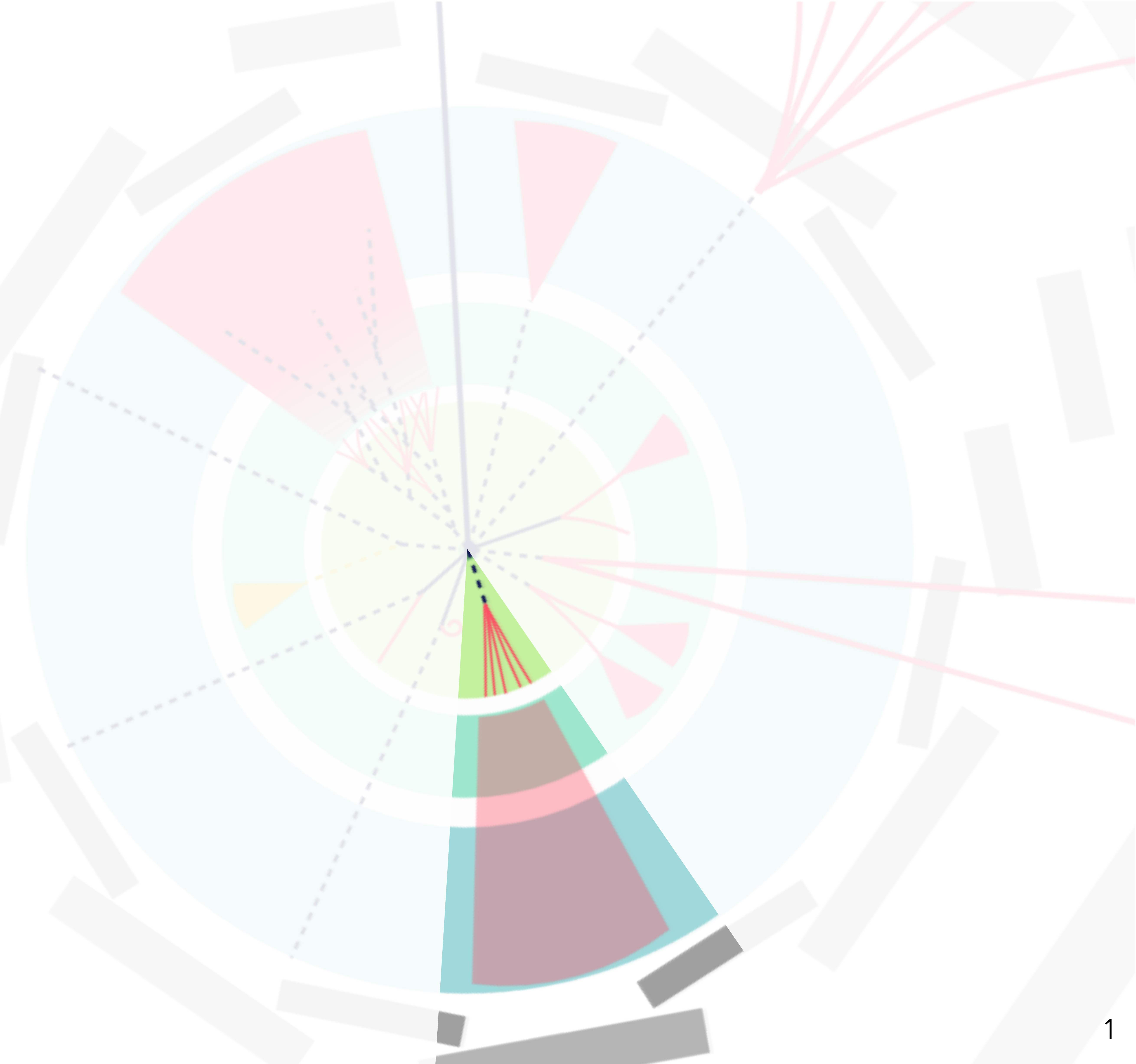

Long-lived particles give rise to a wide range of exotic signatures

I will be focusing on Inner Detector *track-based signatures*

- Displaced hadronic vertices

Overview

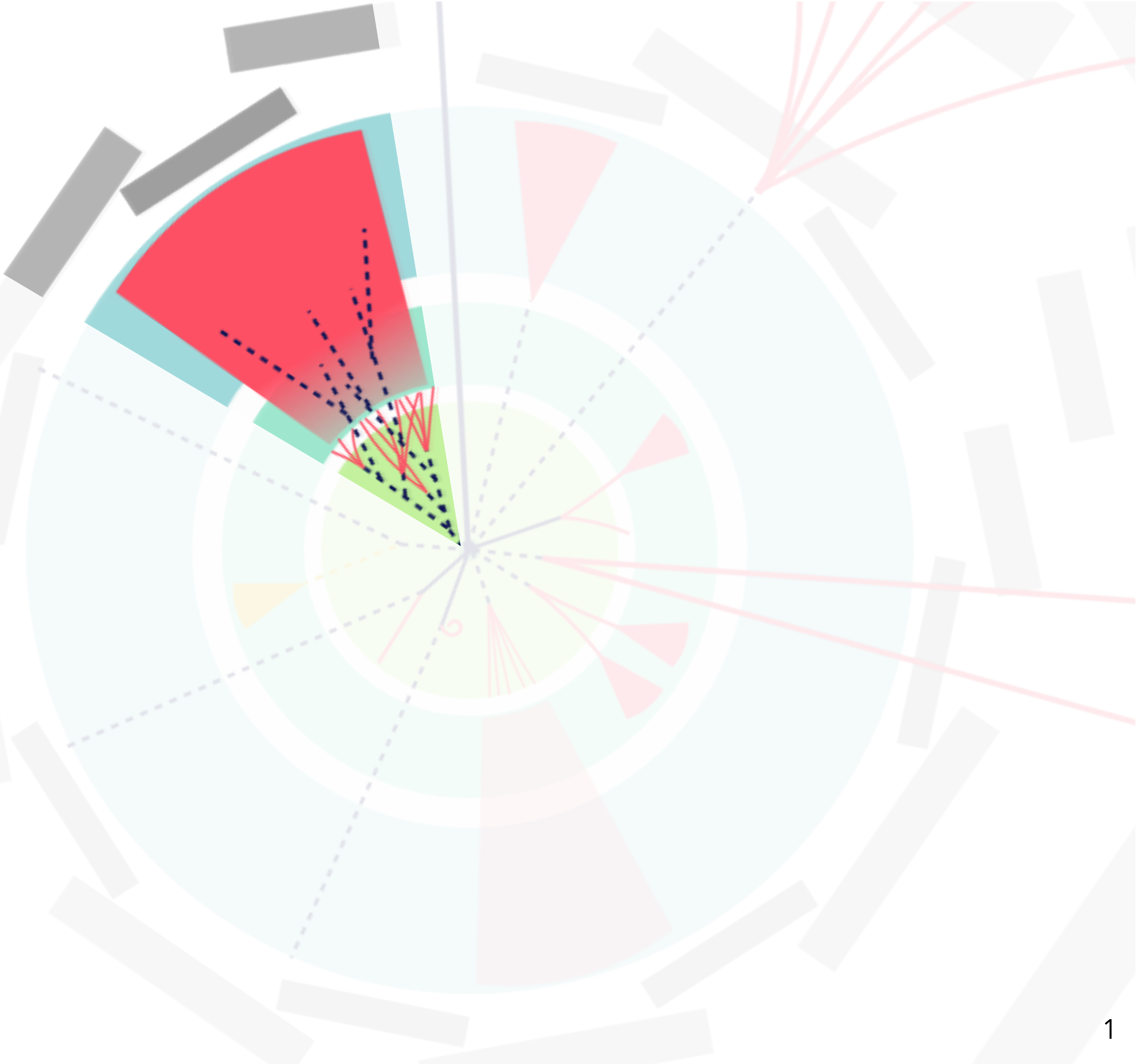

Long-lived particles give rise to a wide range of exotic signatures

I will be focusing on Inner Detector *track-based signatures*

- Displaced hadronic vertices
- Emerging jets

Overview

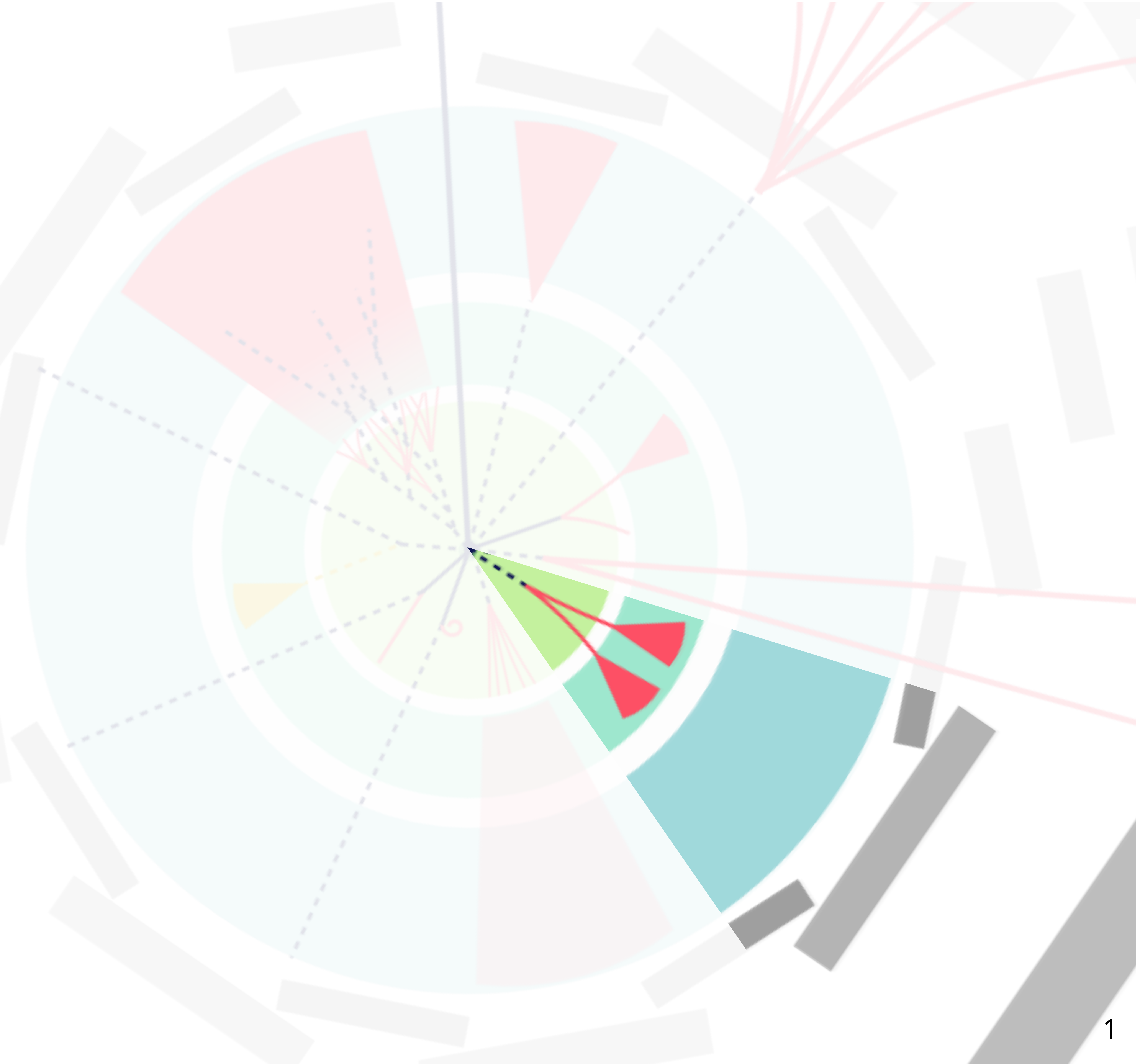

Long-lived particles give rise to a wide range of exotic signatures

I will be focusing on Inner Detector *track-based signatures*

- Displaced hadronic vertices
- Emerging jets
- Heavy neutral leptons

Overview

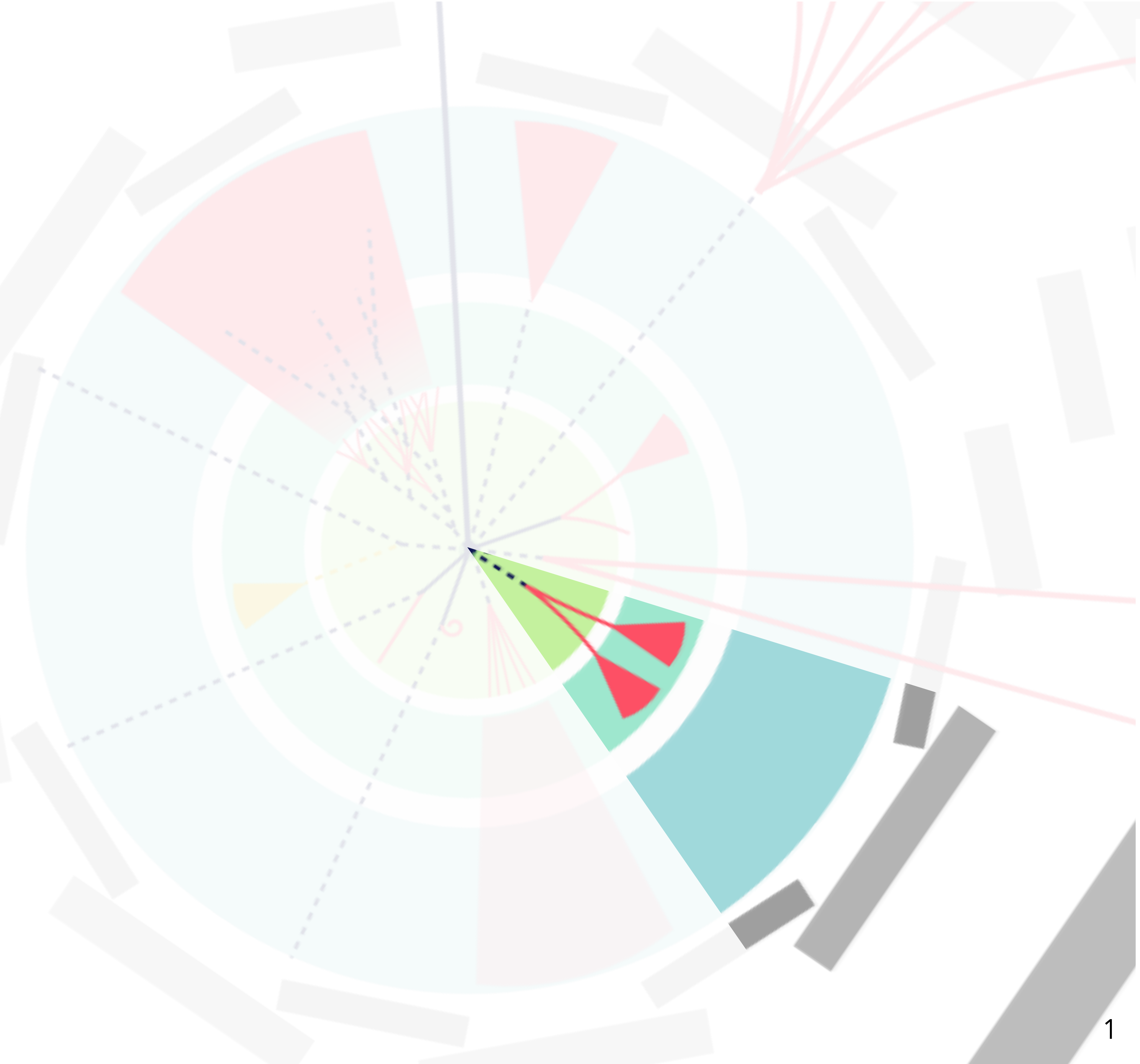

Long-lived particles give rise to a wide range of exotic signatures

I will be focusing on Inner Detector *track-based signatures*

- Displaced hadronic vertices
- Emerging jets
- Heavy neutral leptons

<u>Pair produced LLPs</u> and <u>signatures with MET</u> will be covered by Audrey and Joseph

Hadronic vertex signatures

Benchmark scenario: Higgs portal dark sector

- Bottom-up motivation as one of three renormalizable portal interactions to dark sector
- Top-down motivation from models of Neutral Naturalness

Visible sector 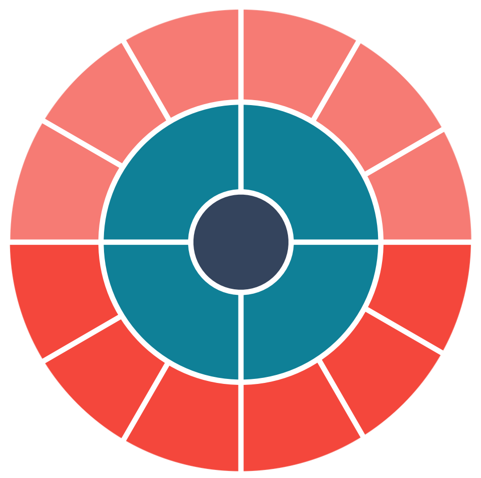 $- - - \left(\mu S + \lambda S^2\right) H^\dagger H - - -$ 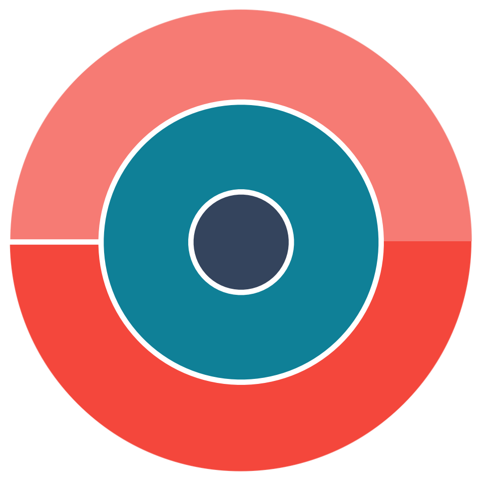 Dark sector

Hadronic vertex signatures

Benchmark scenario: Higgs portal dark sector

- Bottom-up motivation as one of three renormalizable portal interactions to dark sector
- Top-down motivation from models of Neutral Naturalness

Visible sector

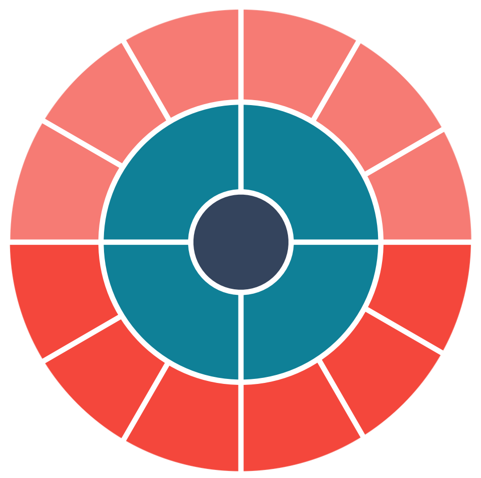

$$- - - \left(\mu S + \lambda S^2\right) H^\dagger H - - -$$

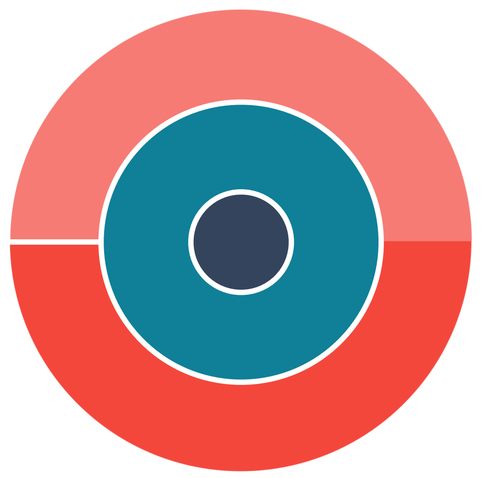

Dark sector

Gives rise to exotic decays of the Higgs boson

- Long-lived mediators → displaced hadronic vertex signatures

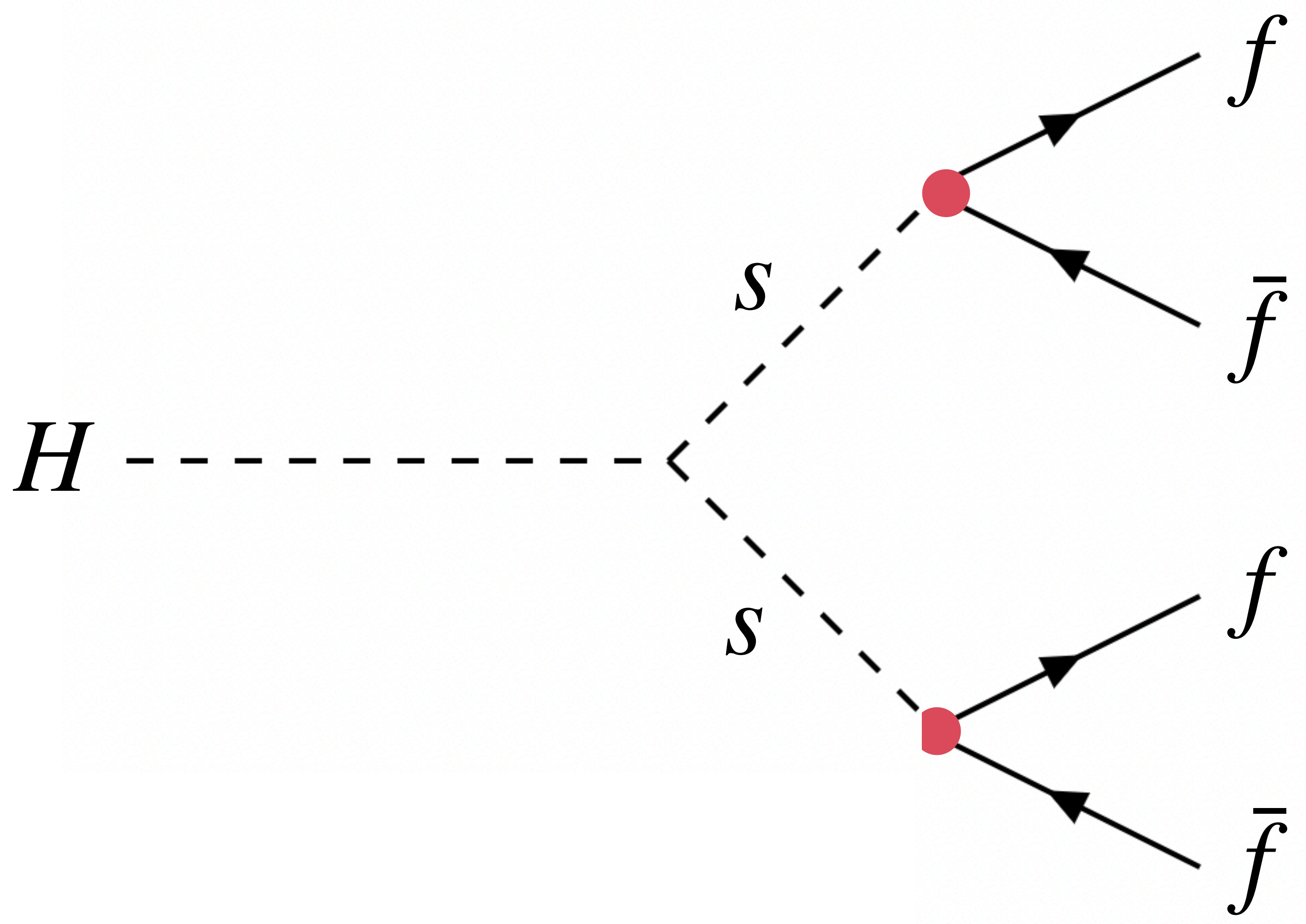

Hadronic vertices in ATLAS ID

2403.15332

New ATLAS results using Run 2 data

- First result to use new displaced track reconstruction
- Probe ZH, WH, and VBF production modes
    - Follow-up to previous ZH-only result: 2107.06092

Hadronic vertices in ATLAS ID

2403.15332

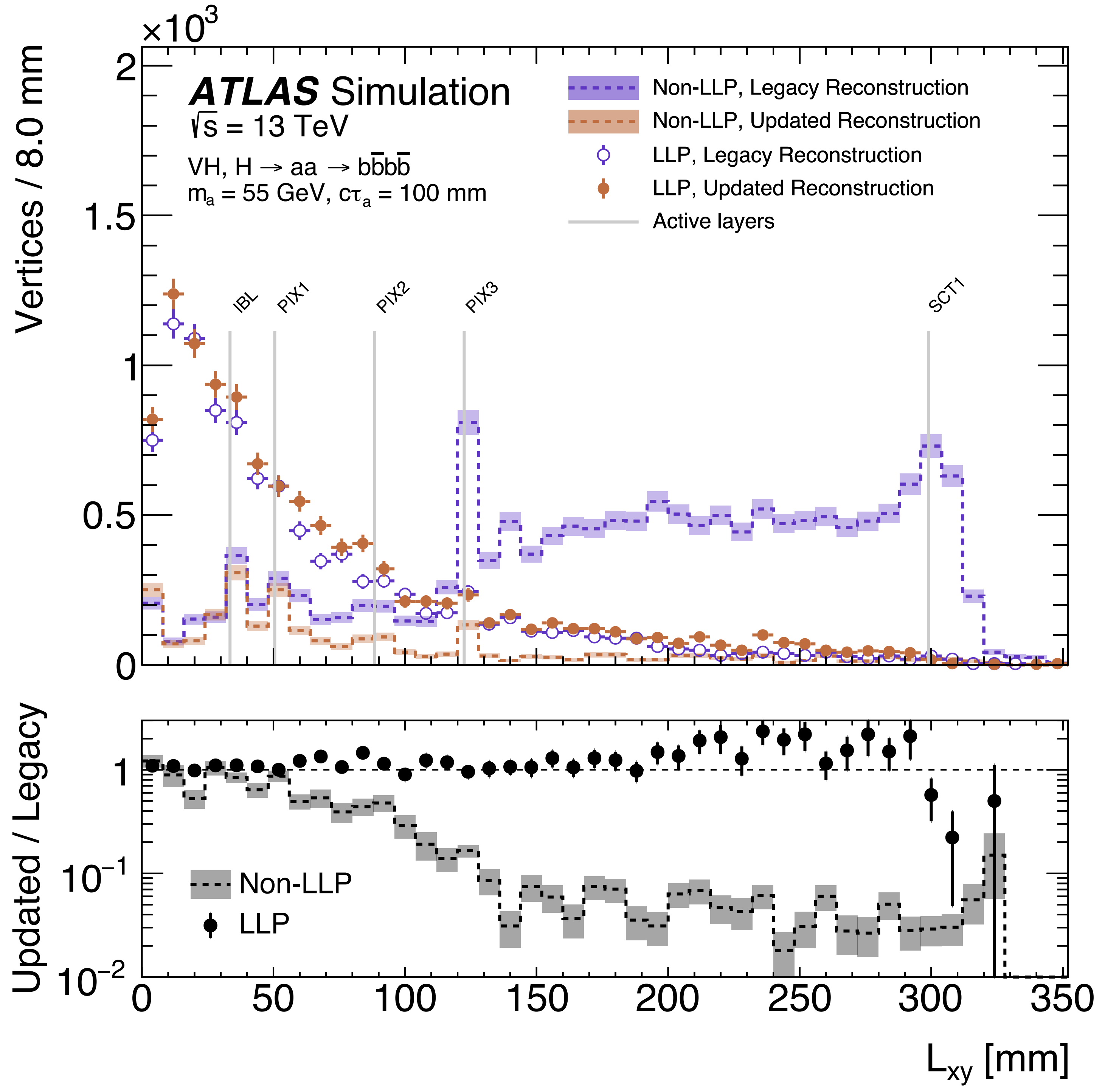

New ATLAS results using Run 2 data

- First result to use new displaced track reconstruction
- Probe ZH, WH, and VBF production modes
  - Follow-up to previous ZH-only result: 2107.06092

Hadronic vertices in ATLAS ID

New ATLAS results using Run 2 data

- First result to use new displaced track reconstruction
- Probe ZH, WH, and VBF production modes
  - Follow-up to previous ZH-only result: 2107.06092

Reconstruct secondary vertices and identify displaced jets using boosted decision tree

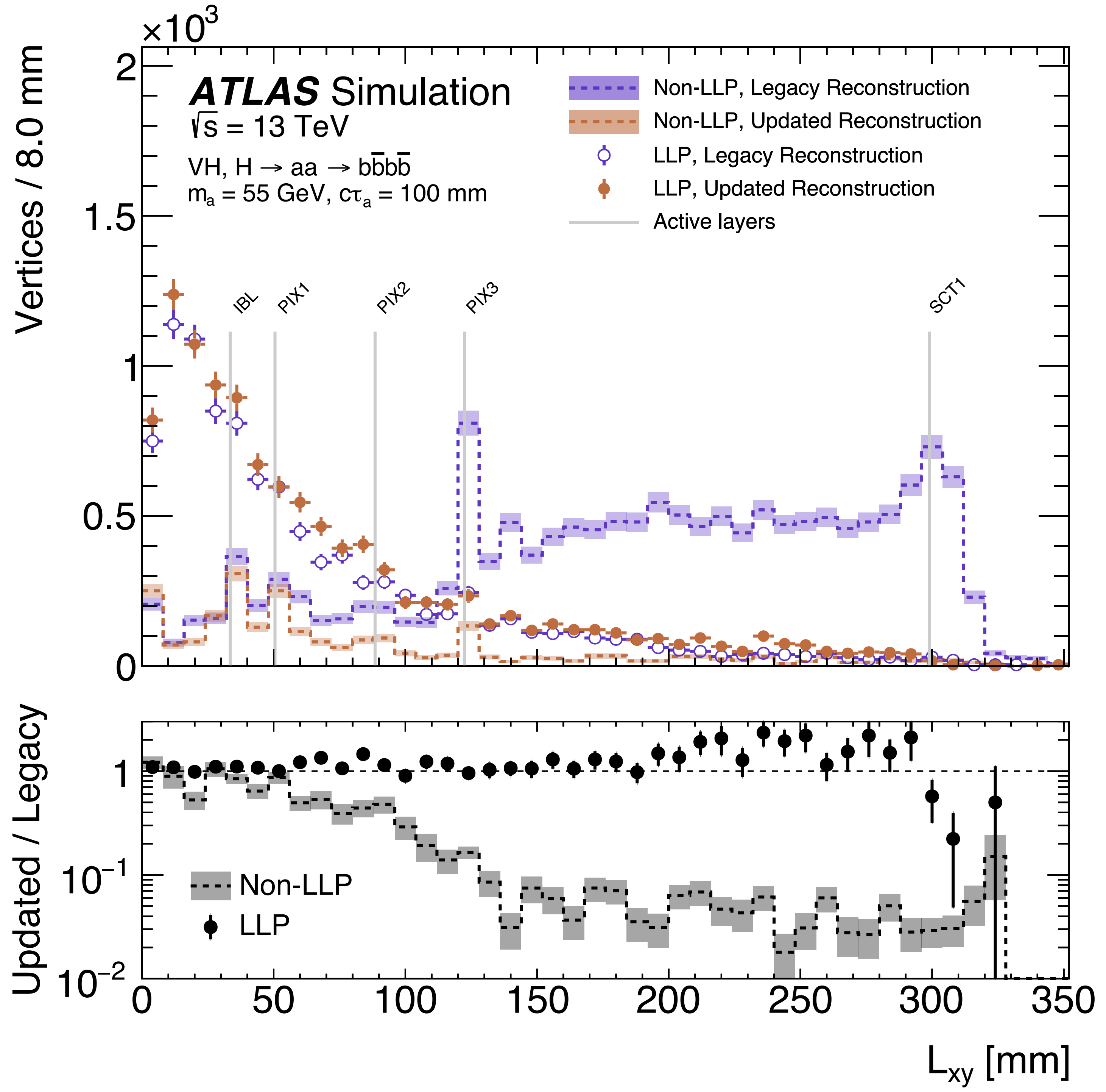

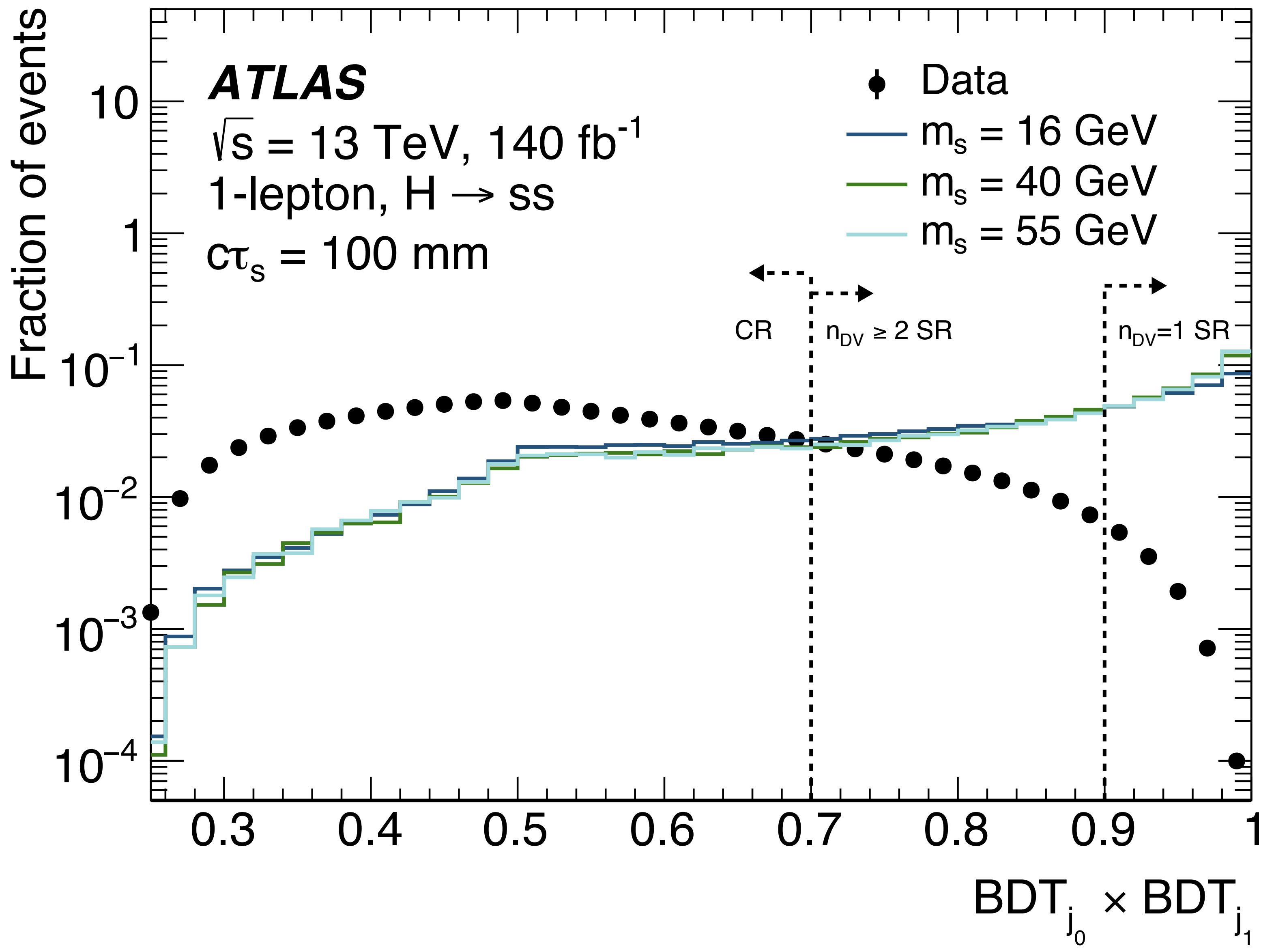

Hadronic vertices in ATLAS ID

2403.15332

New ATLAS results using Run 2 data

- First result to use new displaced track reconstruction
- Probe ZH, WH, and VBF production modes
  - Follow-up to previous ZH-only result: 2107.06092

Reconstruct secondary vertices and identify displaced jets using boosted decision tree

Data-driven background estimate derived by parameterizing per-jet vertex match probability

- Used to estimate distribution of event-level discriminant in events with $n_{\mathrm{DV}} = 1$ and $n_{\mathrm{DV}} \geq 2$

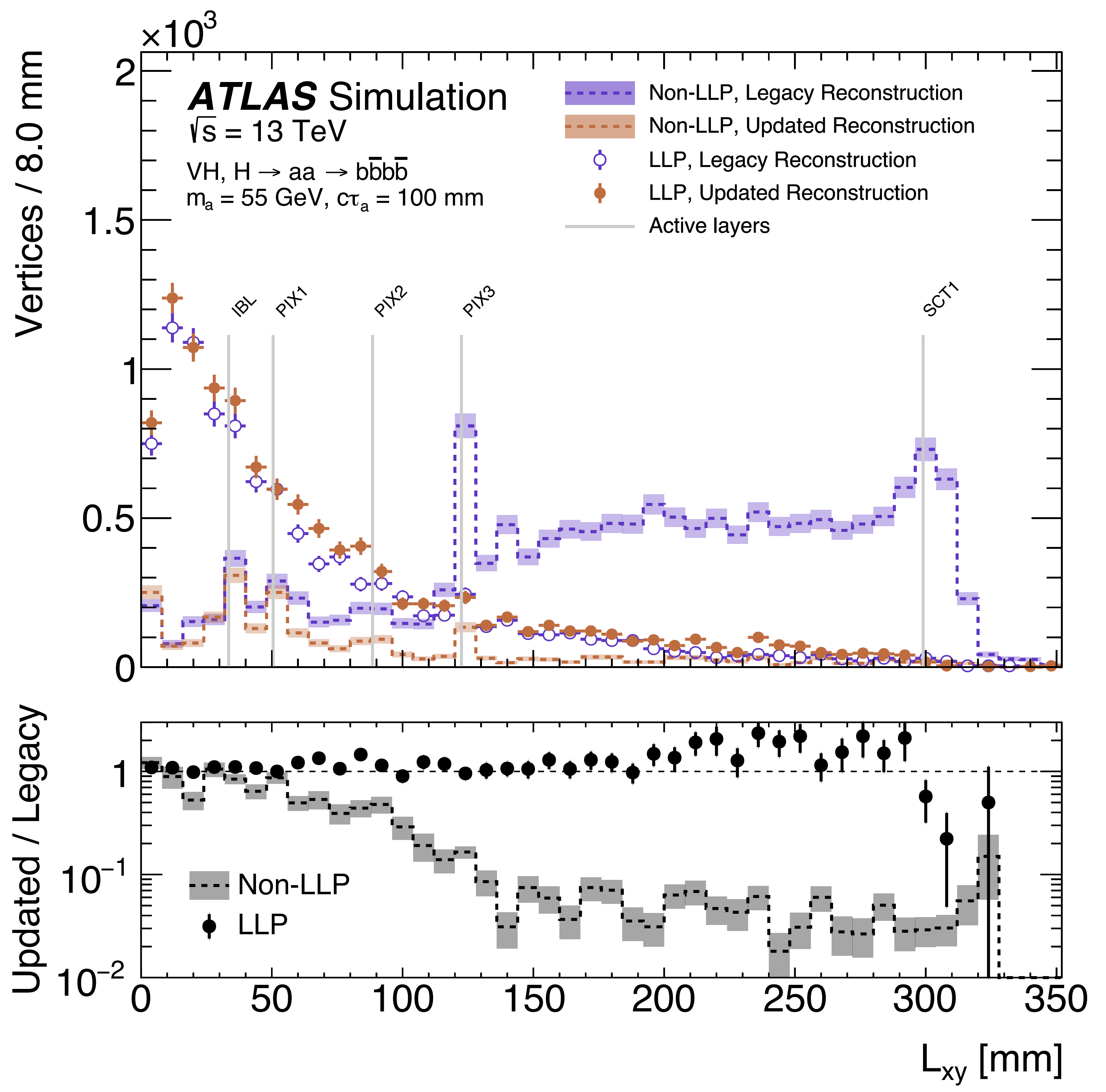

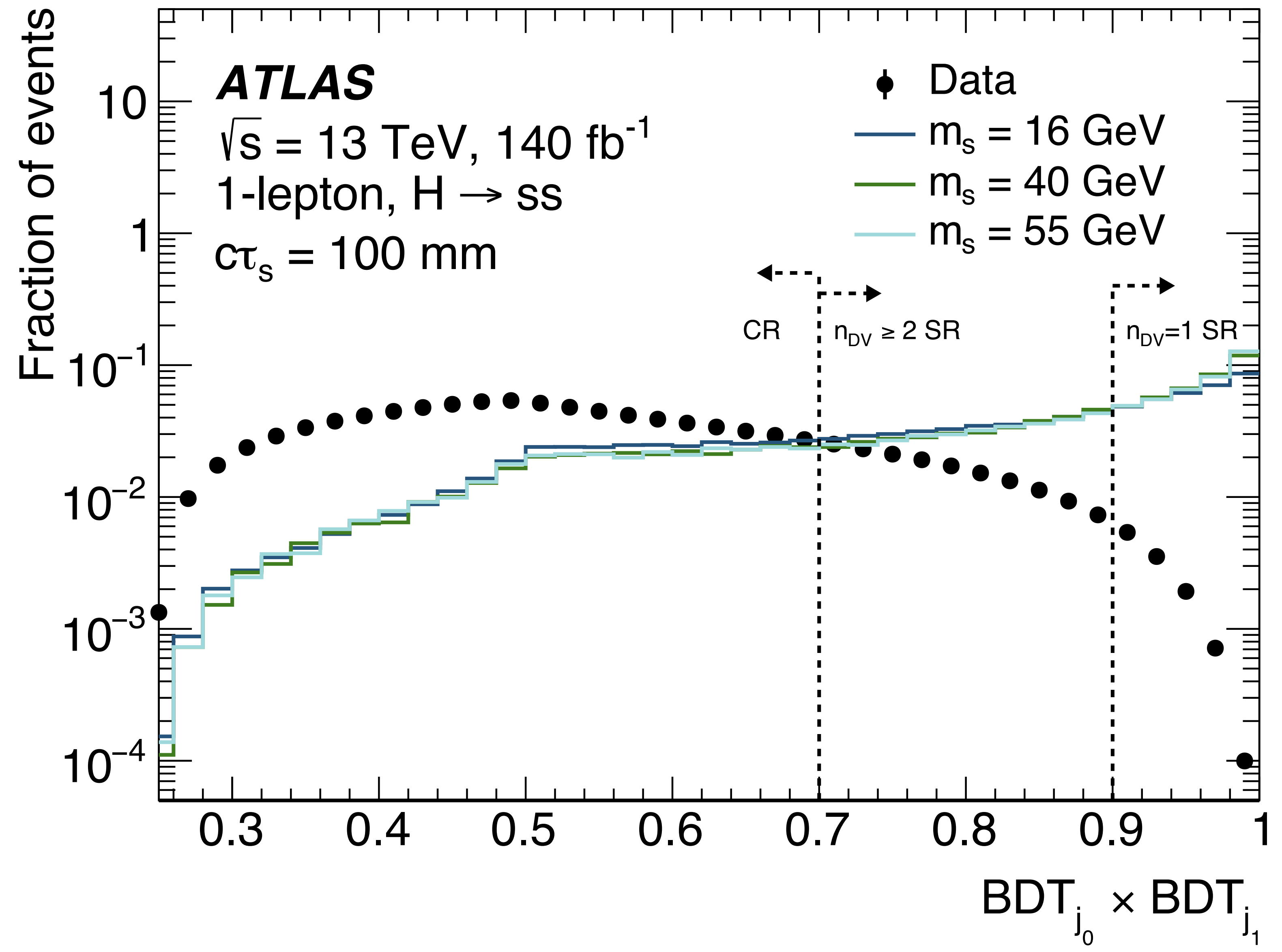

Hadronic vertices in ATLAS ID

Six signal regions based on Higgs production mode and vertex multiplicity

- Binned in event-level discriminant formed from jet-level BDT scores

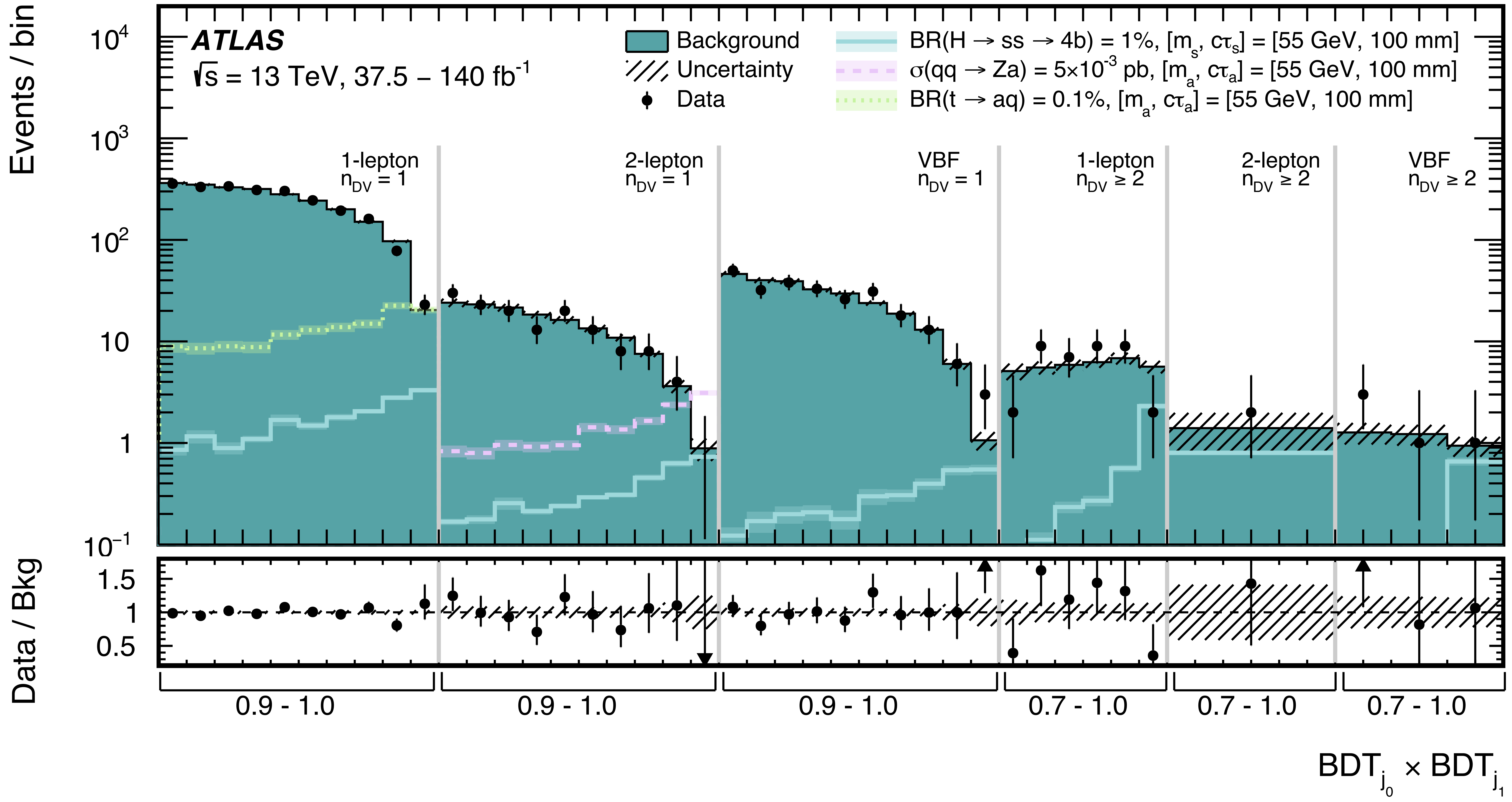

Hadronic vertices in ATLAS ID

Six signal regions based on Higgs production mode and vertex multiplicity

- Binned in event-level discriminant formed from jet-level BDT scores

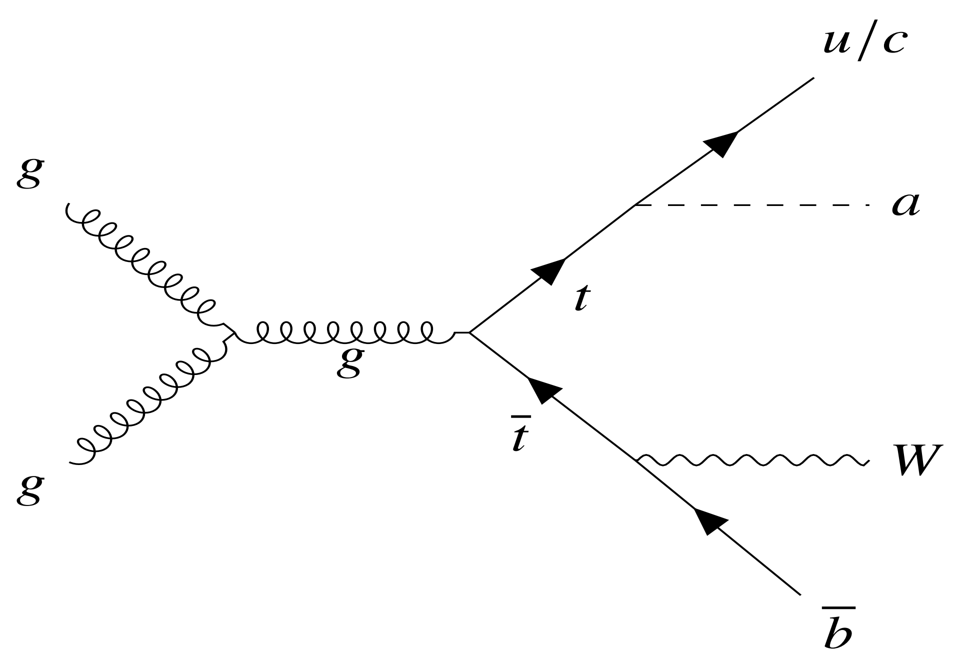

Sensitivity also to axion-like particles from top decays and vector boson couplings

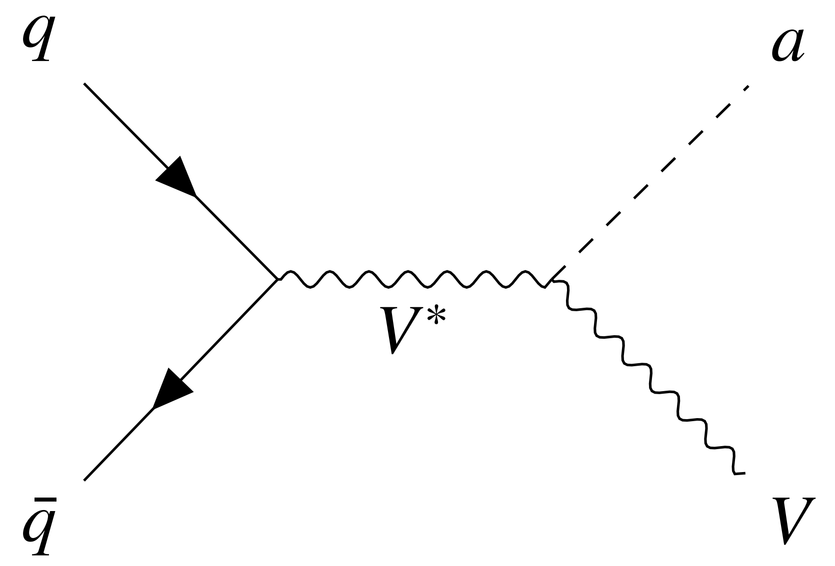

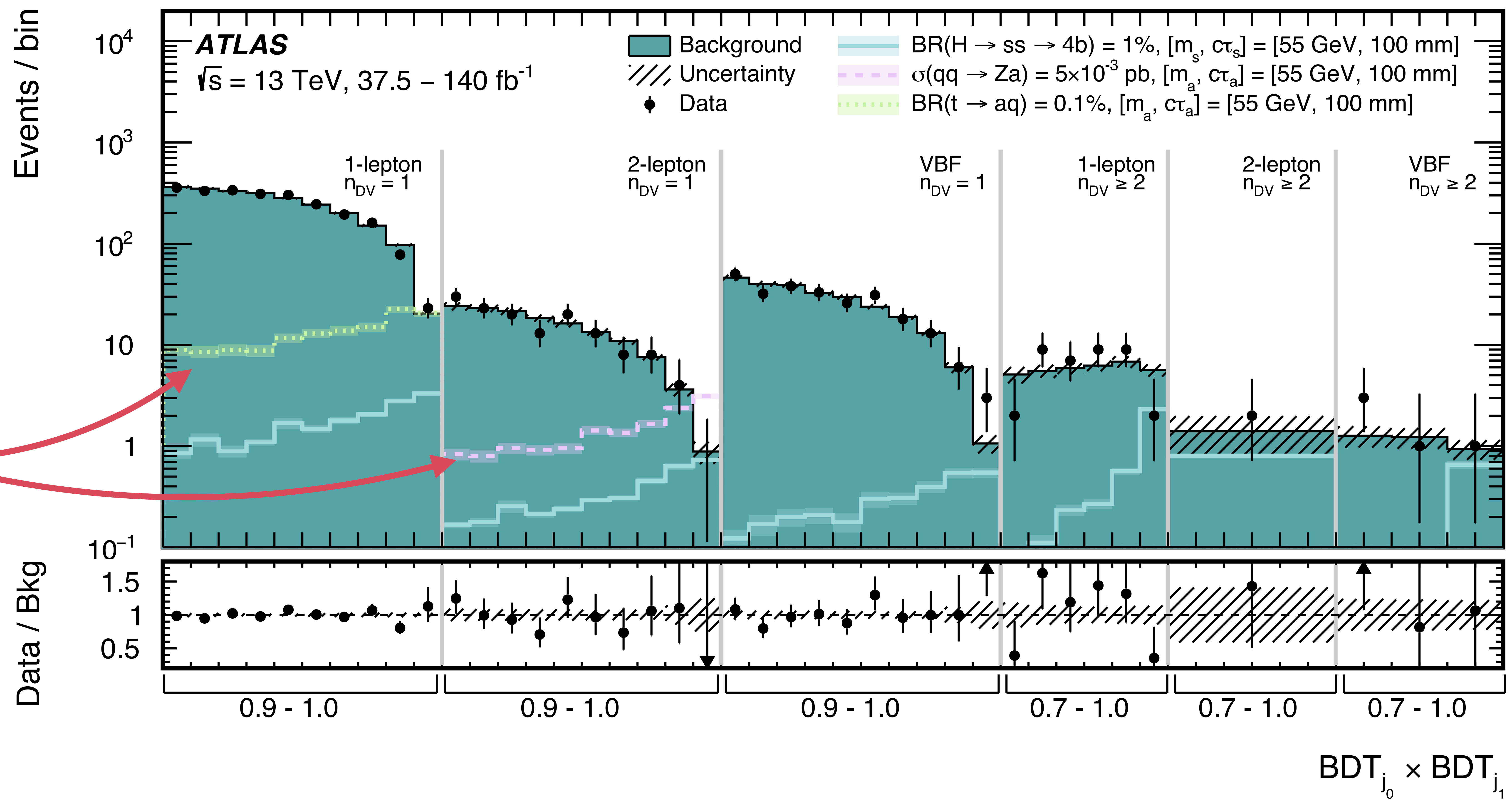

Hadronic vertices in ATLAS ID

Updated ATLAS results are 10-100x more sensitive than previous results using the same dataset

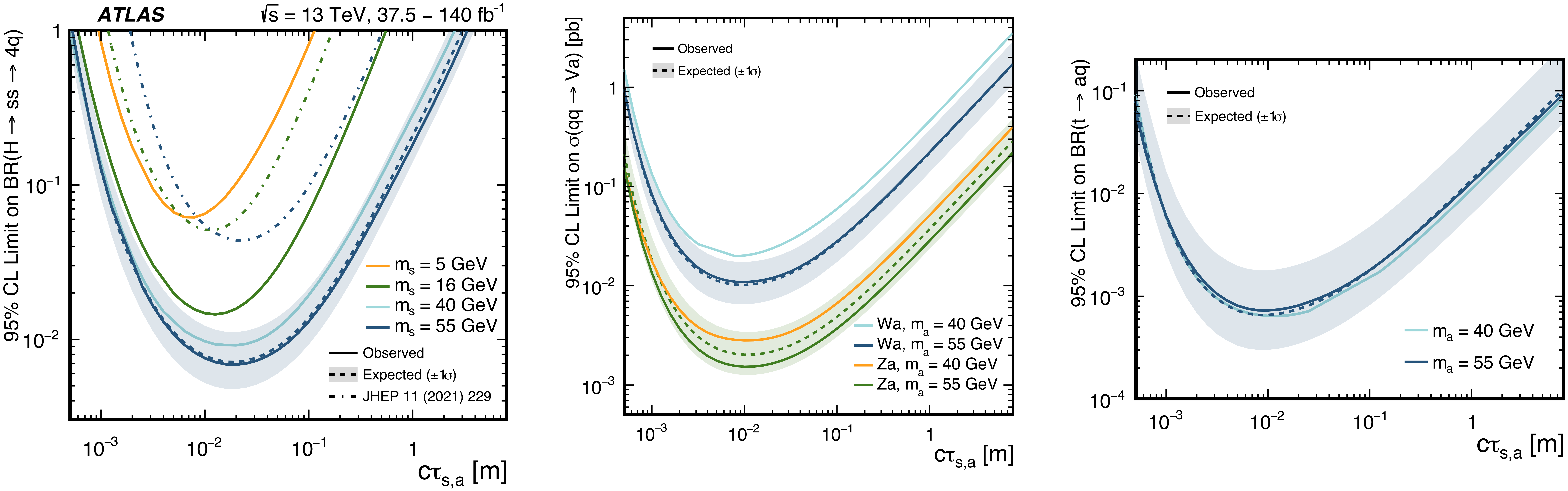

Hadronic vertices in ATLAS ID

Updated ATLAS results are 10-100x more sensitive than previous results using the same dataset

- First limits on photophobic ALP from $V \to Va$ and $t\bar{t}, t \to aq$ ALP models

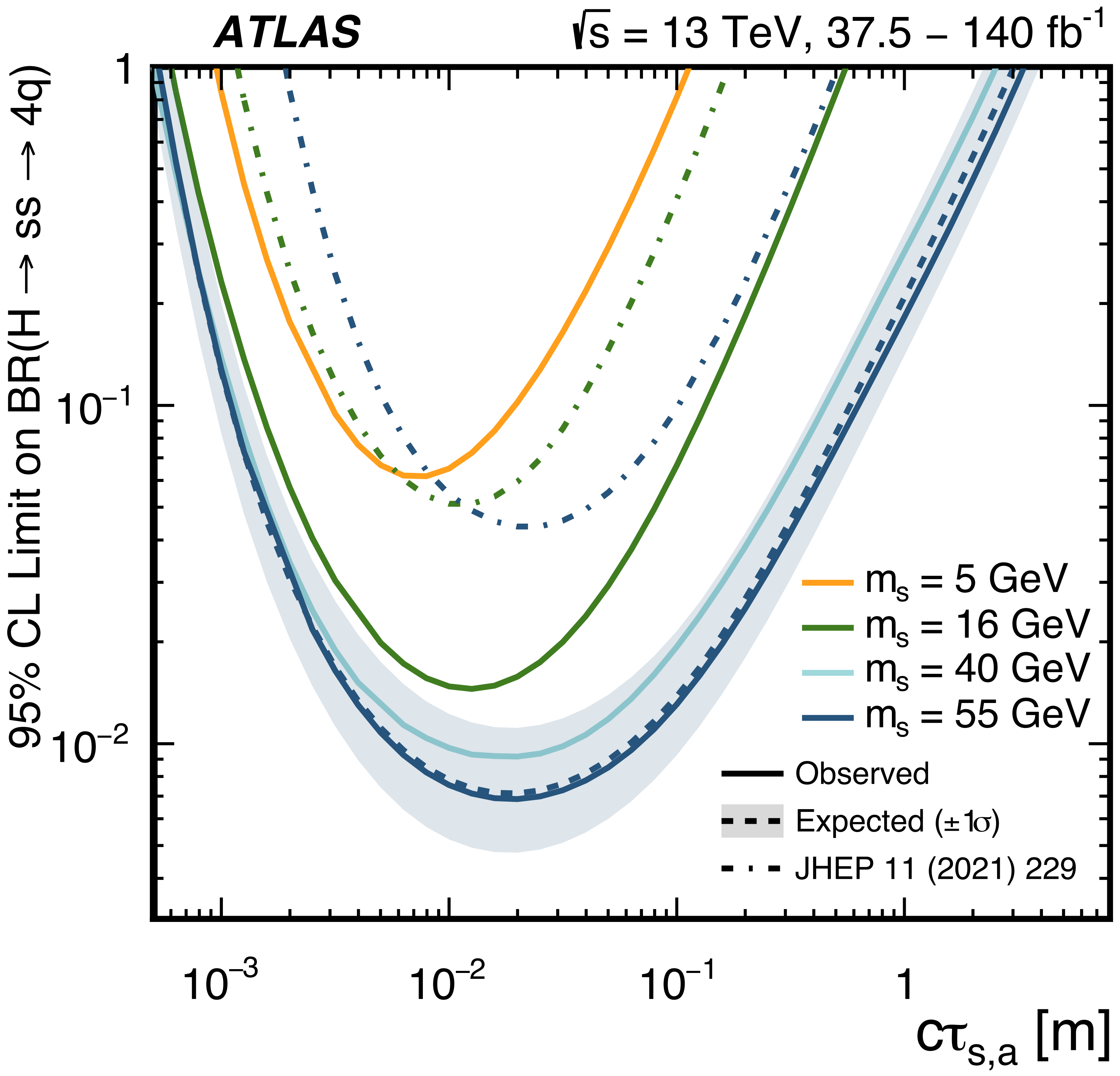

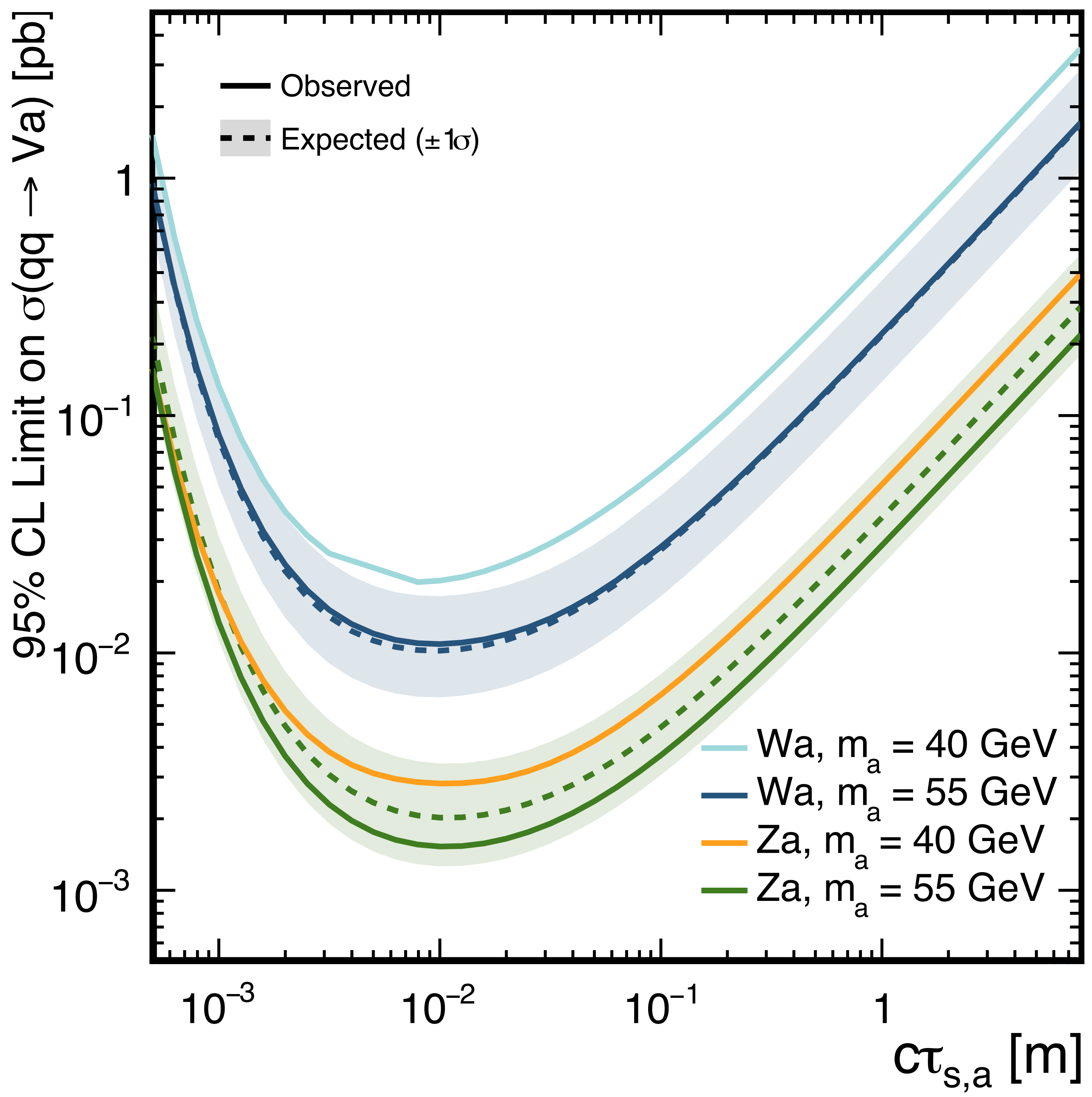

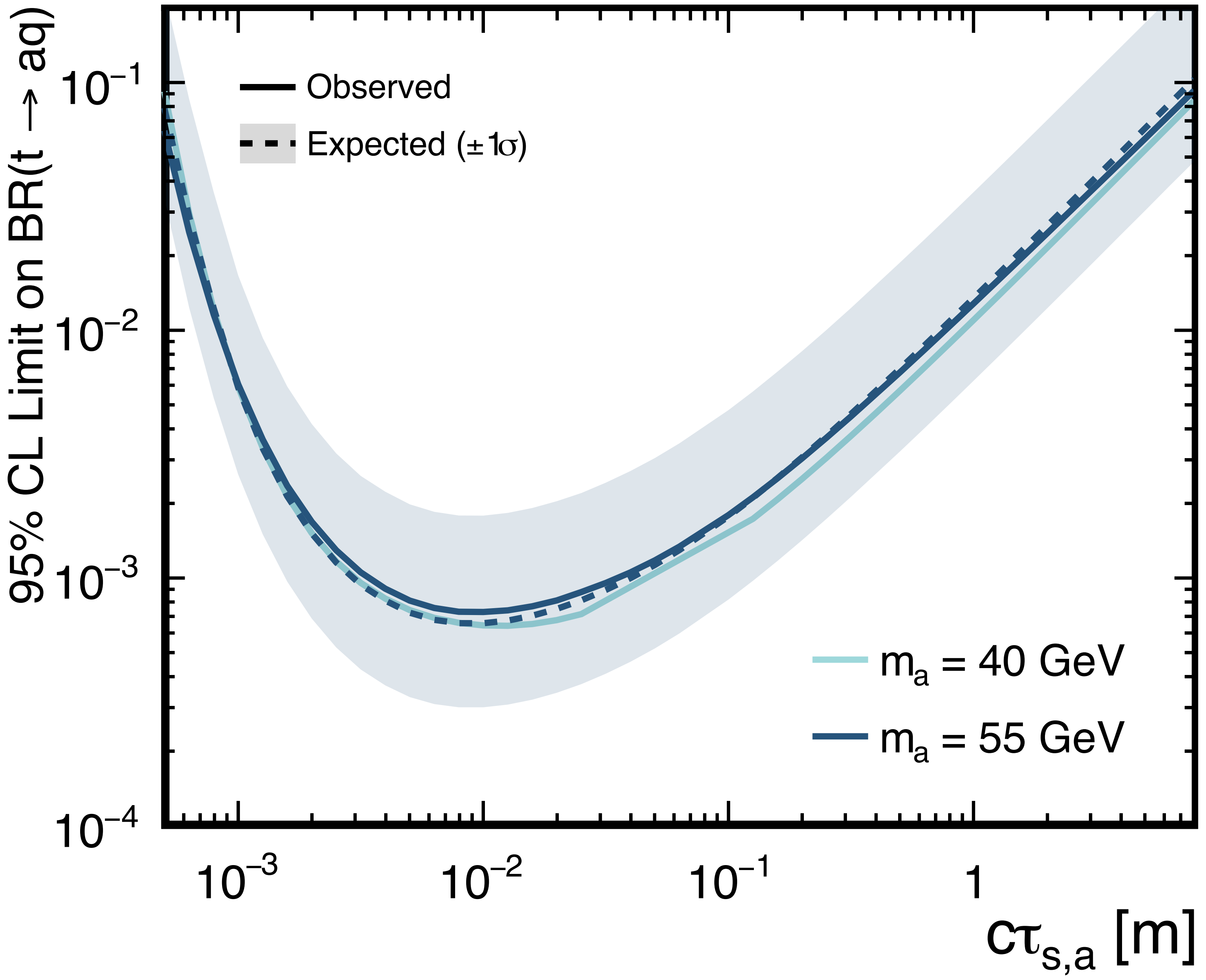

Hadronic vertices in CMS

CMS-PAS-EXO-23-013

New CMS Run 3 results using 2022+2023 data

- Displaced jet trigger efficiencies in Run 3 are a factor of 4 to 17 higher than in Run 2 for $H \rightarrow ss \rightarrow 4b$
- Allows for efficient probe of ggH production!

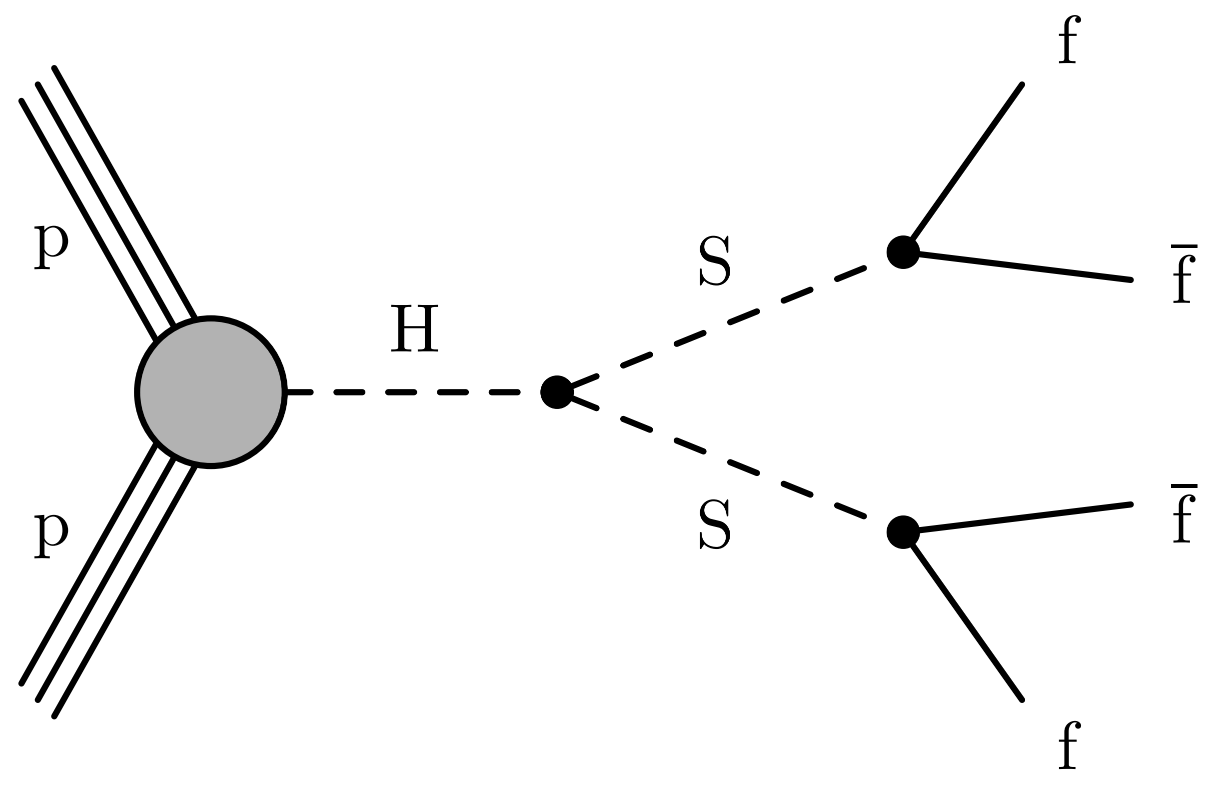

Hadronic vertices in CMS

CMS-PAS-EXO-23-013

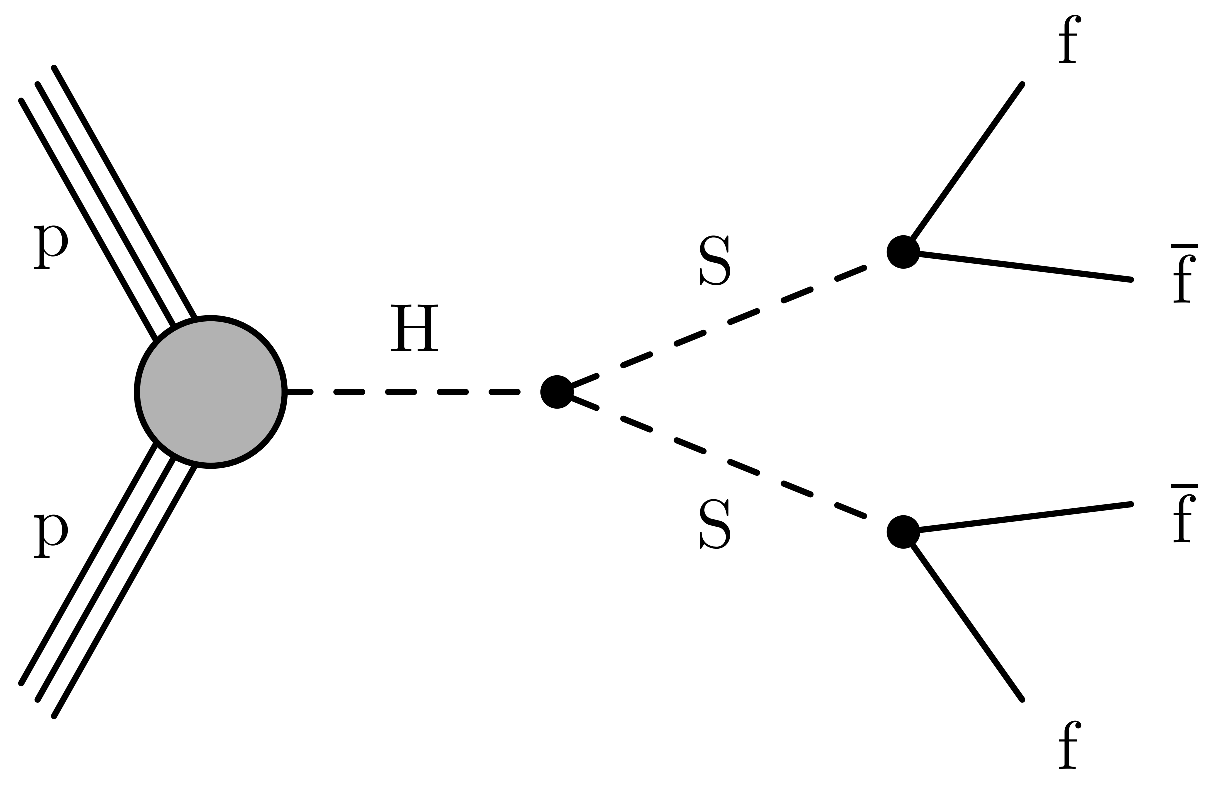

New CMS Run 3 results using 2022+2023 data

- Displaced jet trigger efficiencies in Run 3 are a factor of 4 to 17 higher than in Run 2 for $H \to ss \to 4b$
- Allows for efficient probe of ggH production!

Di-jet-level graph neural network (GNN) taggers used to separate signal and background

- Use track-level and vertex-level information
- Two independent taggers define ABCD plane

Hadronic vertices in CMS

CMS-PAS-EXO-23-013

New CMS Run 3 results using 2022+2023 data

- Displaced jet trigger efficiencies in Run 3 are a factor of 4 to 17 higher than in Run 2 for $H \to ss \to 4b$
- Allows for efficient probe of ggH production!

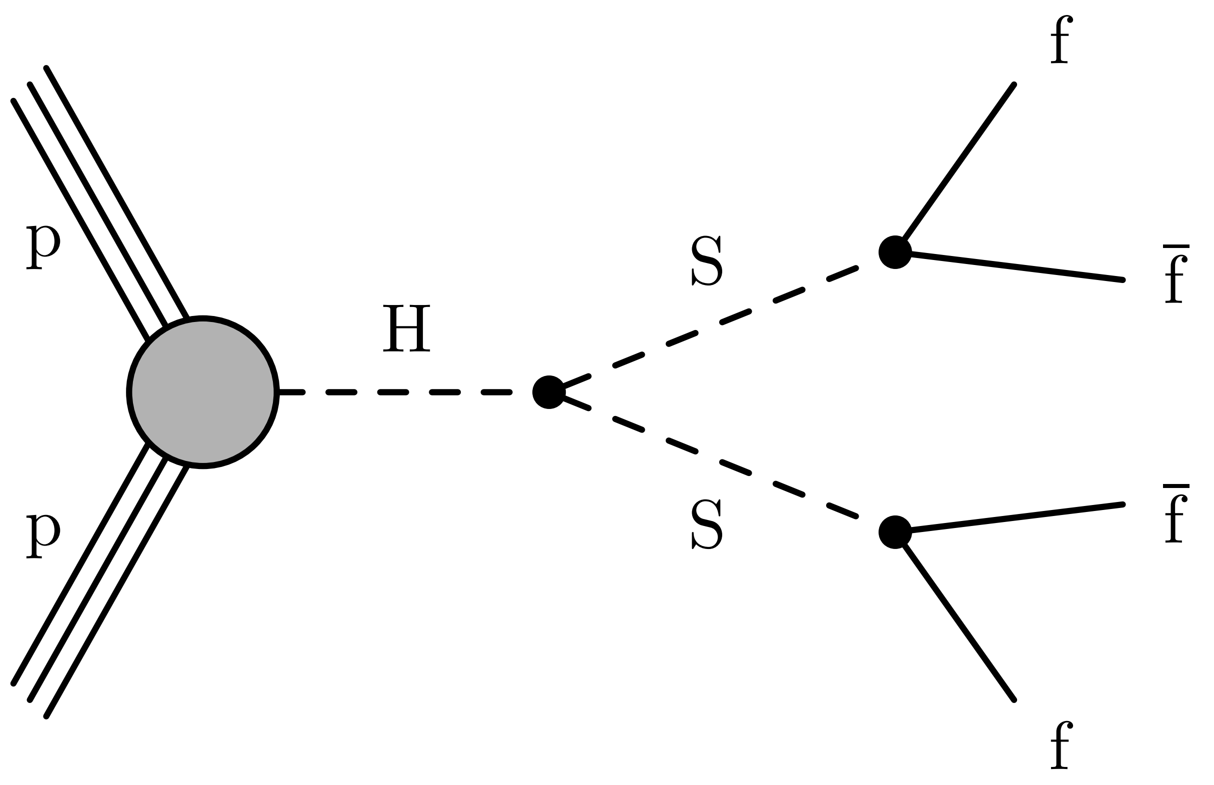

Di-jet-level graph neural network (GNN) taggers used to separate signal and background

- Use track-level and vertex-level information
- Two independent taggers define ABCD plane

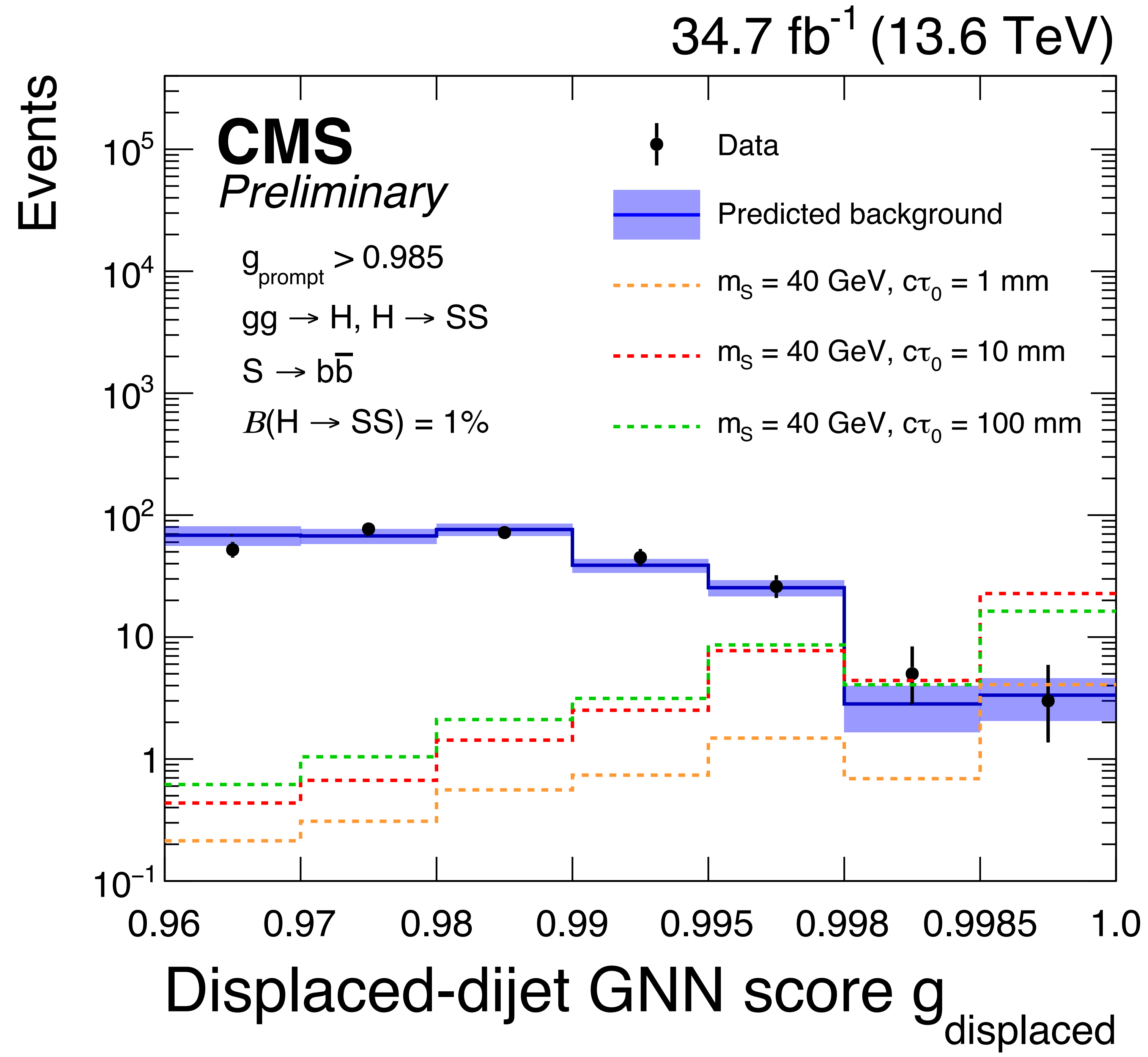

Good agreement observed between data and data-driven ABCD background estimate in signal region

Hadronic vertices in CMS

Model independent limits set on $\mathrm{Br}(H \to ss)$

- 10x improvement w.r.t. previous CMS Run 2 results with only 1/4 the data!

Results also interpreted in NN models with dark glueballs: Twin Higgs and Folded SUSY

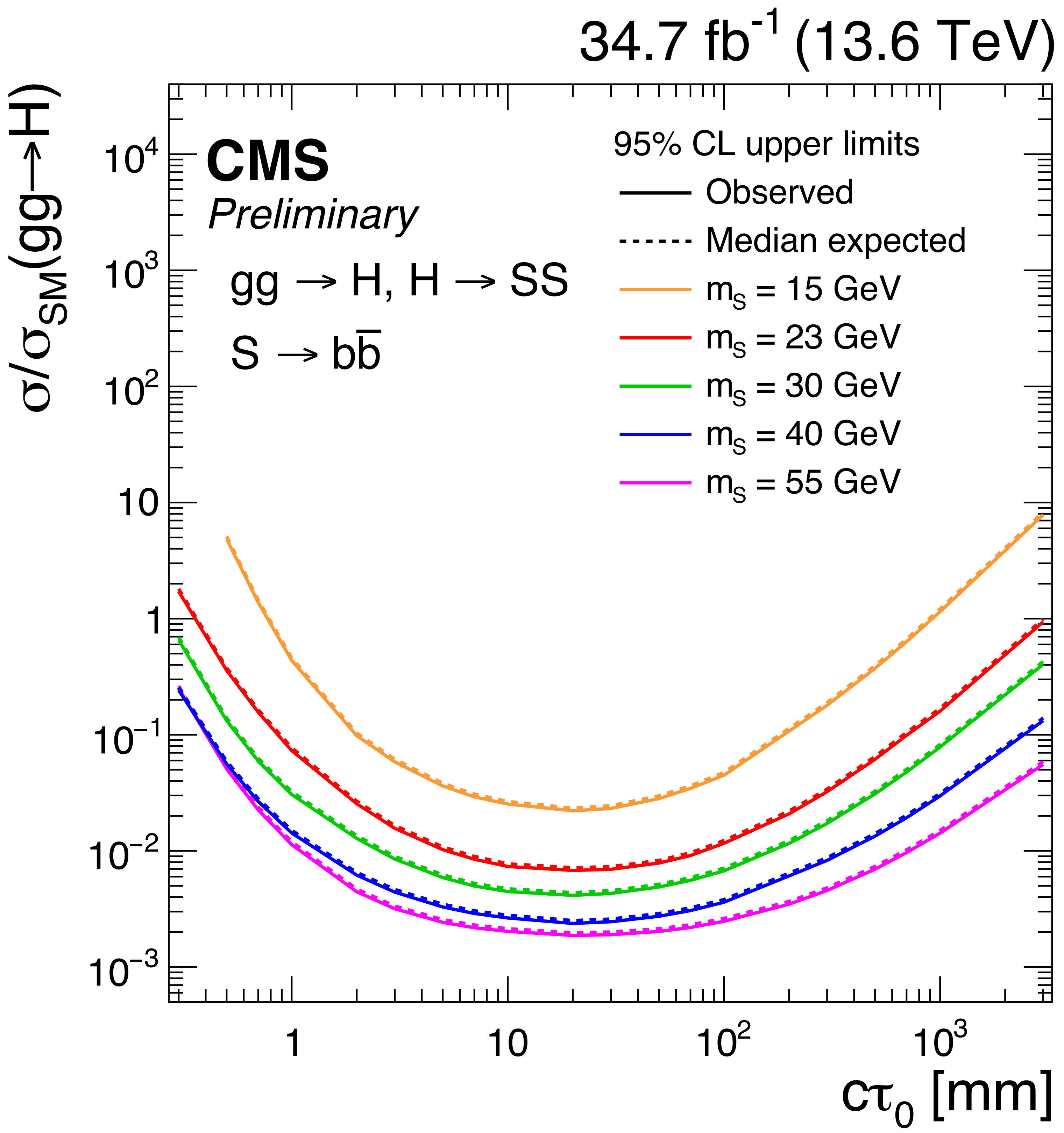

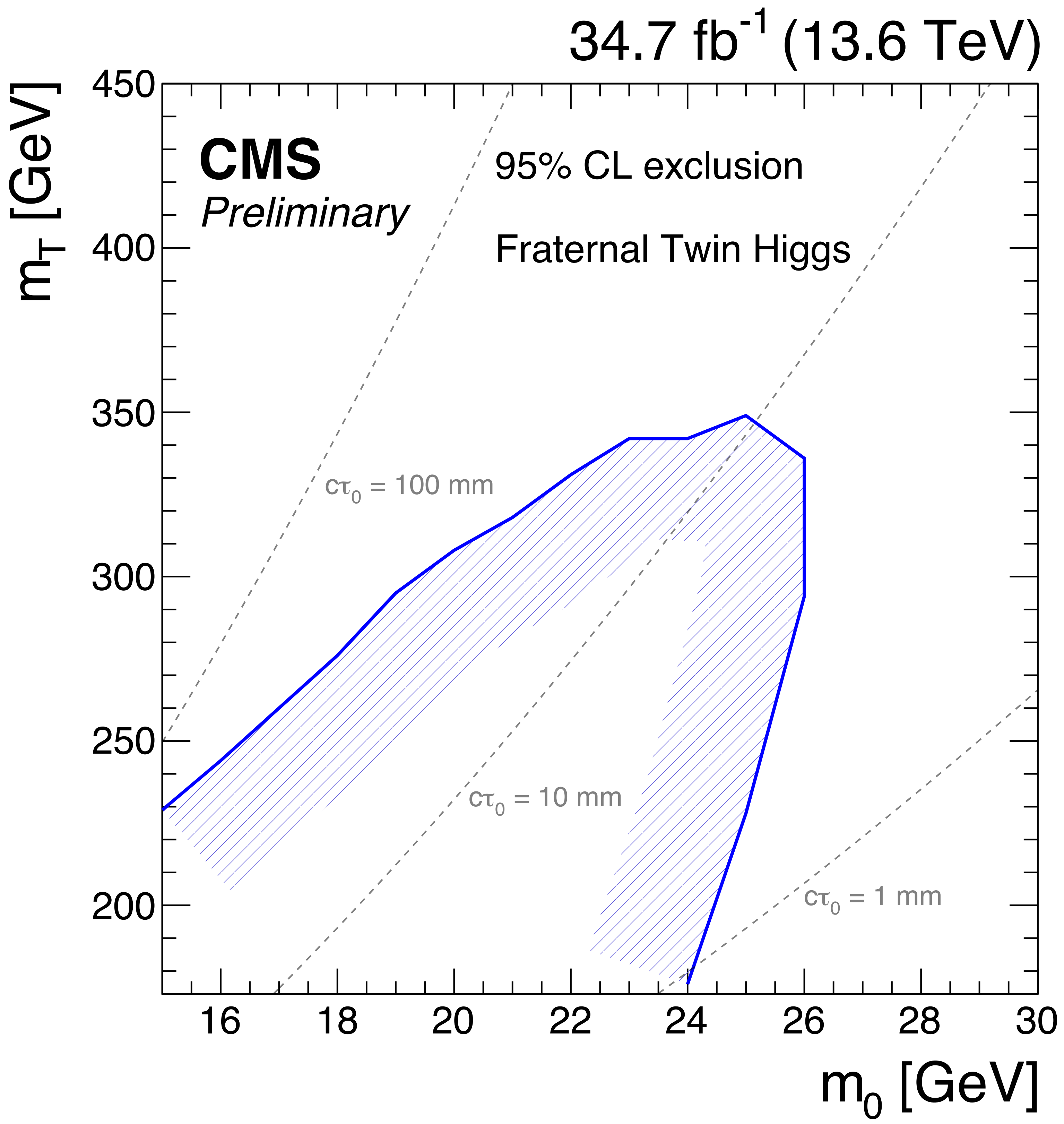

LHCb Run 3 prospects

2312.14016

LHCb Run 3 projections are expected to add considerable sensitivity for dark scalar decays thanks to new downstream track reconstruction algorithm

- Able to trigger on decays with displacements up to ~2m

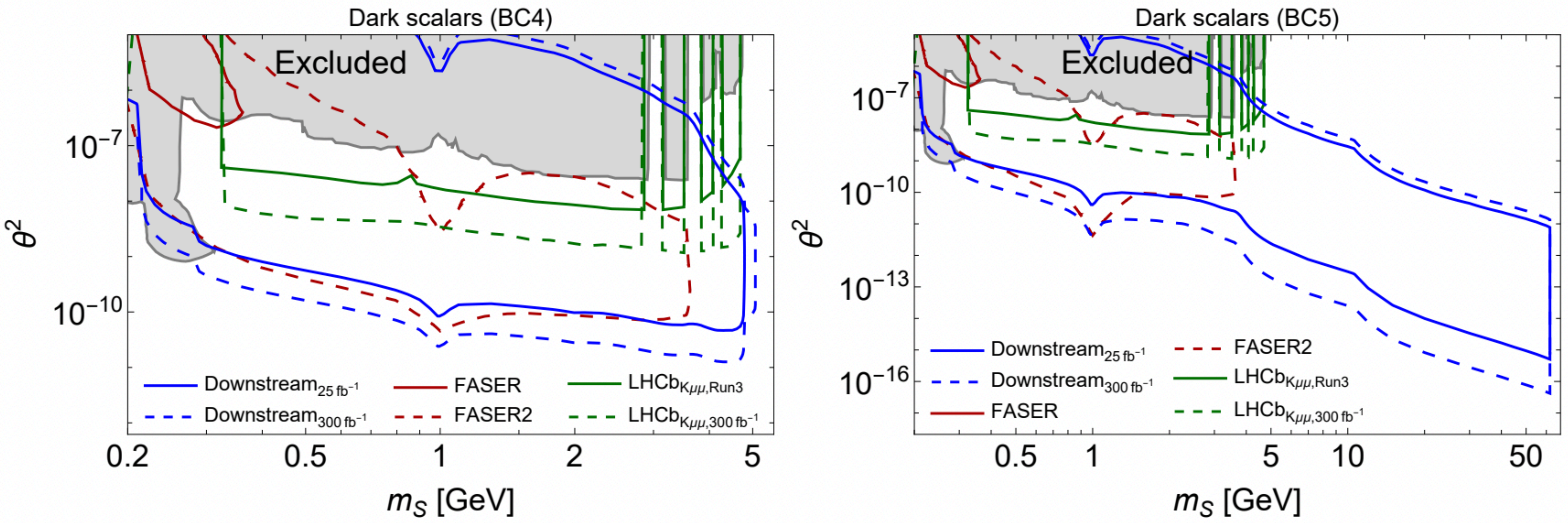

Especially interesting for $m_s < 5$ GeV where ATLAS+CMS lose sensitivity

Dark QCD signatures

Dark QCD searches offer a different window into the dark sector by directly probing the dark gauge structure

$$\mathcal{L}_d = \bar{q}'_i (i \not{D} - m_{q'_i}) q'_i - \frac{1}{4} G'^{\mu\nu} G'_{\mu\nu},$$

Dark QCD signatures

Dark QCD searches offer a different window into the dark sector by directly probing the dark gauge structure

$$\mathcal{L}_d = \bar{q}'_i (i \not{D} - m_{q'_i}) q'_i - \frac{1}{4} G'^{\mu\nu} G'_{\mu\nu},$$

Depending on the dark QCD model parameters, a variety of exotic jet phenomena are possible

- If DS states are LLPs, emerging jets with large numbers of displaced vertices are expected

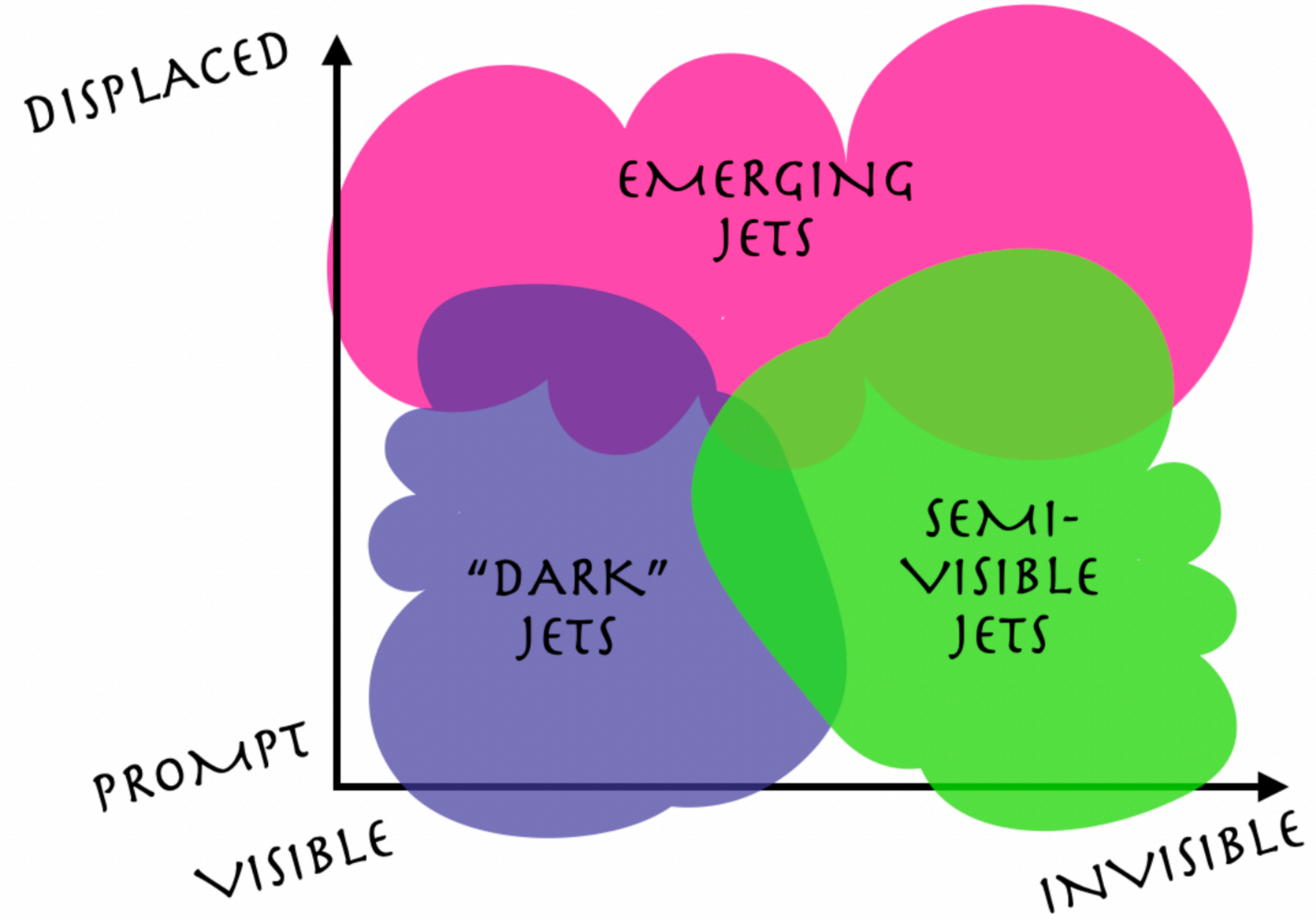

Dark QCD signatures

Dark QCD searches offer a different window into the dark sector by directly probing the dark gauge structure

$$\mathcal{L}_d = \bar{q}'_i(i\not{D} - m_{q'_i})q'_i - \frac{1}{4}G'^{\mu\nu}G'_{\mu\nu},$$

Depending on the dark QCD model parameters, a variety of exotic jet phenomena are possible

- If DS states are LLPs, emerging jets with large numbers of displaced vertices are expected

LHC searches typically focus on production via bifundamental mediator for triggering

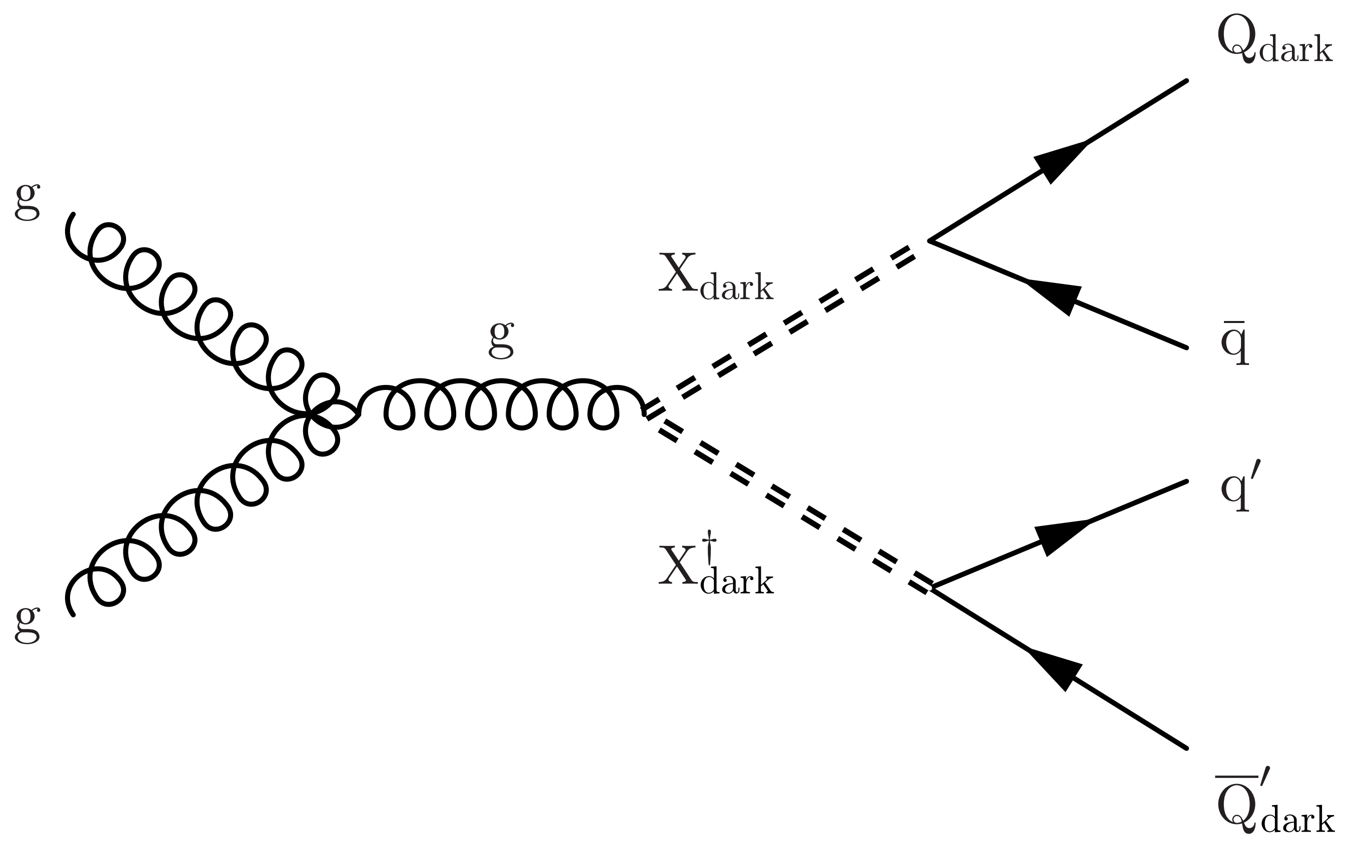

$$\mathcal{L}_{\text{med}} = (D^{\mu}X)^{\dagger}(D_{\mu}X) - M_X^2 X^{\dagger}X + \kappa_{ij} X\,\bar{q}'_i q_j + h.c.$$

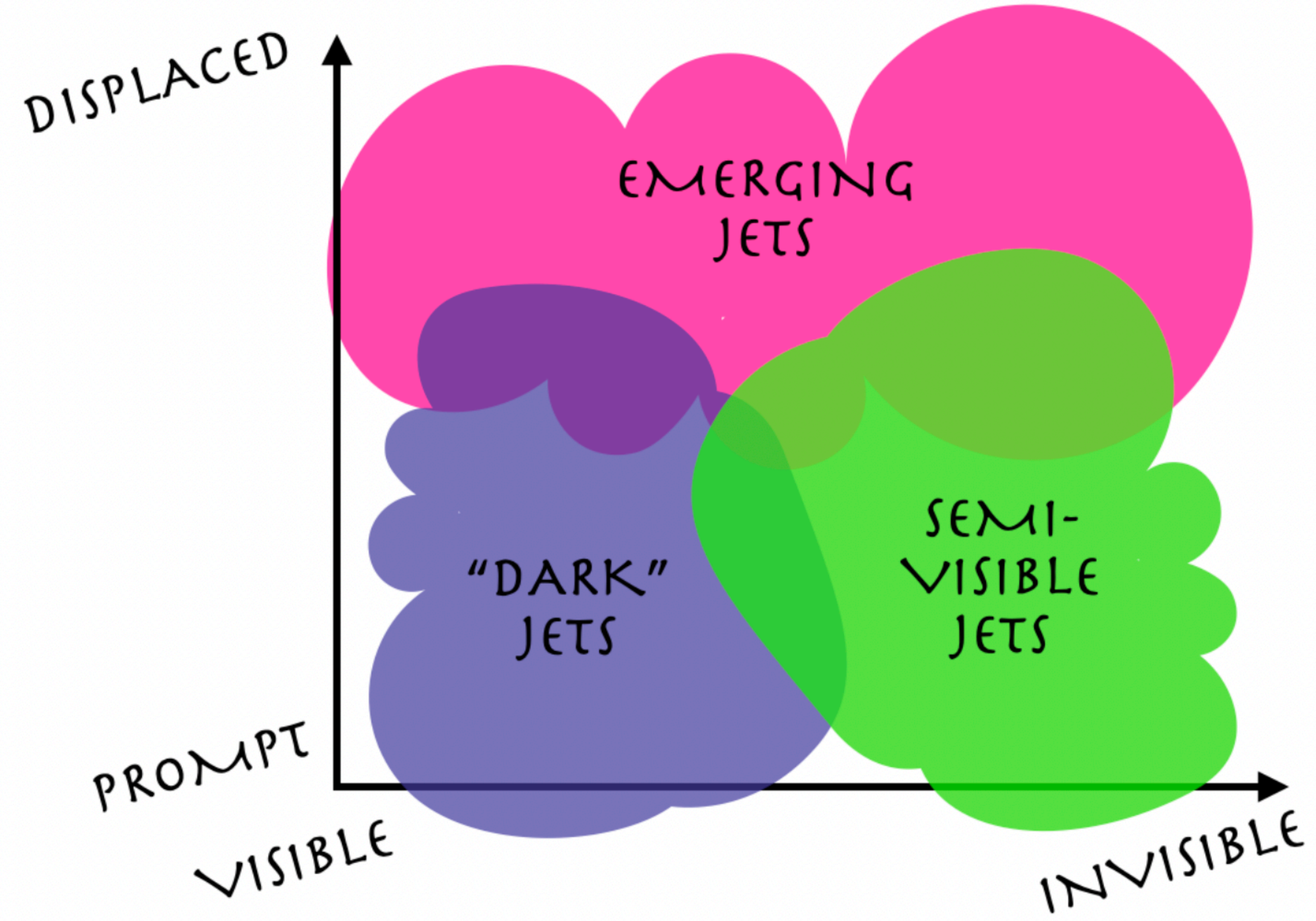

Emerging jets in CMS

New CMS emerging jet search using full Run 2 data

- Follow up to 2016 partial Run 2 results

2403.01556

Emerging jets in CMS

New CMS emerging jet search using full Run 2 data

- Follow up to 2016 partial Run 2 results

Two benchmark models considered:

1. Unflavoured: only consider coupling to d-quarks
2. Flavour-aligned: diagonal couplings between SM quarks and three dark quark flavours

→ Results in a large number of b-quarks in the decays

2403.01556

Emerging jets in CMS

New CMS emerging jet search using full Run 2 data

- Follow up to 2016 partial Run 2 results

Two benchmark models considered:

1. Unflavoured: only consider coupling to d-quarks
2. Flavour-aligned: diagonal couplings between SM quarks and three dark quark flavours

   → Results in a large number of b-quarks in the decays

For each model, two different search strategies are used

1. Model agnostic results using high-level observables based on track displacement
2. Model dependent results using GNN

2403.01556

Emerging jets in CMS

New CMS emerging jet search using full Run 2 data

- Follow up to 2016 partial Run 2 results

Two benchmark models considered:

1. Unflavoured: only consider coupling to d-quarks
2. Flavour-aligned: diagonal couplings between SM quarks and three dark quark flavours

   → Results in a large number of b-quarks in the decays

For each model, two different search strategies are used

1. Model agnostic results using high-level observables based on track displacement
2. Model dependent results using GNN

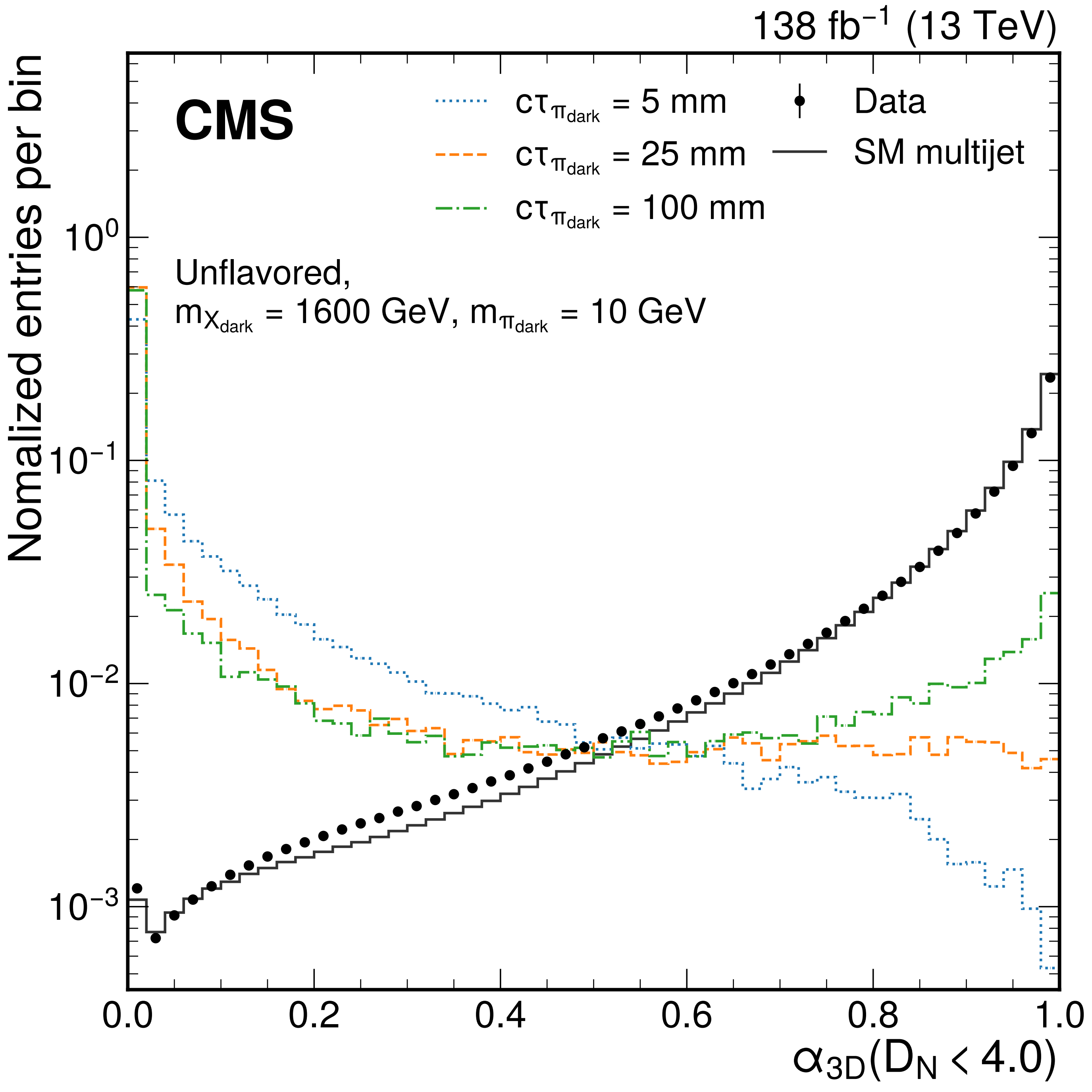

2403.01556

Emerging jets in CMS

New CMS emerging jet search using full Run 2 data

- Follow up to 2016 partial Run 2 results

Two benchmark models considered:

1. Unflavoured: only consider coupling to d-quarks
2. Flavour-aligned: diagonal couplings between SM quarks and three dark quark flavours

   → Results in a large number of b-quarks in the decays

For each model, two different search strategies are used

1. Model agnostic results using high-level observables based on track displacement
2. Model dependent results using GNN

2403.01556

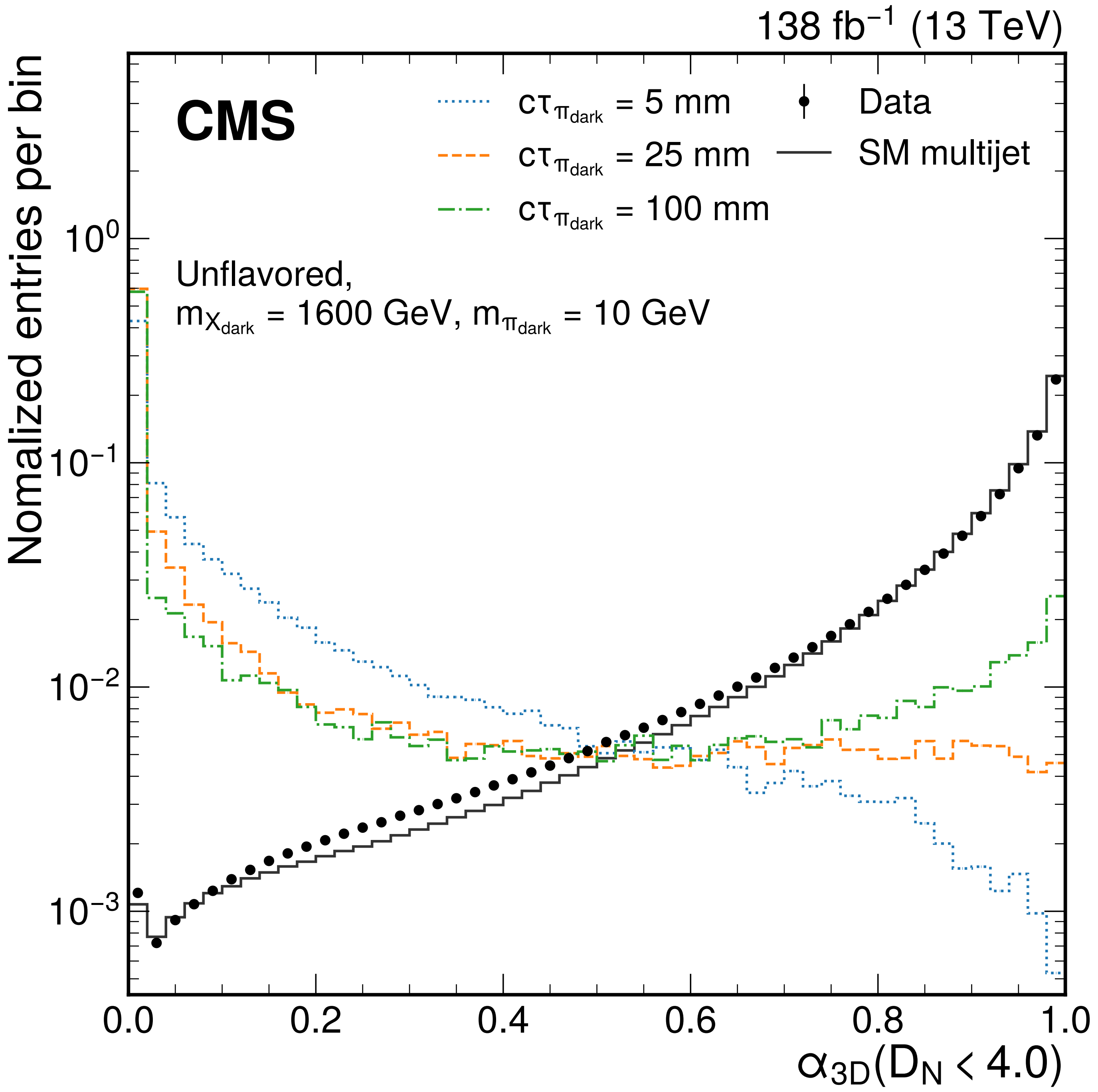

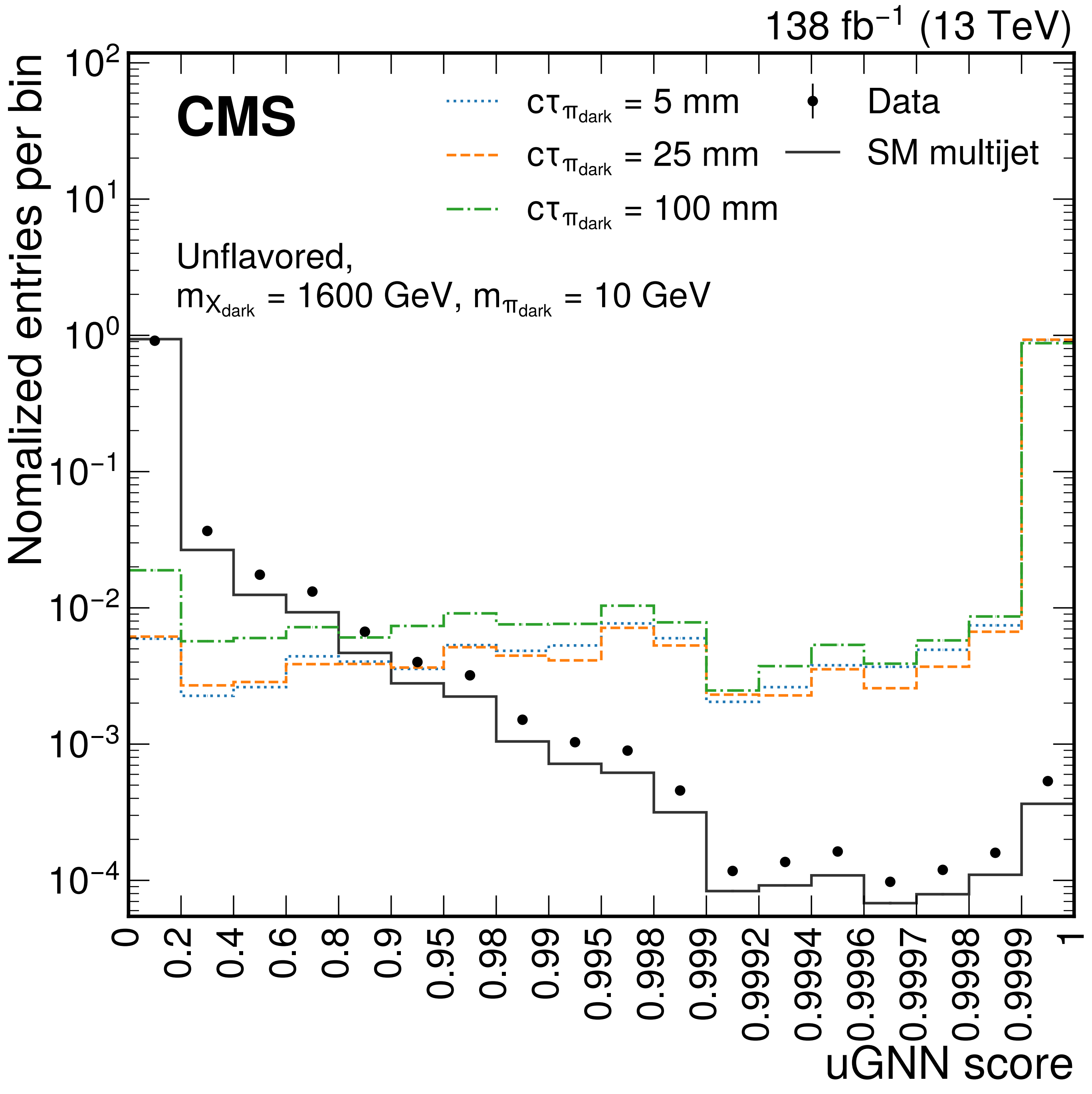

Emerging jets in CMS

Limits set as a function of mediator mass ($m_{X_{\rm dark}}$) and dark pion lifetime

- Both model independent and model-dependent results significantly expand sensitivity w.r.t. previous results
- First search to probe a flavoured dark QCD sector!

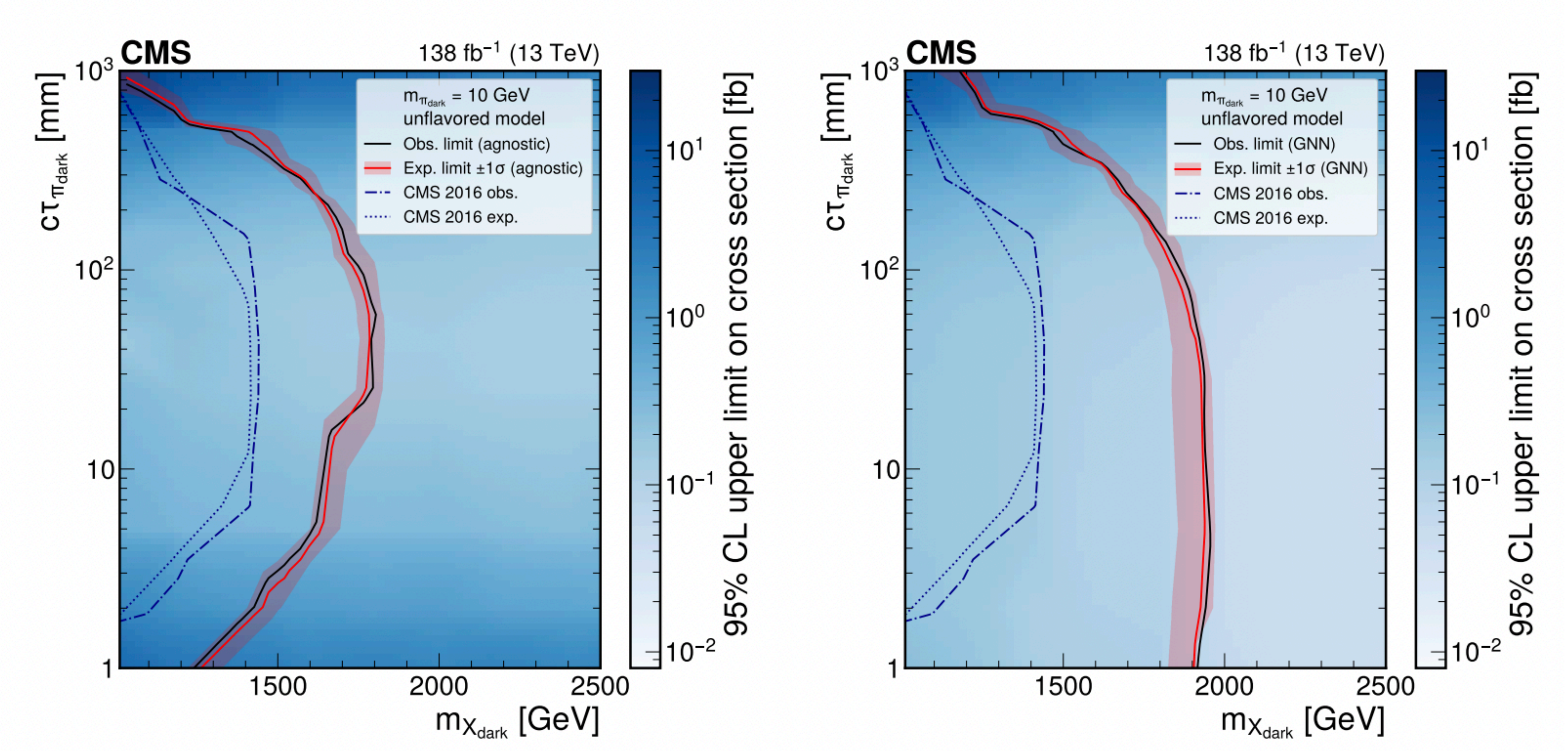

Run 3 prospects for emerging jets

Dark QCD parameter space still largely unexplored!

Run 3 prospects for emerging jets

Dark QCD parameter space still largely unexplored!

Explore beyond bifundamental mediators in Run 3: e.g. Higgs portal, Z'

- New ATLAS triggers will enable searches for s-channel emerging jet production via Z' mediator

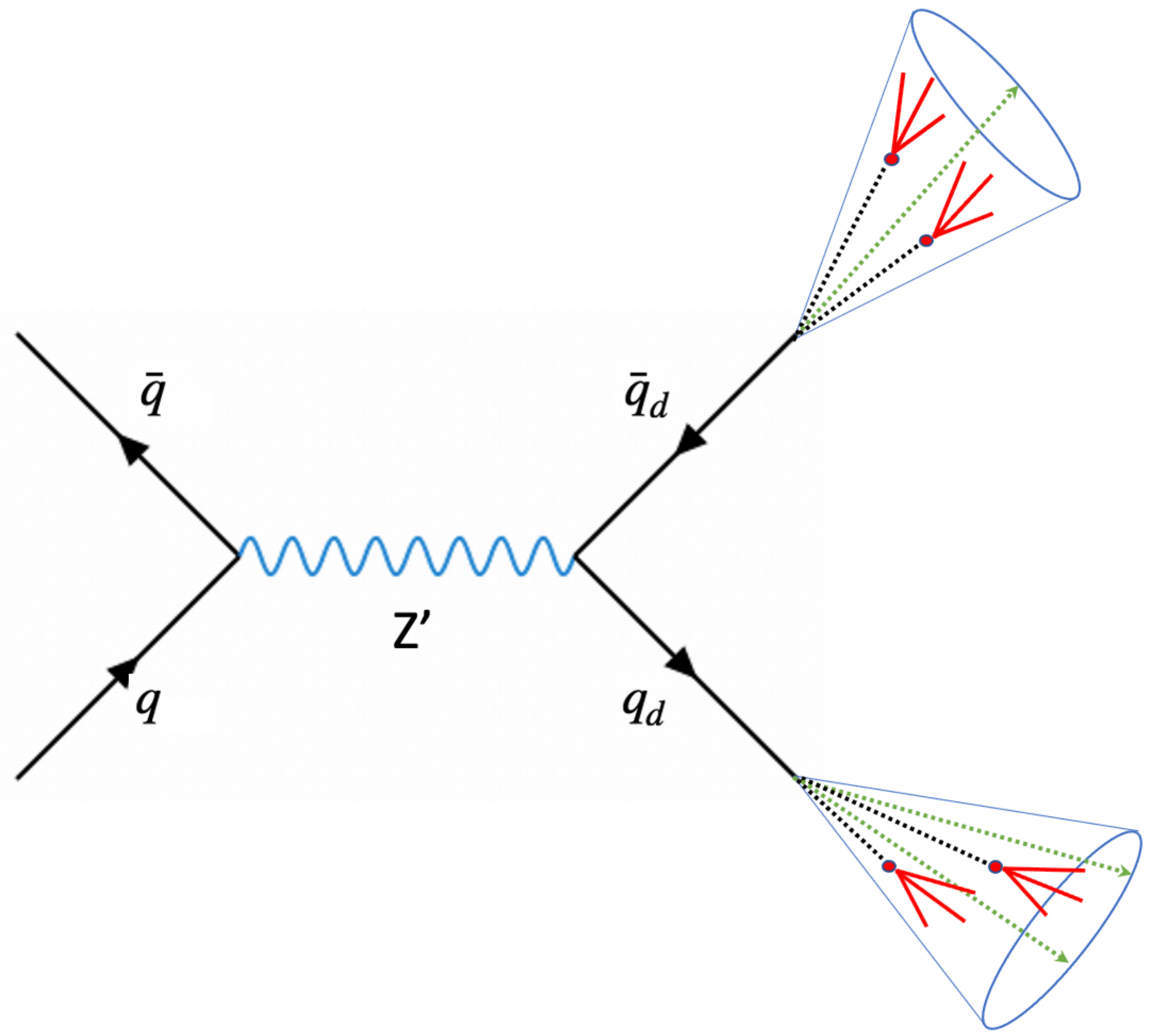

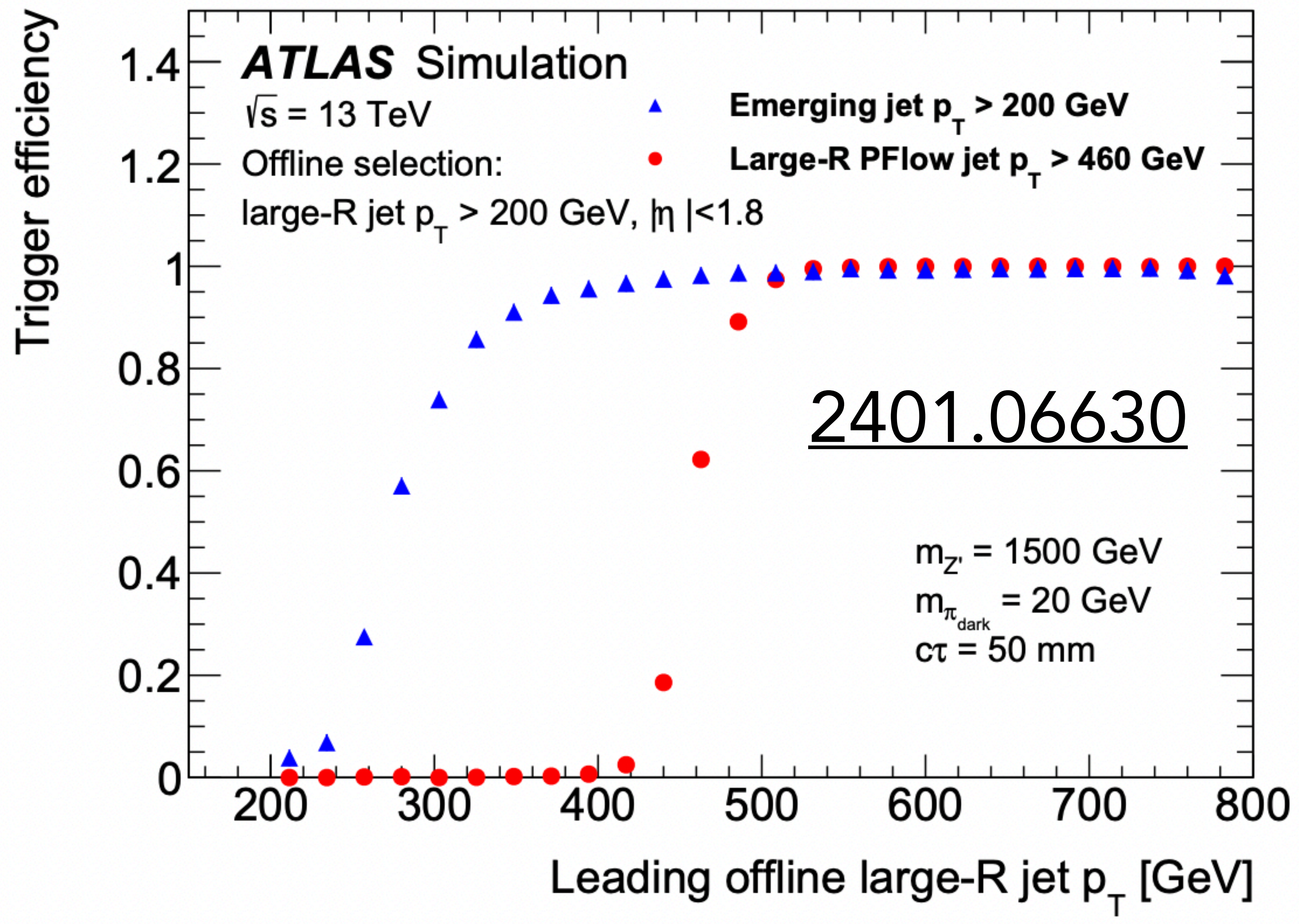

Run 3 prospects for emerging jets

Dark QCD parameter space still largely unexplored!

Explore beyond bifundamental mediators in Run 3: e.g. Higgs portal, Z'

- New ATLAS triggers will enable searches for s-channel emerging jet production via Z' mediator

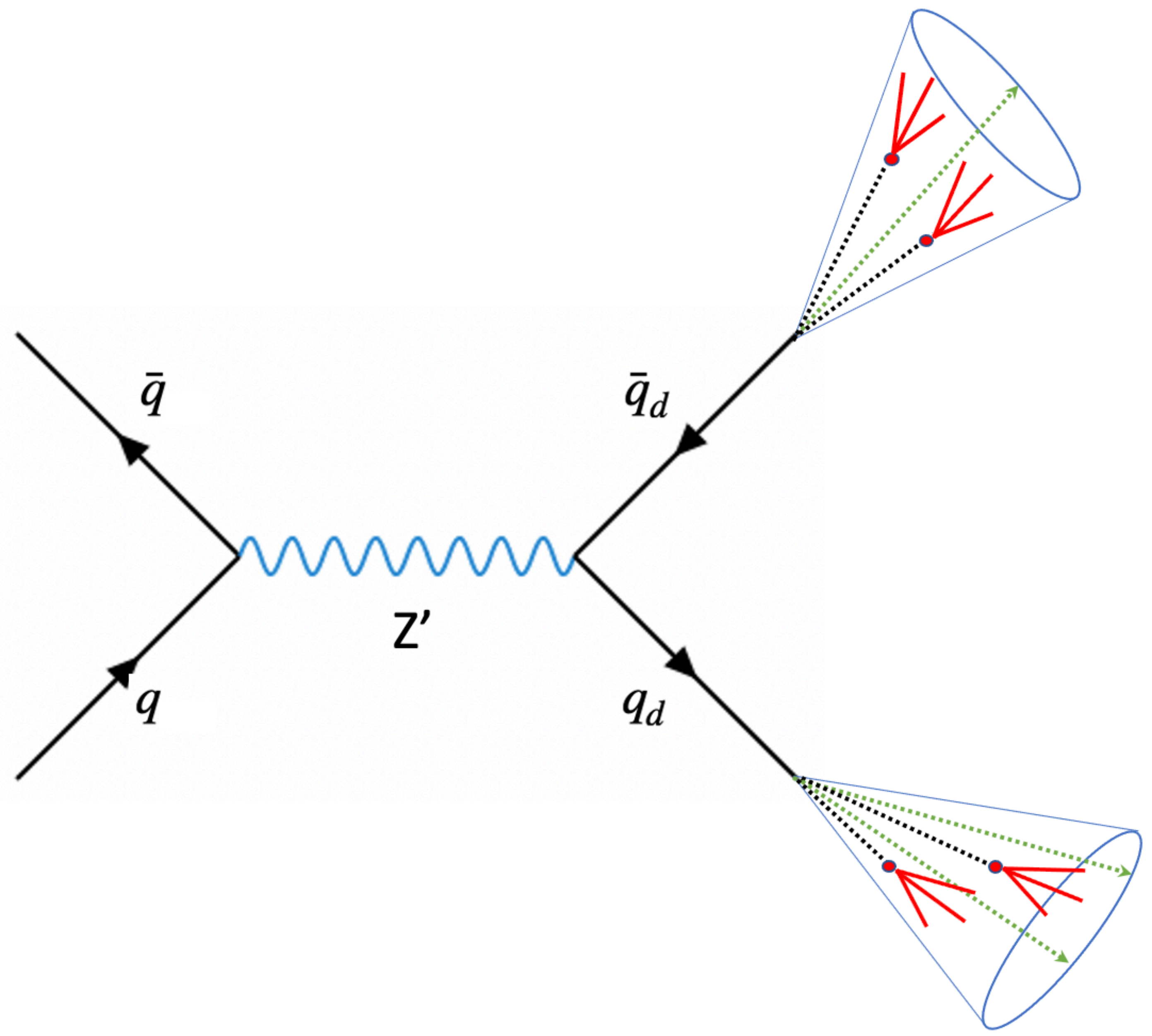

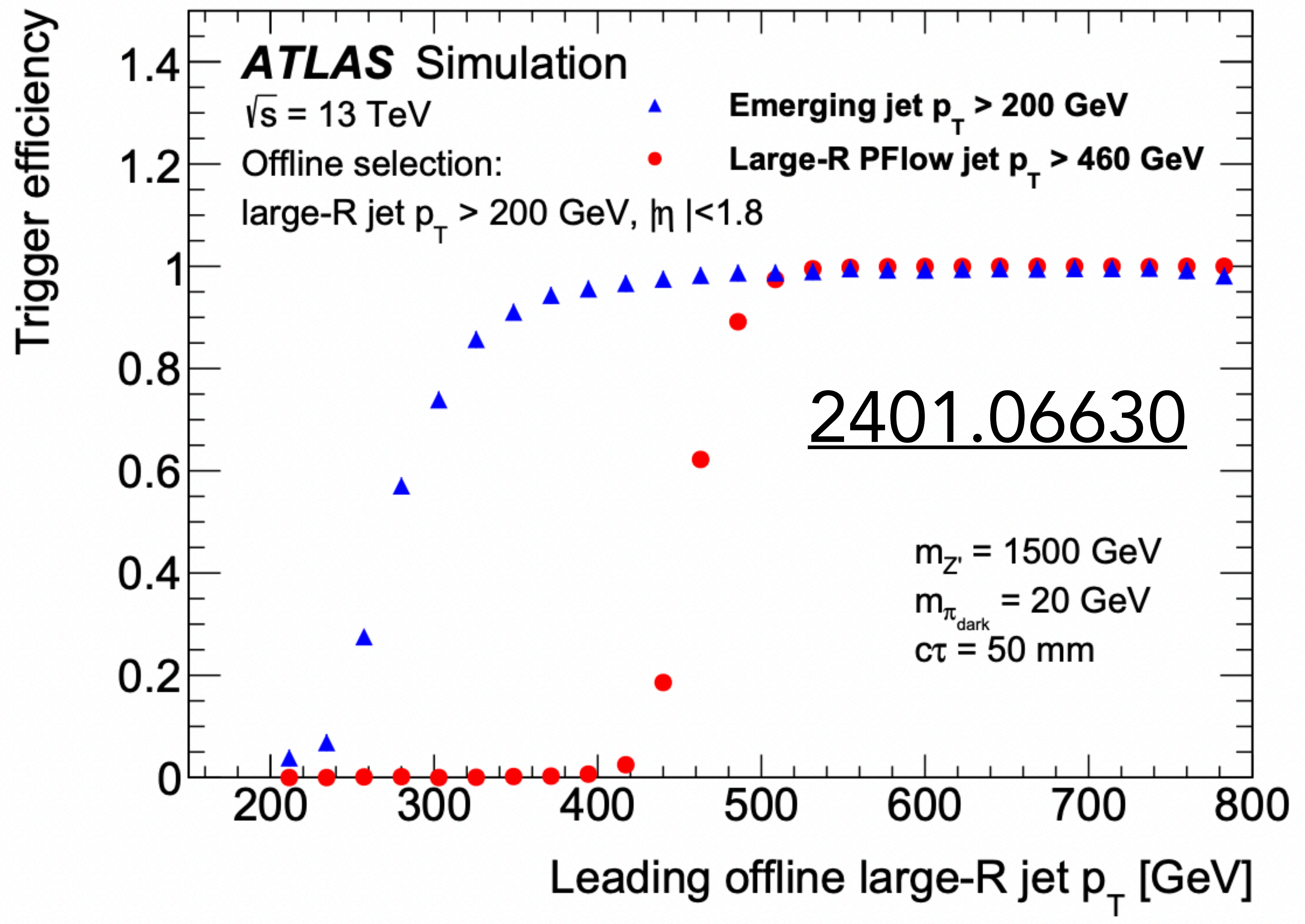

Coordinate with searches for semi-visible jets and dark jets to effectively cover model space

Heavy Neutral Leptons

Neutrino sector offers another renormalizable portal to the dark sector

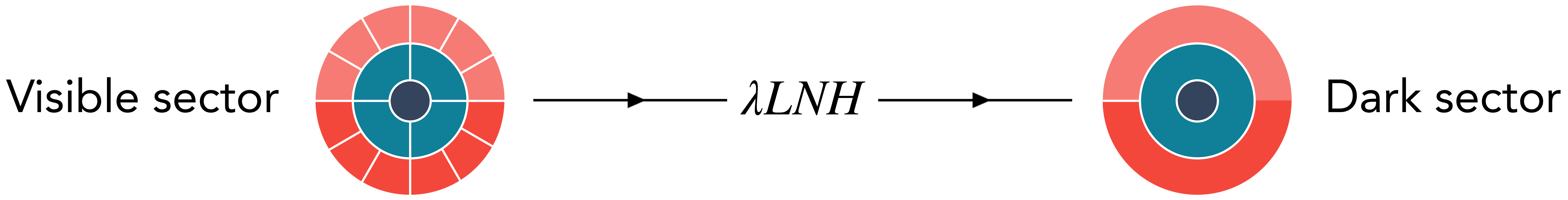

Heavy Neutral Leptons

Neutrino sector offers another renormalizable portal to the dark sector

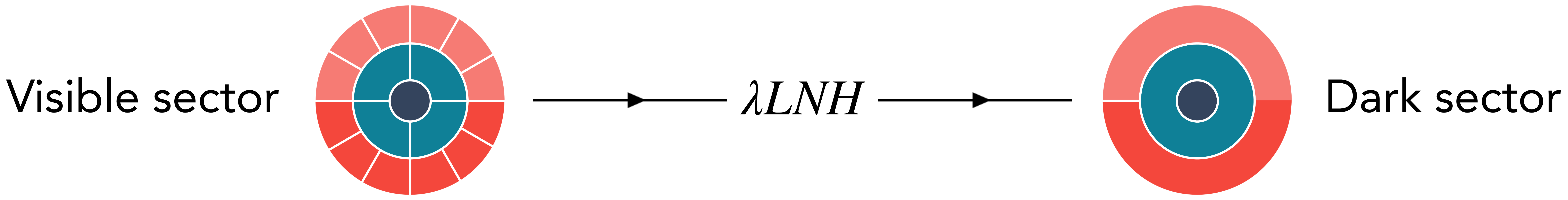

Extension of SM with right-handed neutrinos can simultaneously explain neutrino masses, dark matter, and baryon asymmetry

Heavy Neutral Leptons

Neutrino sector offers another renormalizable portal to the dark sector

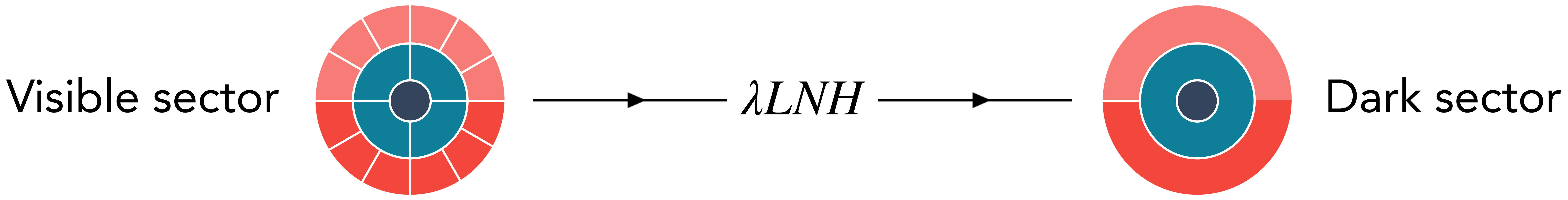

Extension of SM with right-handed neutrinos can simultaneously explain neutrino masses, dark matter, and baryon asymmetry

Dirac

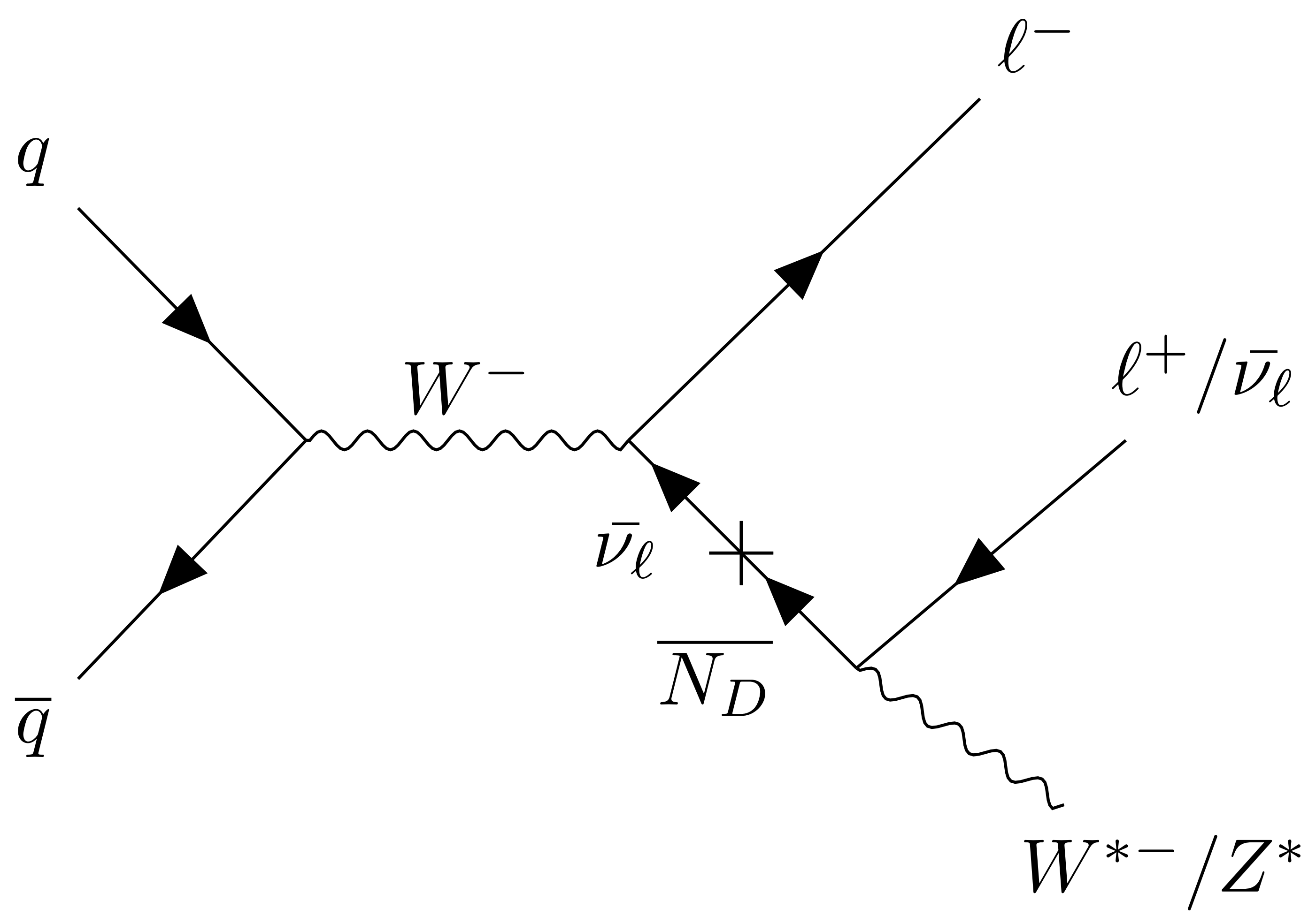

Heavy Neutral Leptons

Neutrino sector offers another renormalizable portal to the dark sector

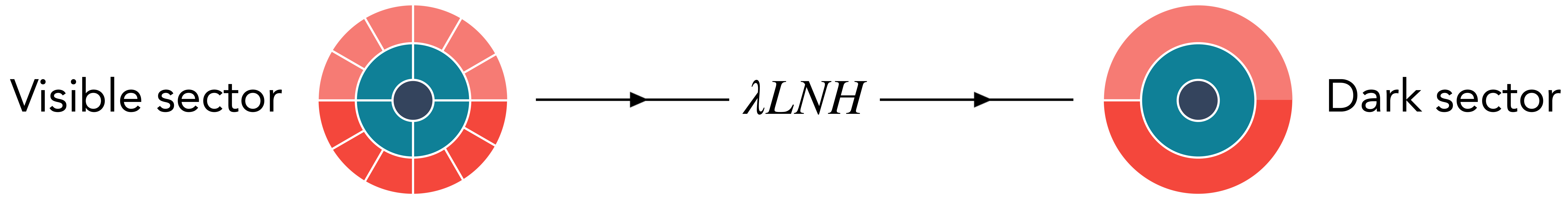

Extension of SM with right-handed neutrinos can simultaneously explain neutrino masses, dark matter, and baryon asymmetry

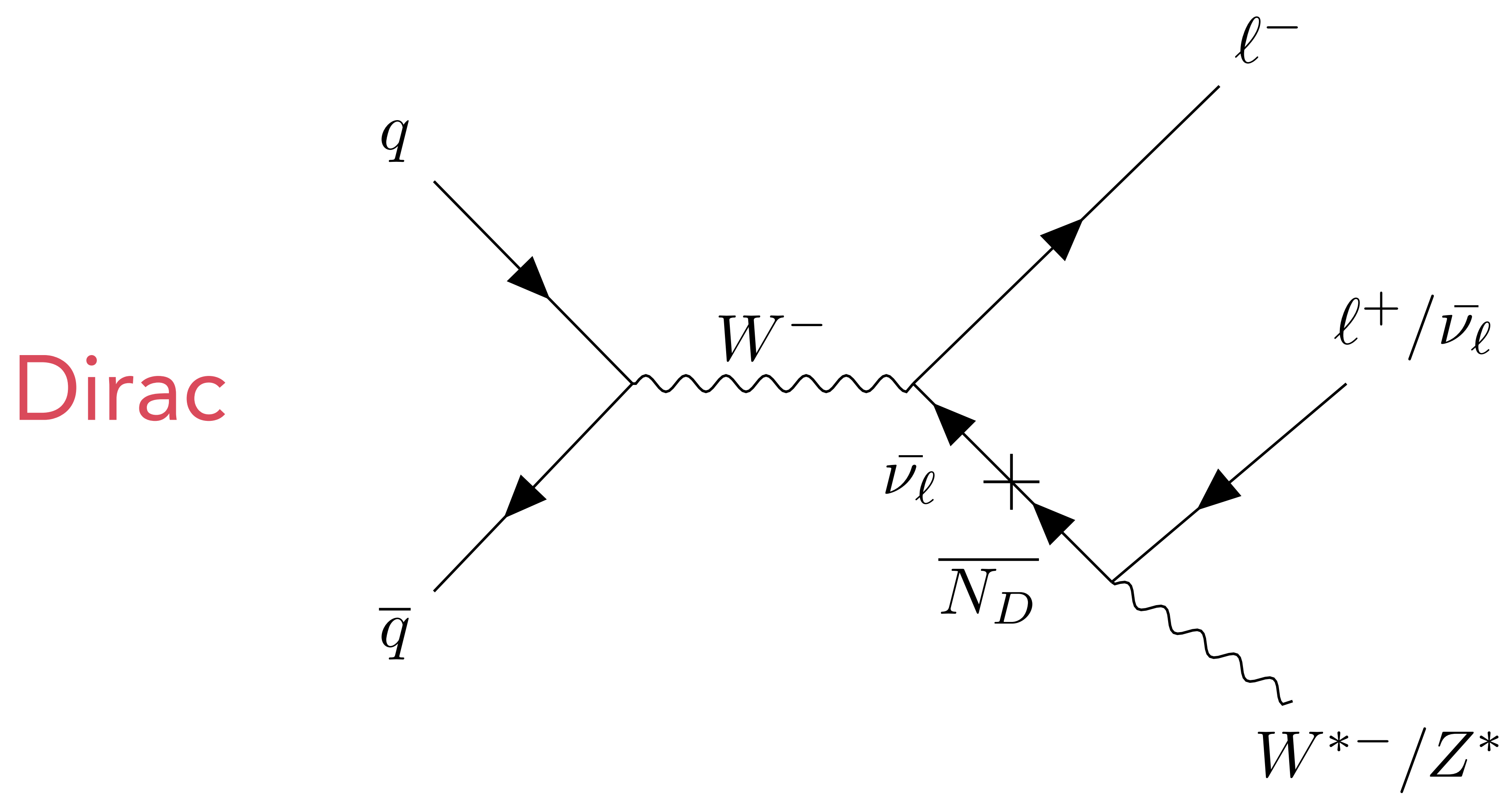

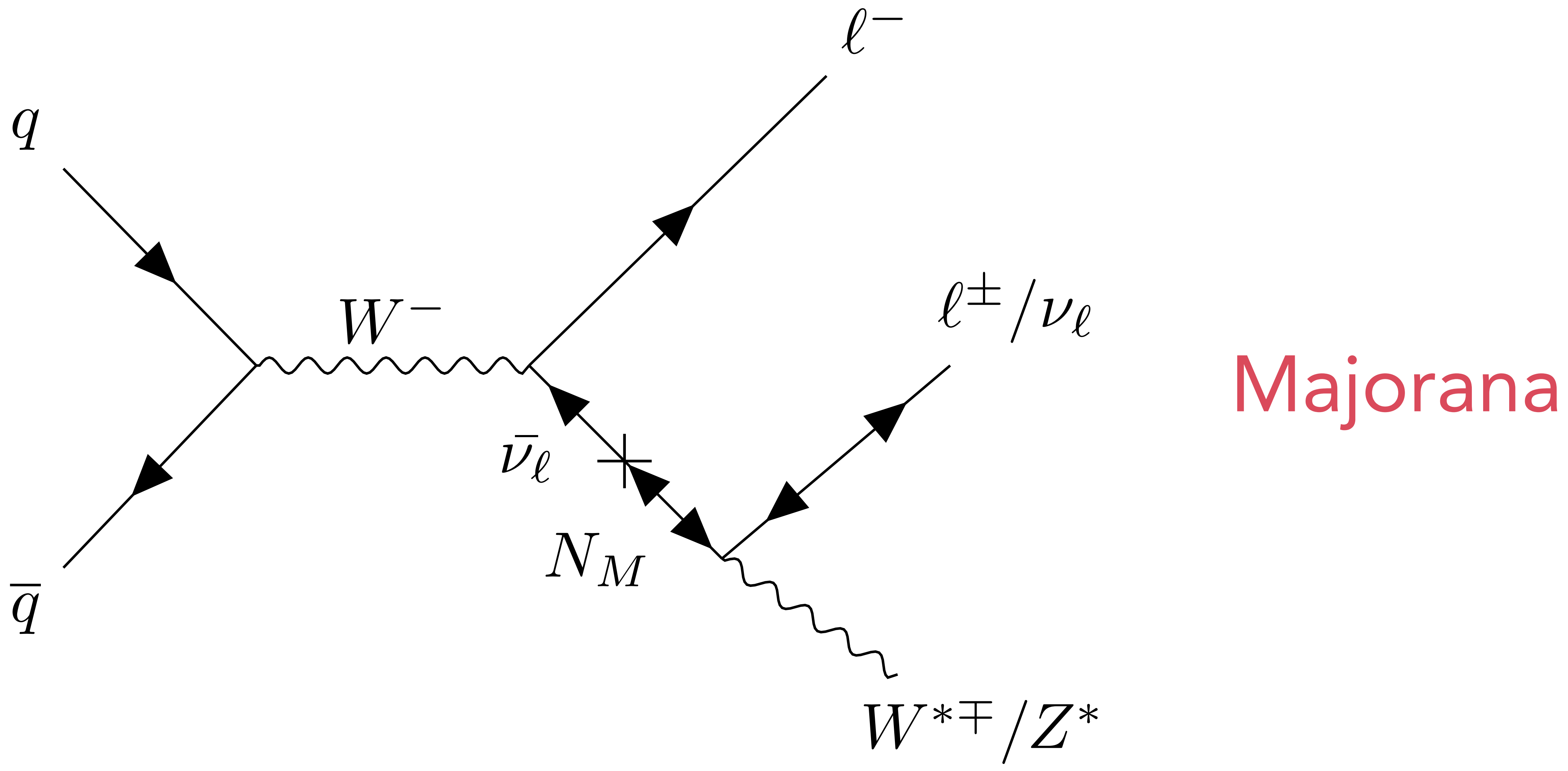

Displaced Heavy Neutral Lepton searches

Both ATLAS and CMS have probed fully-leptonic displaced HNL decays using the full Run 2 datasets

- "Workhorse" channel providing sensitivity for wide range of masses and lifetimes

Displaced Heavy Neutral Lepton searches

Both ATLAS and CMS have probed fully-leptonic displaced HNL decays using the full Run 2 datasets

- "Workhorse" channel providing sensitivity for wide range of masses and lifetimes

Clean channel of displaced dilepton vertex in the inner detectors

Displaced Heavy Neutral Lepton searches

Both ATLAS and CMS have probed fully-leptonic displaced HNL decays using the full Run 2 datasets

- "Workhorse" channel providing sensitivity for wide range of masses and lifetimes

Clean channel of displaced dilepton vertex in the inner detectors

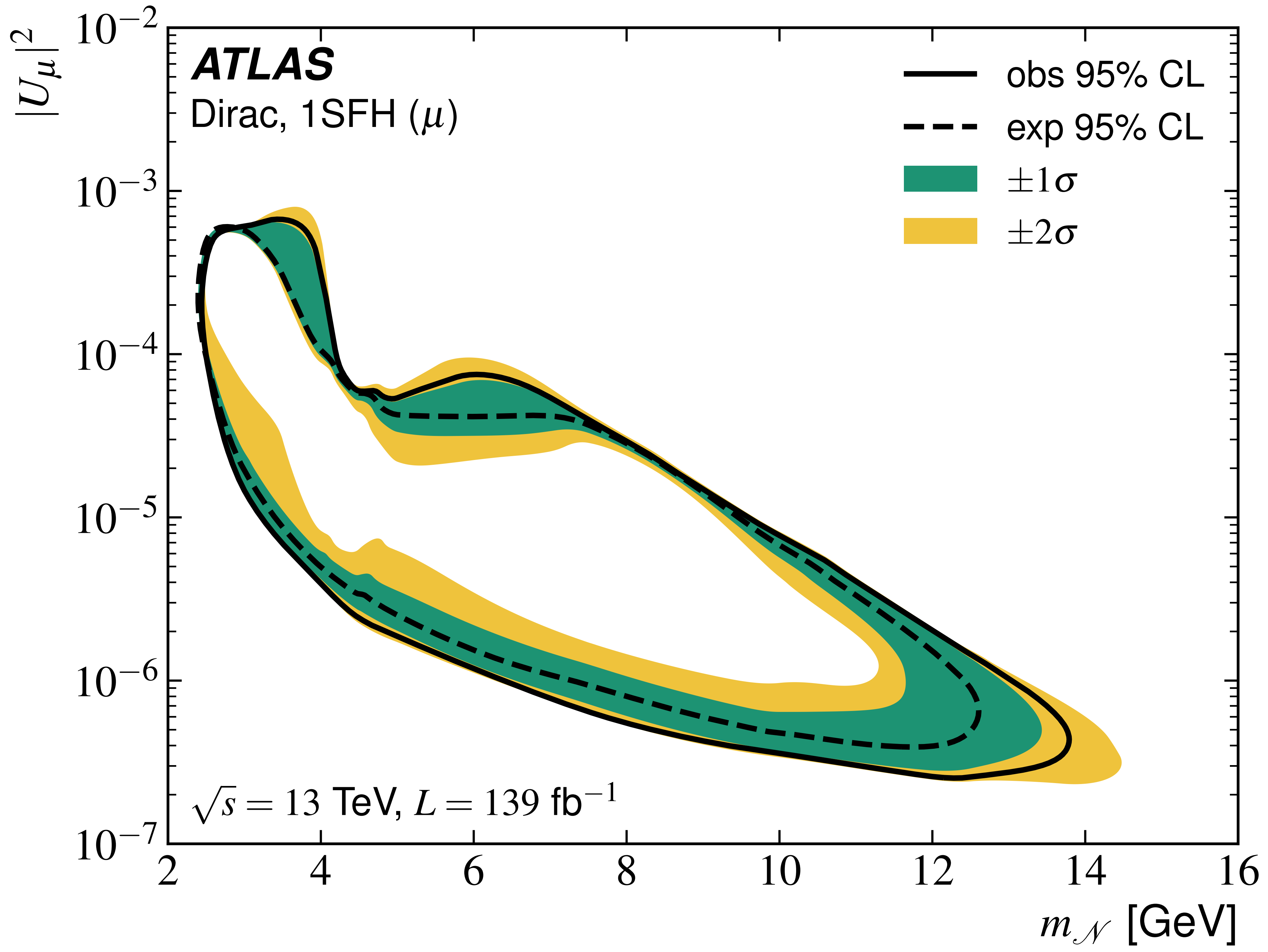

2204.11988

Displaced Heavy Neutral Lepton searches

Both ATLAS and CMS have probed fully-leptonic displaced HNL decays using the full Run 2 datasets

- “Workhorse” channel providing sensitivity for wide range of masses and lifetimes

Clean channel of displaced dilepton vertex in the inner detectors

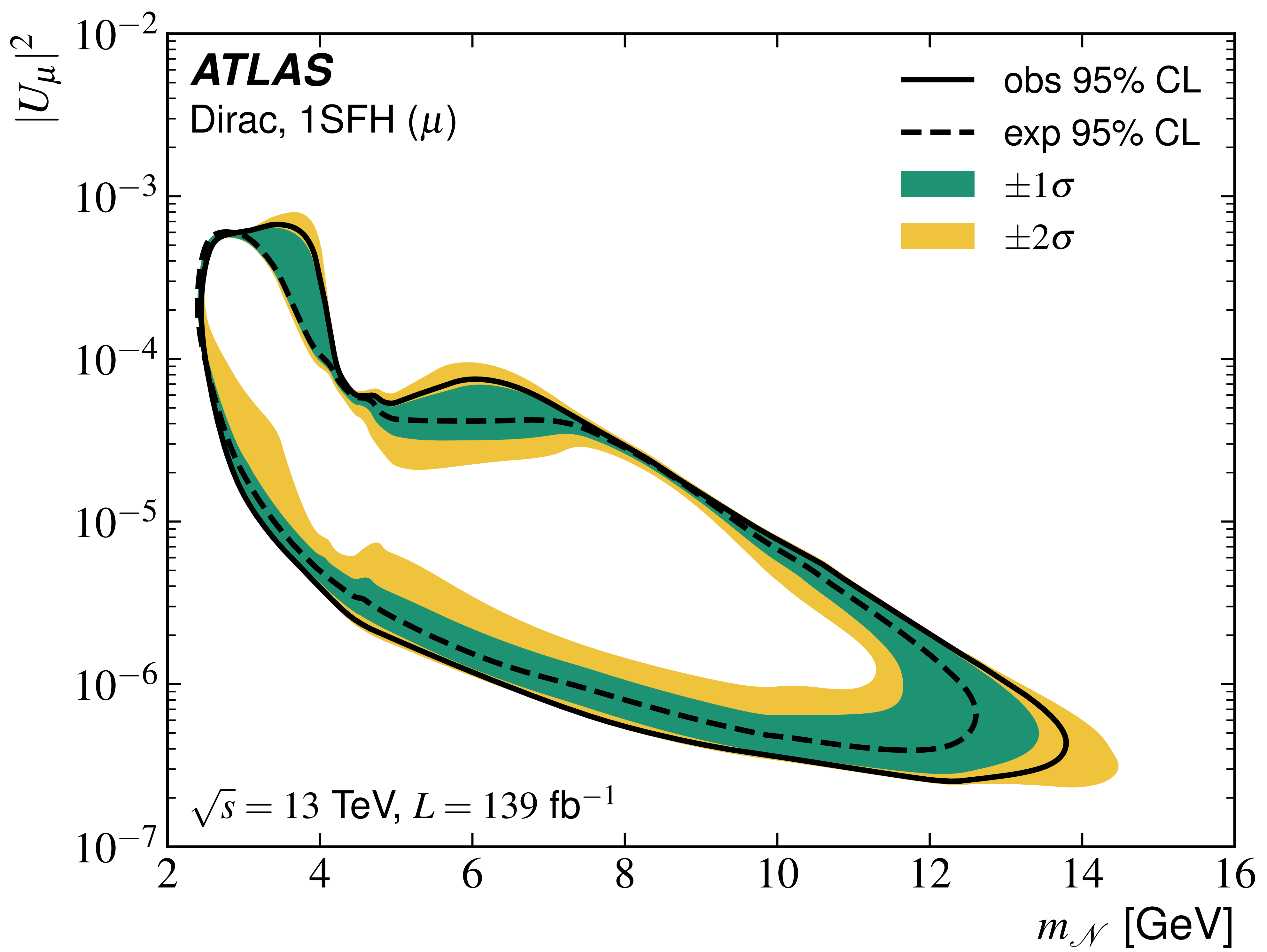

2204.11988

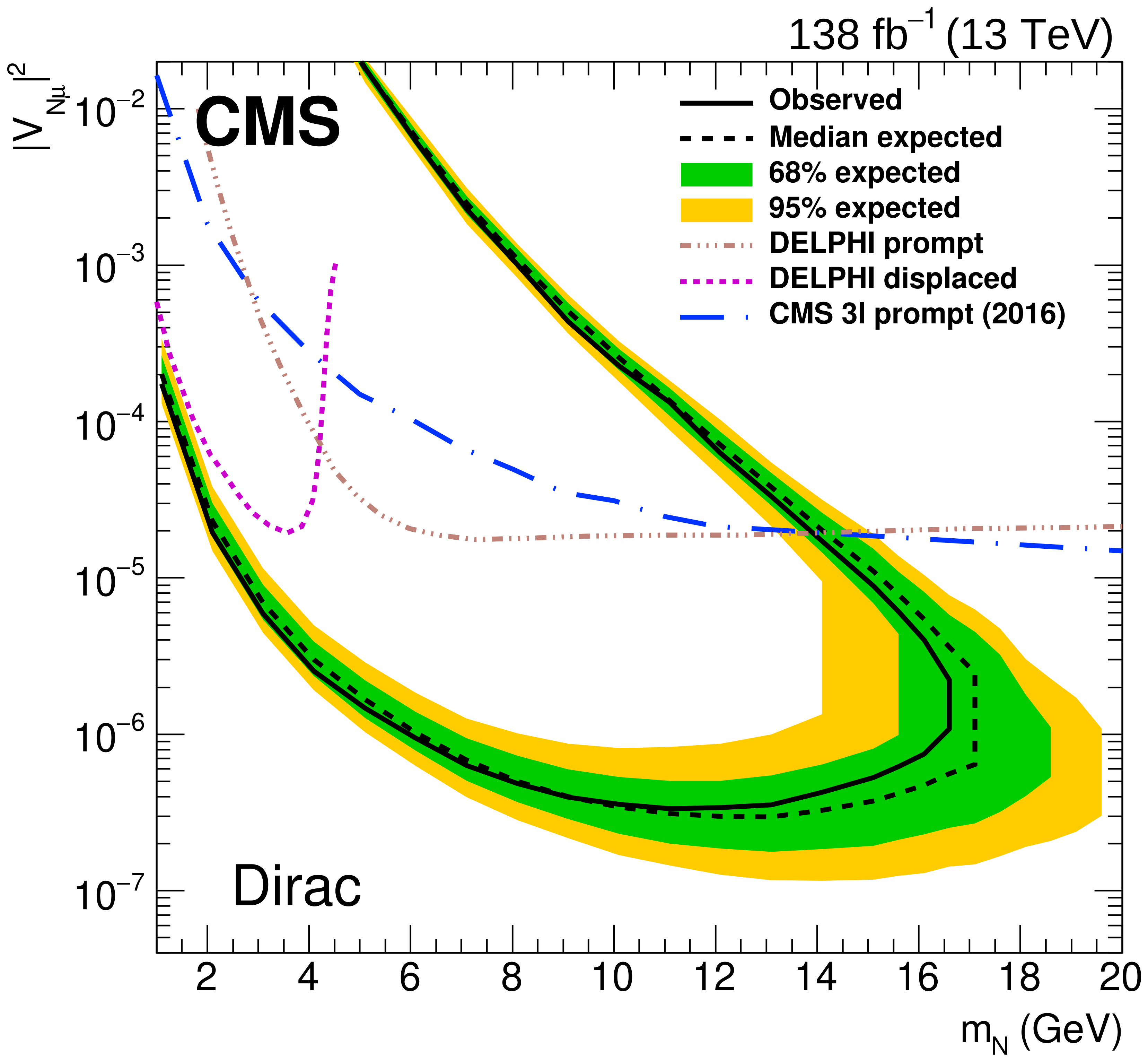

2201.05578

Semi-leptonic HNL decays

2312.07484

CMS has recently probed semi-leptonic HNL decays for the first time at the LHC

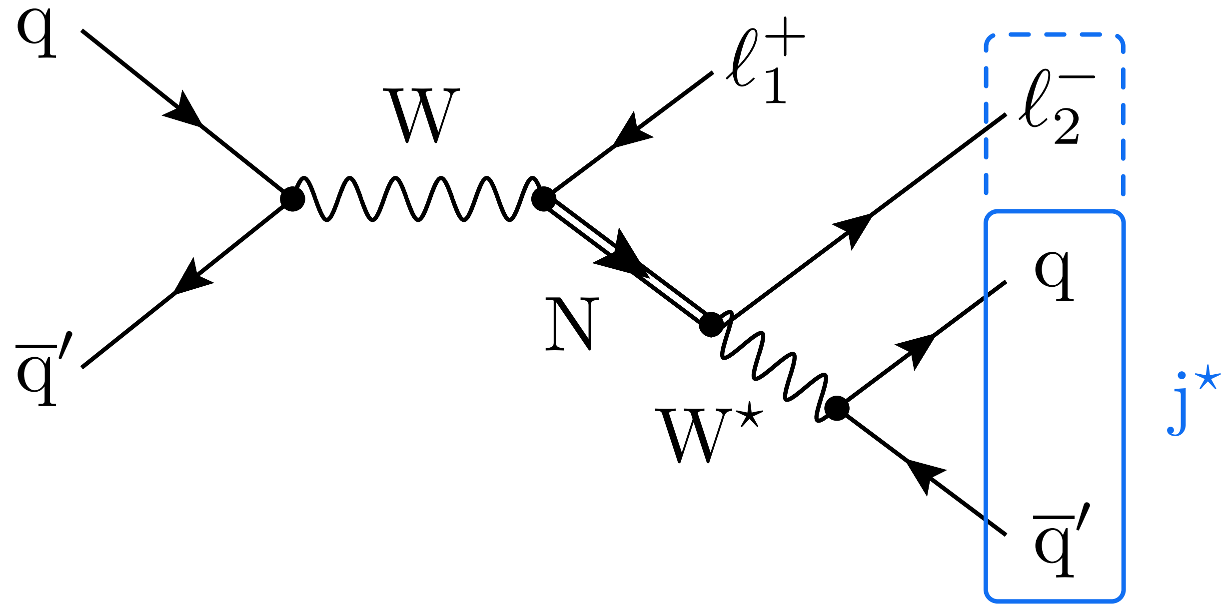

Semi-leptonic HNL decays

2312.07484

CMS has recently probed semi-leptonic HNL decays for the first time at the LHC

- Use a displaced jet tagger to identify signal

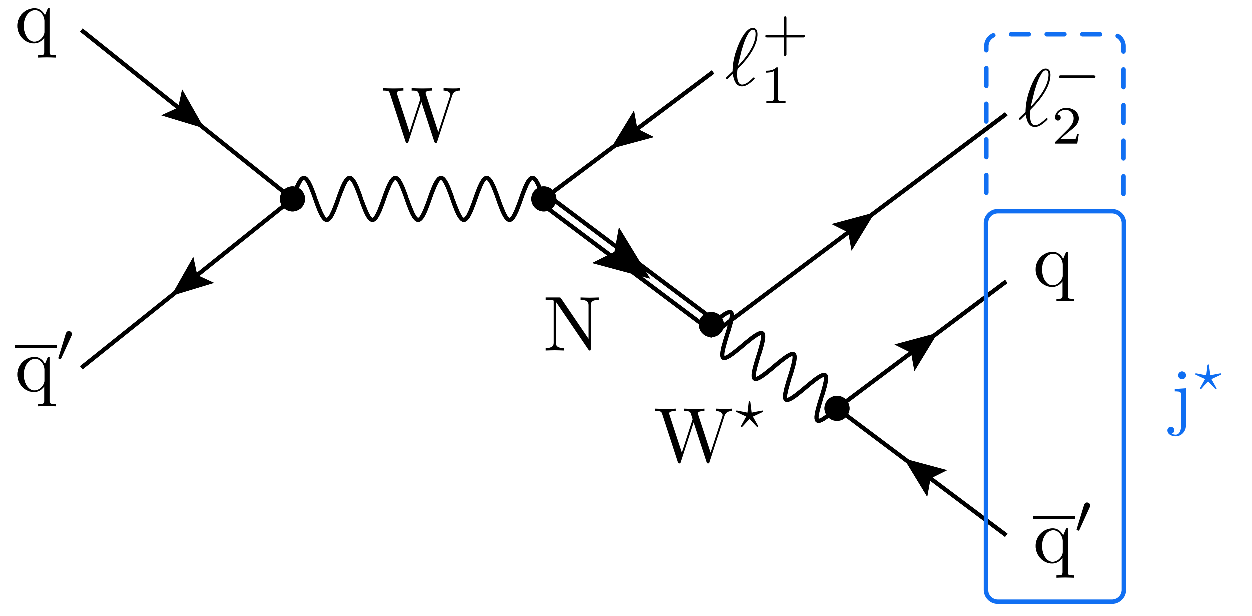

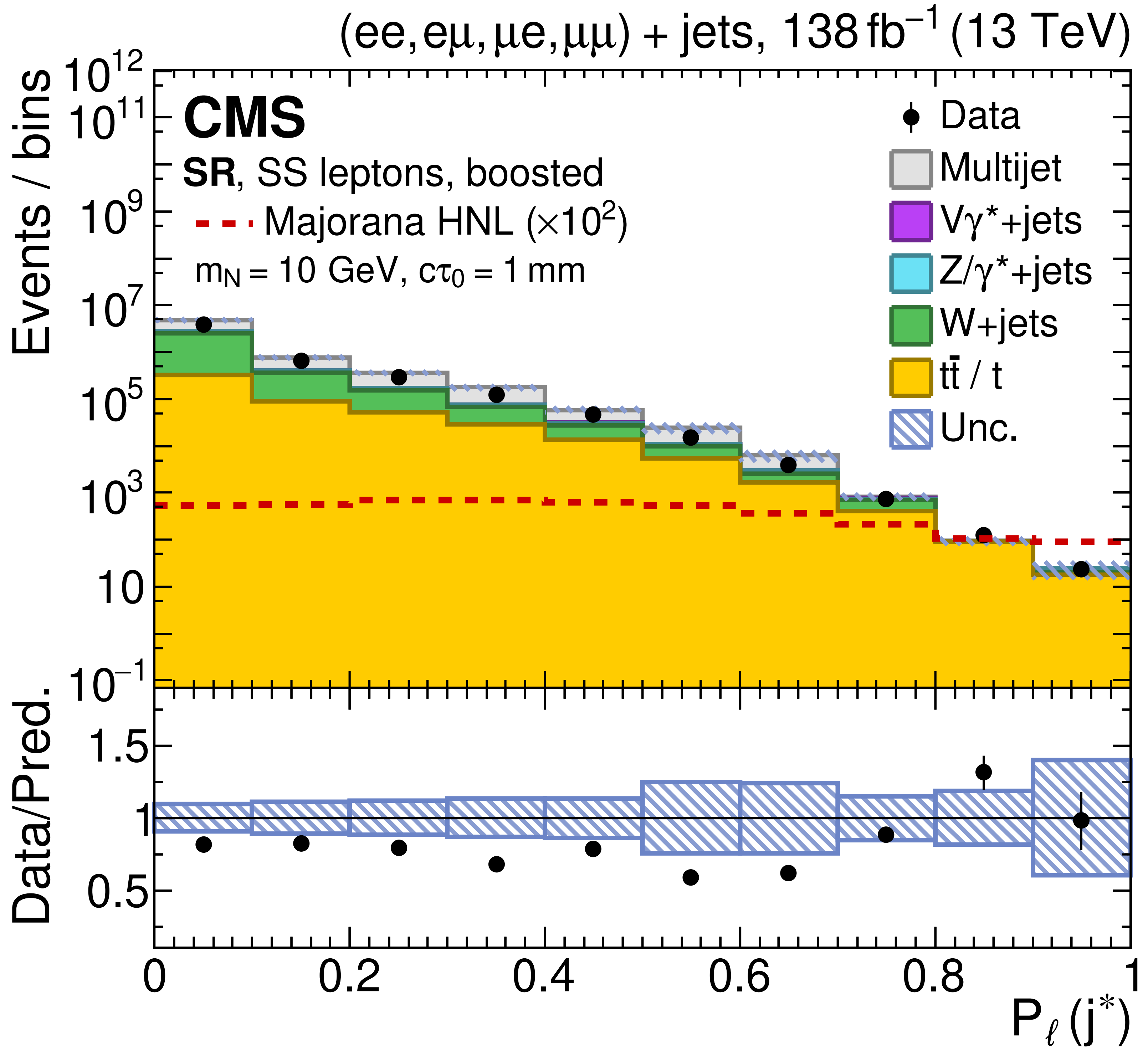

Semi-leptonic HNL decays

2312.07484

CMS has recently probed semi-leptonic HNL decays for the first time at the LHC

- Use a displaced jet tagger to identify signal
- ABCD background estimate using sidebands of m_{llj}

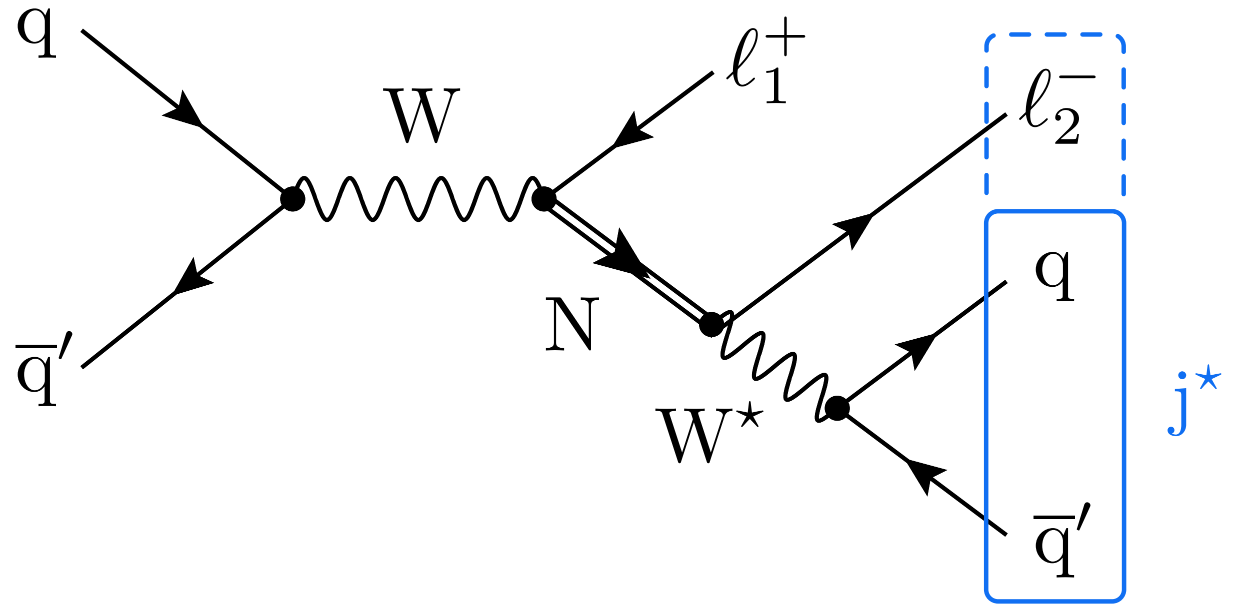

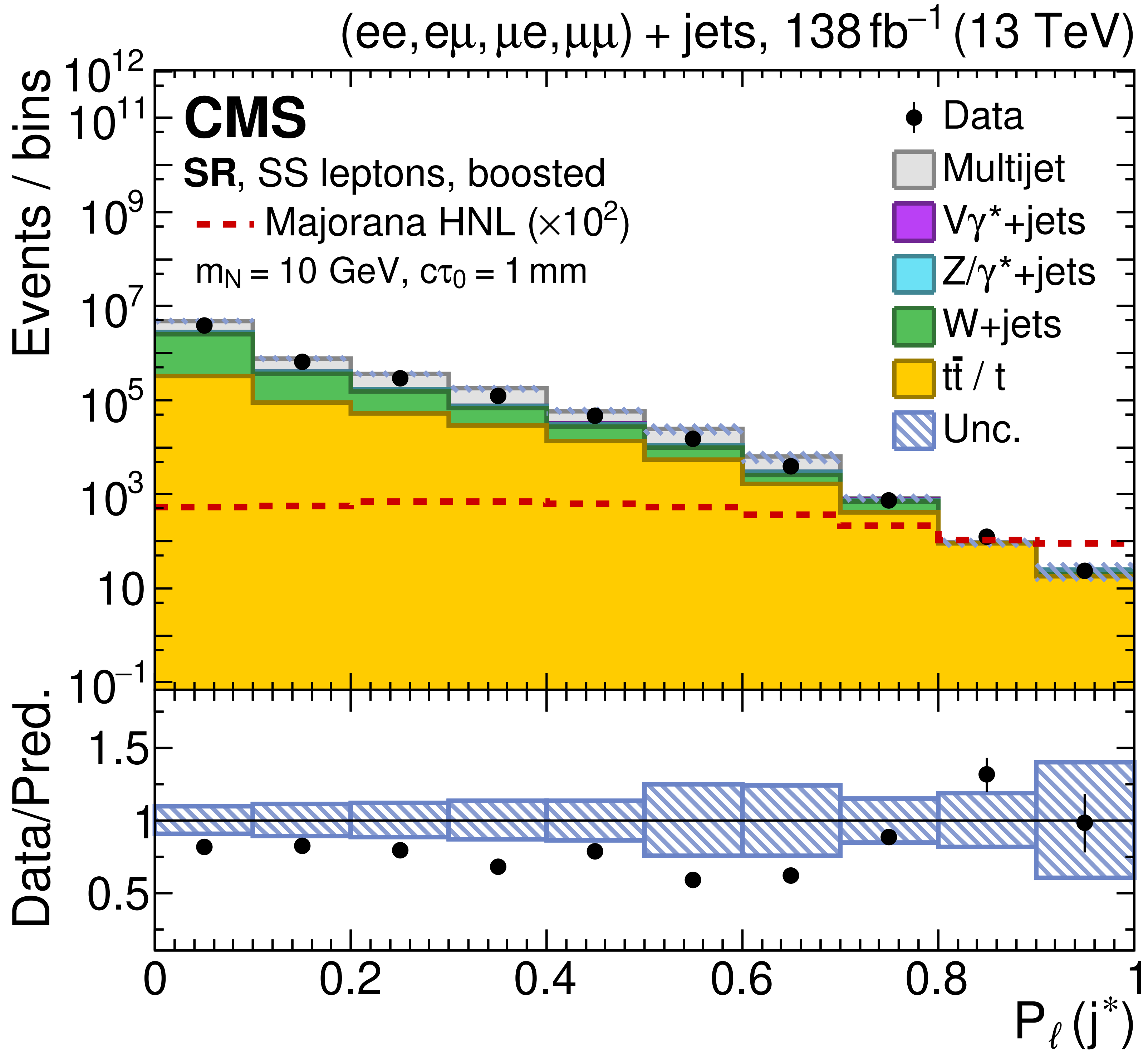

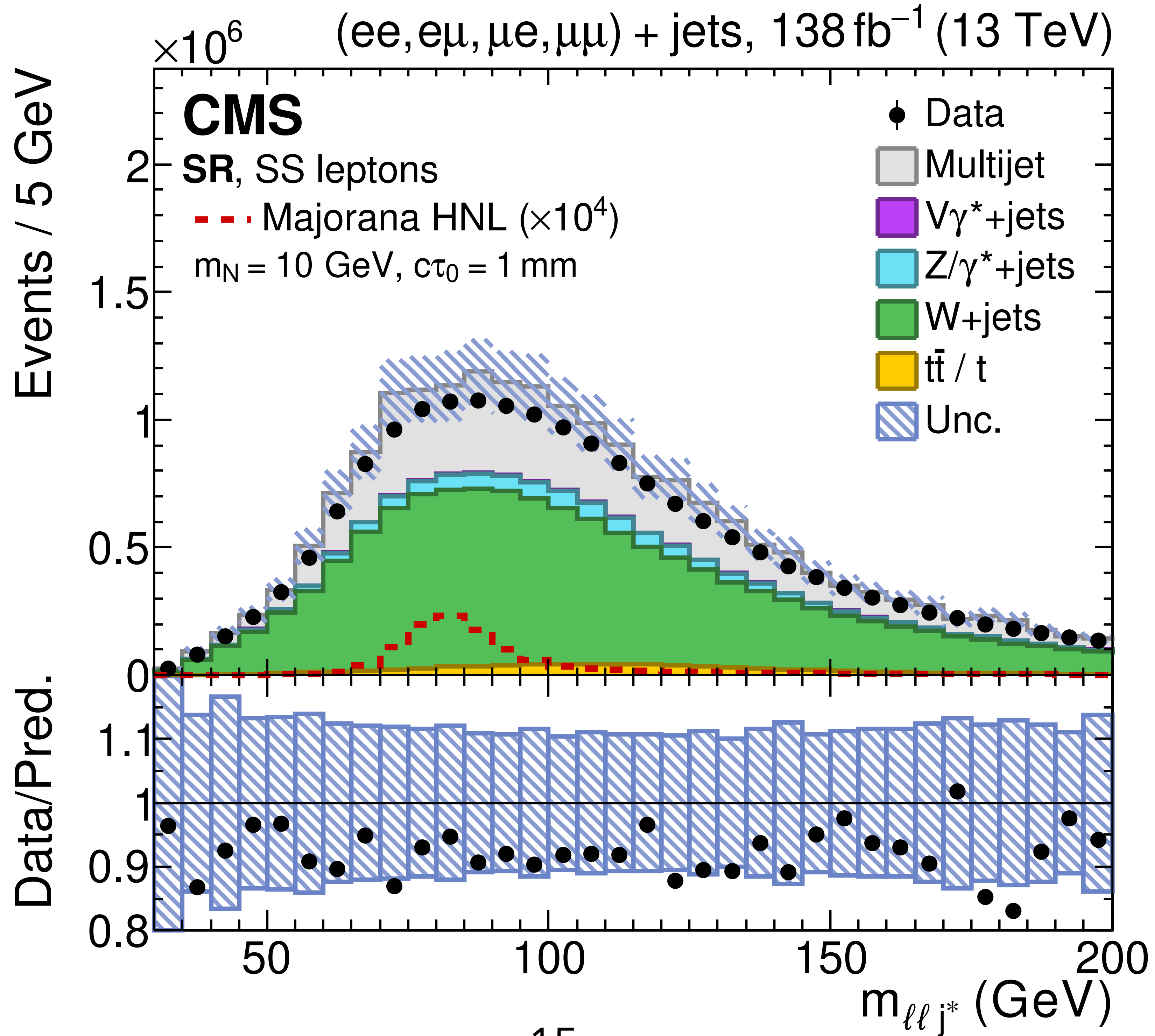

Semi-leptonic HNL decays

2312.07484

CMS has recently probed semi-leptonic HNL decays for the first time at the LHC

- Use a displaced jet tagger to identify signal
- ABCD background estimate using sidebands of m_{llj}
- Comparable sensitivity to fully leptonic analysis

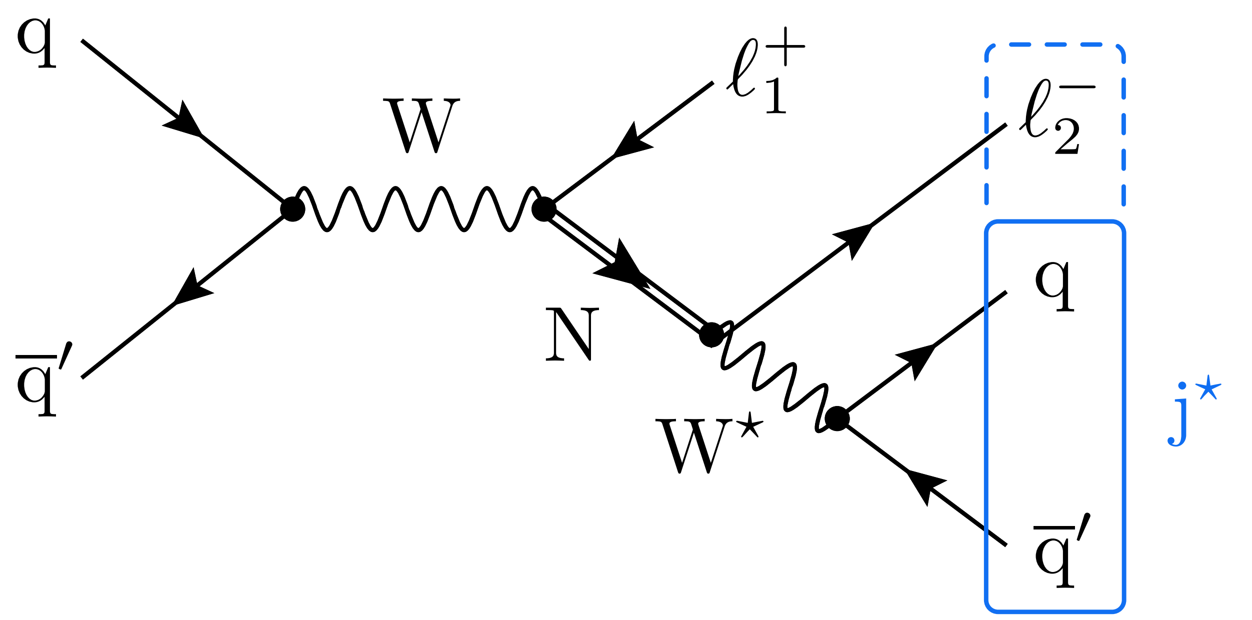

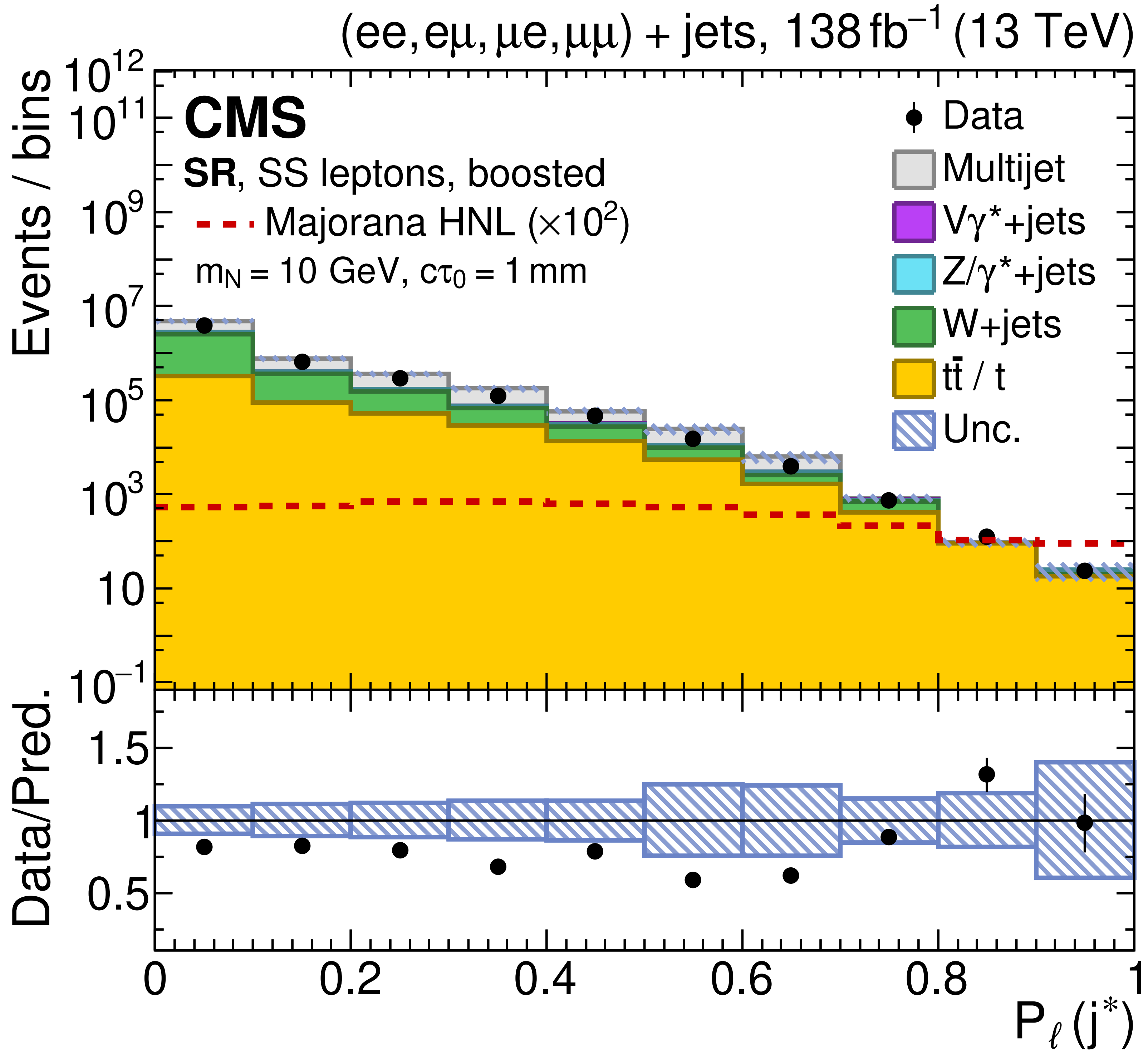

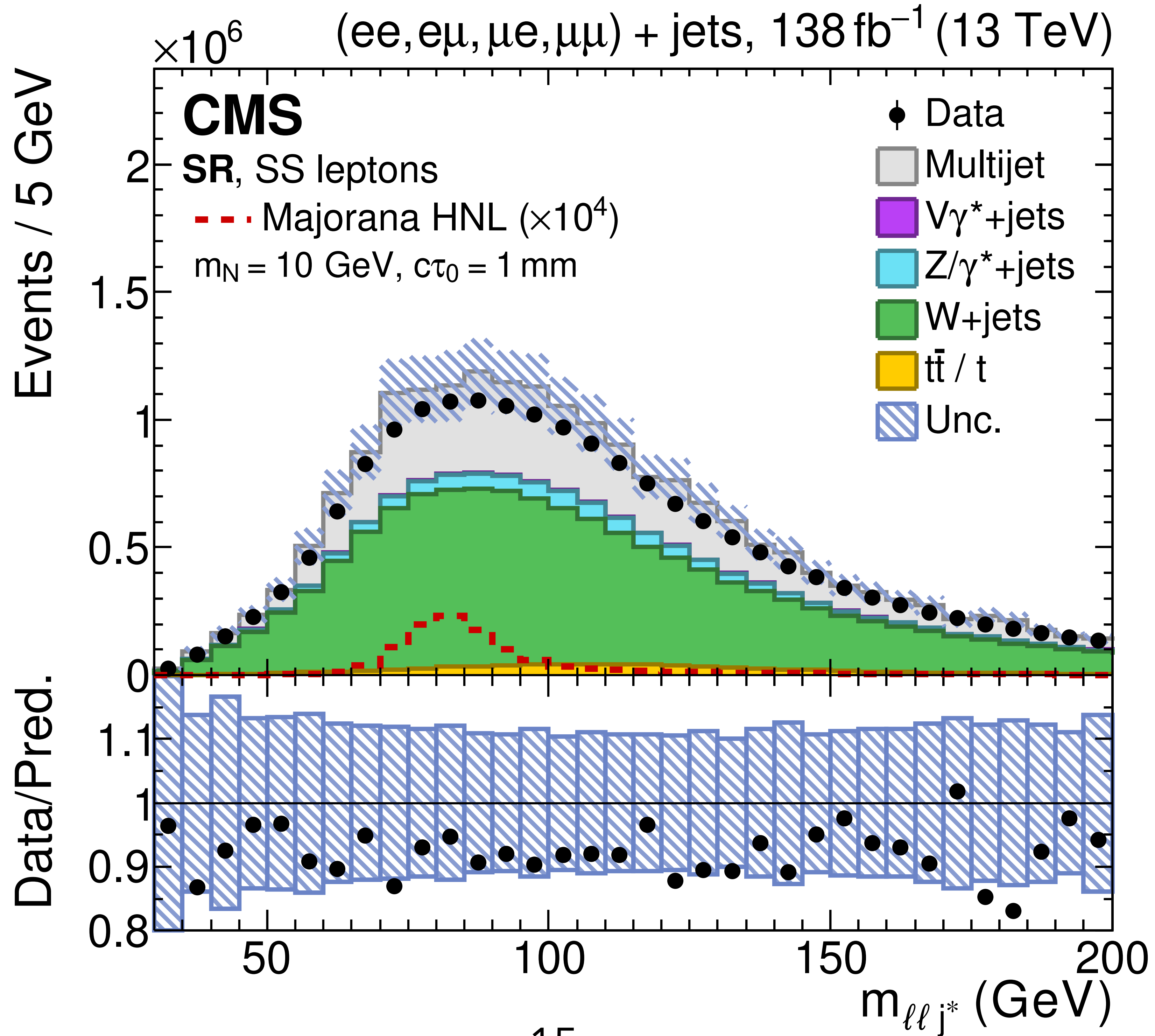

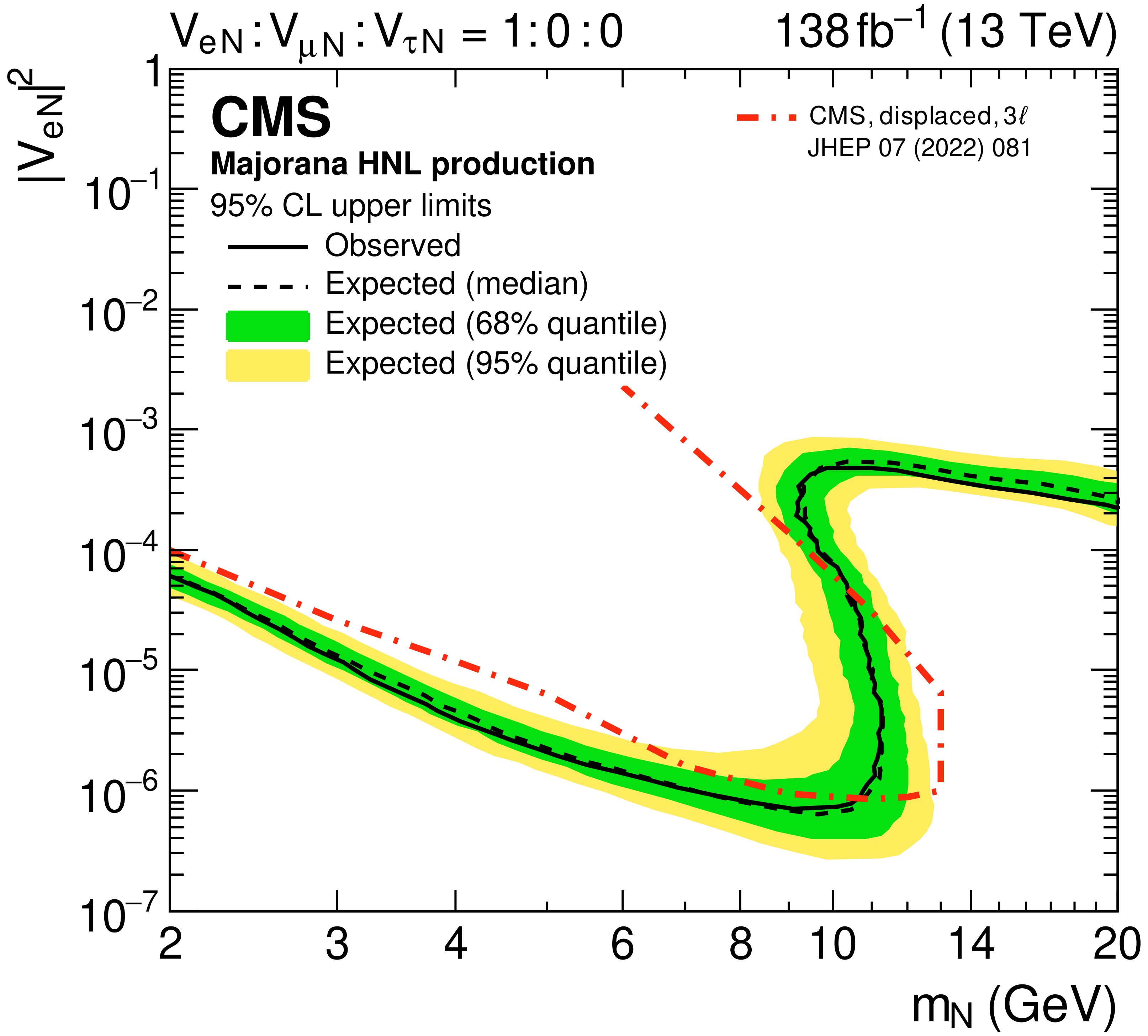

Low mass HNLs

2402.18658

To probe lower masses, CMS uses two novel search strategies which expand sensitivity to lower m_N

1. Search for HNLs decaying in the muon system

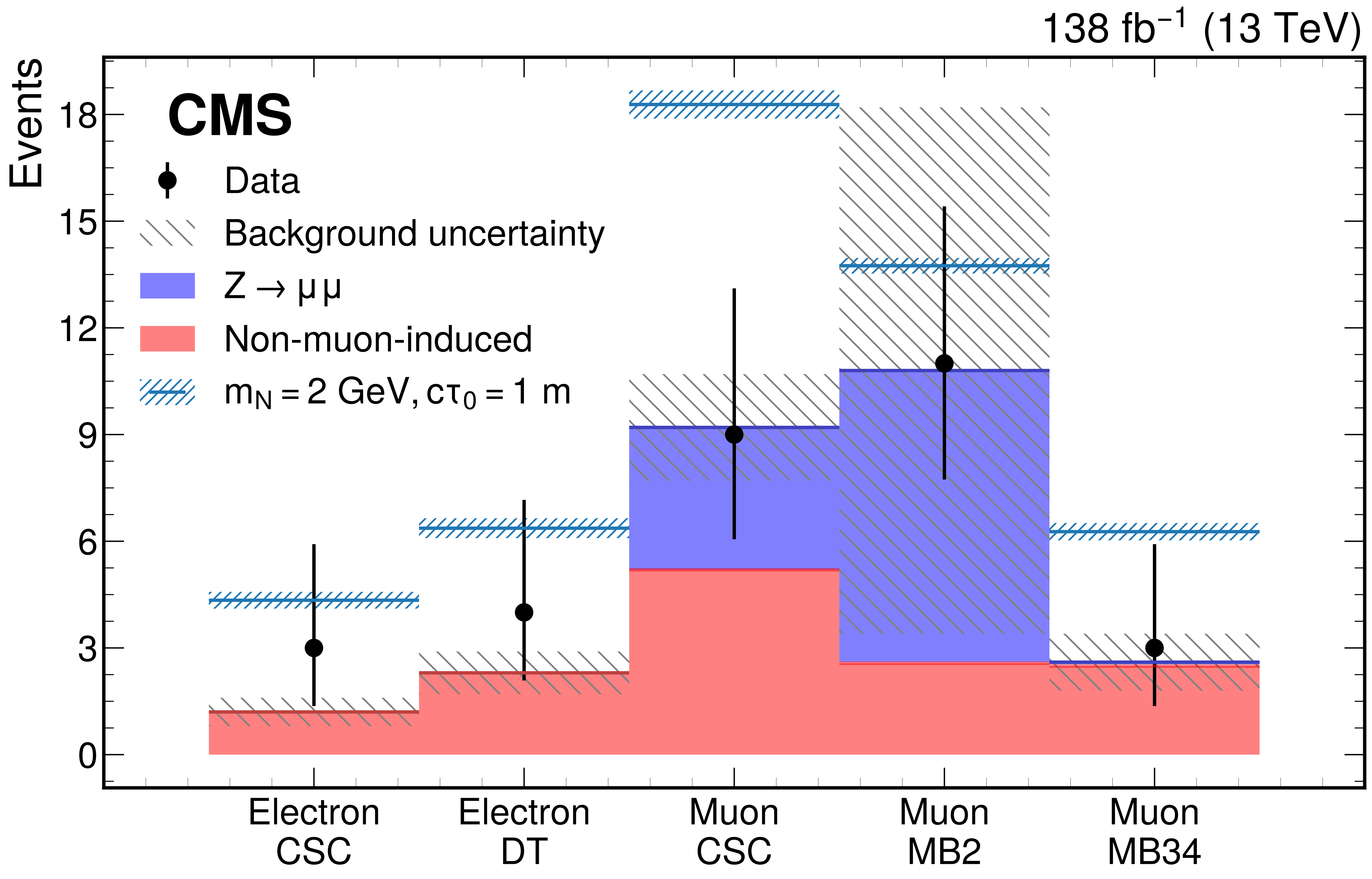

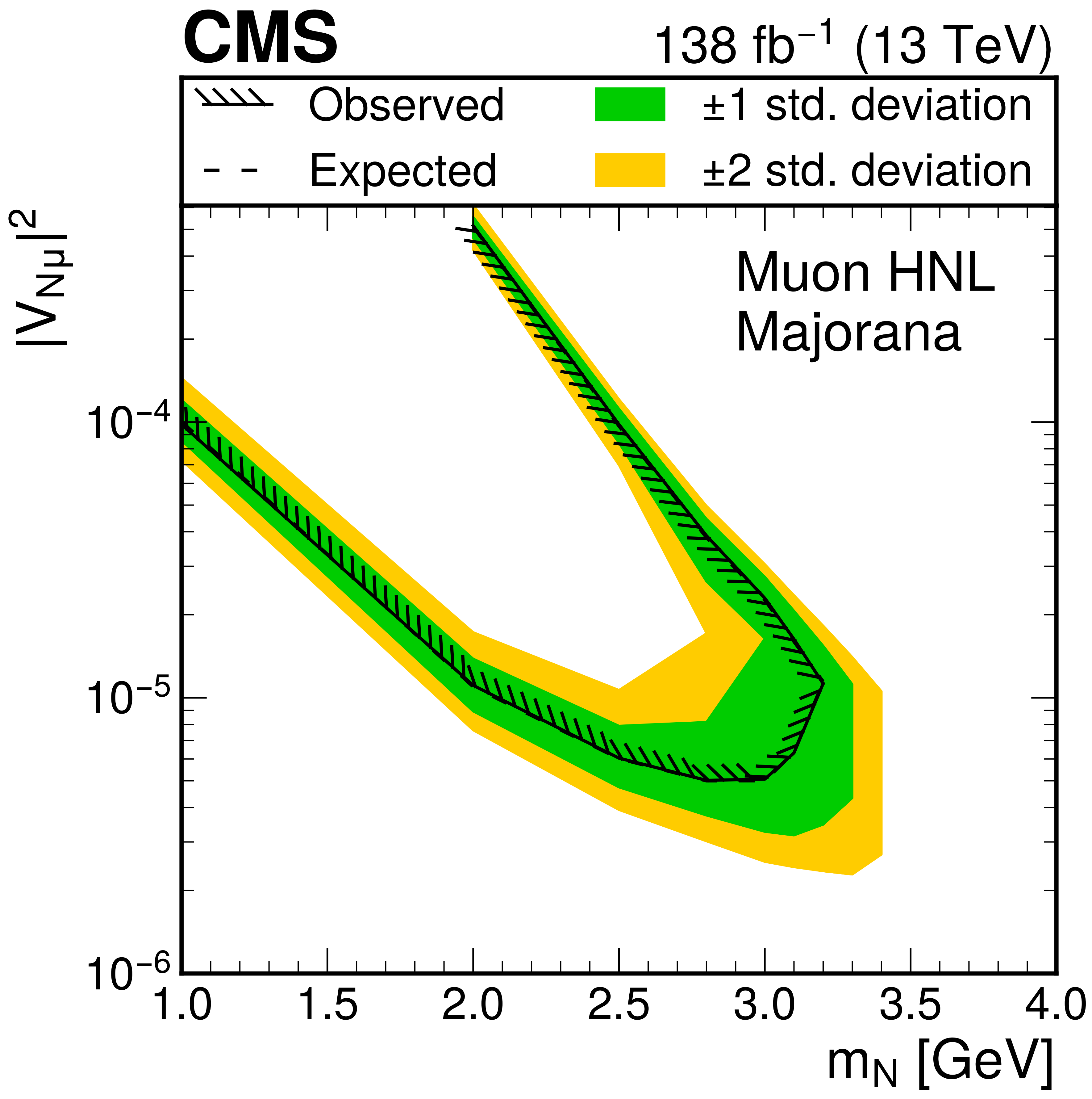

Low mass HNLs

2403.04584

To probe lower masses, CMS uses two novel search strategies which expand sensitivity to lower m_N

2. Search for HNLs produced in B-meson decays using B-parking data stream

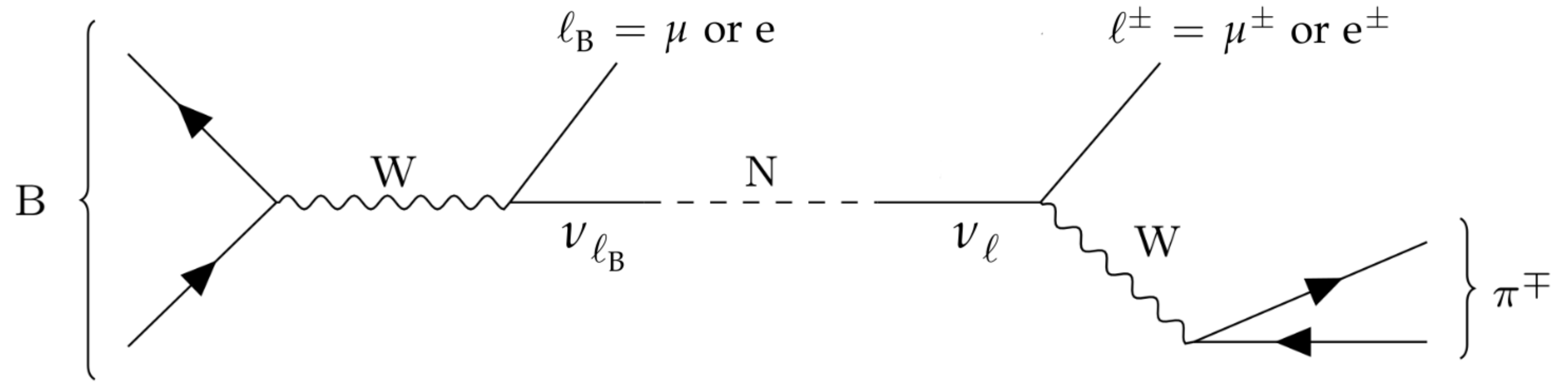

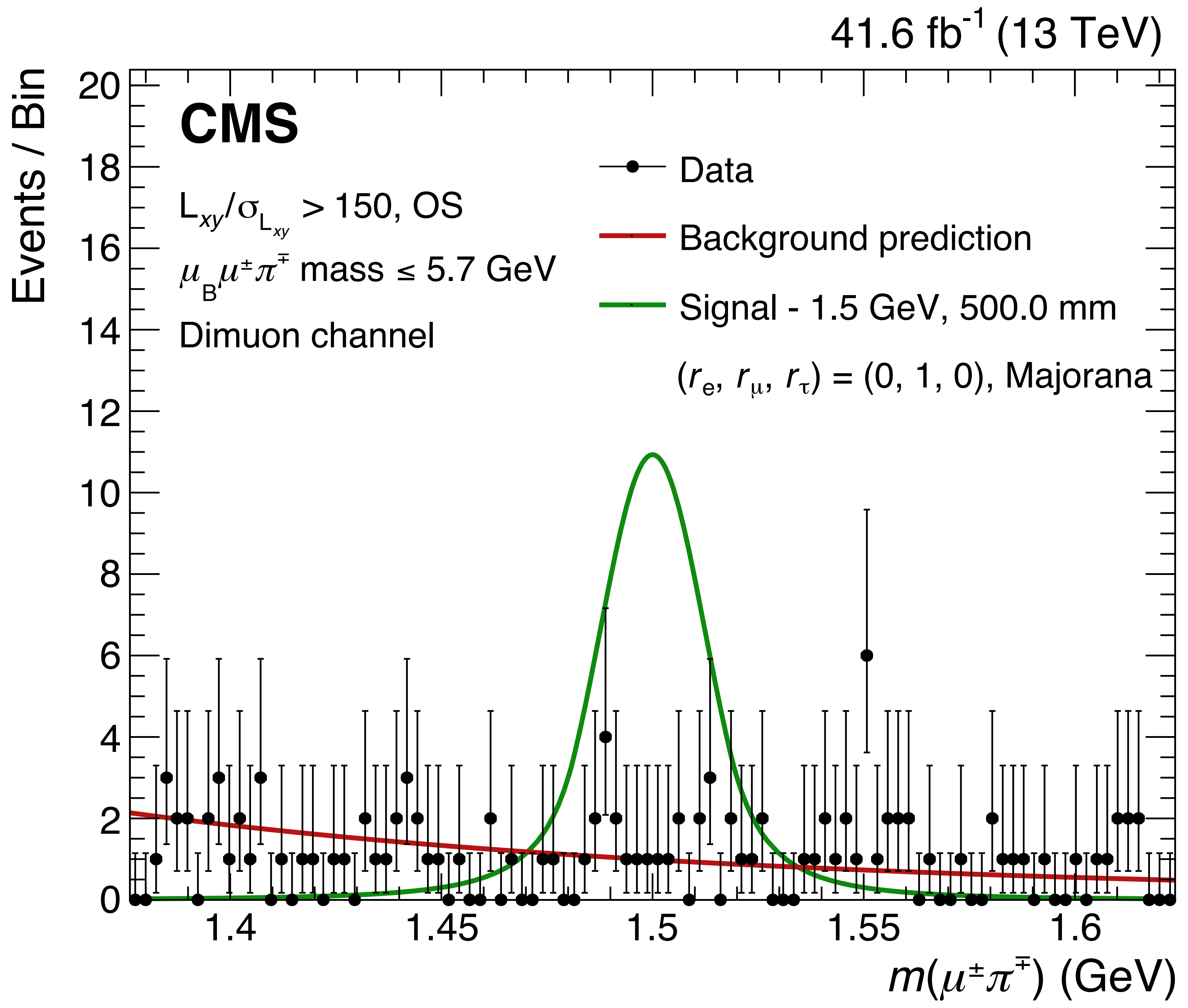

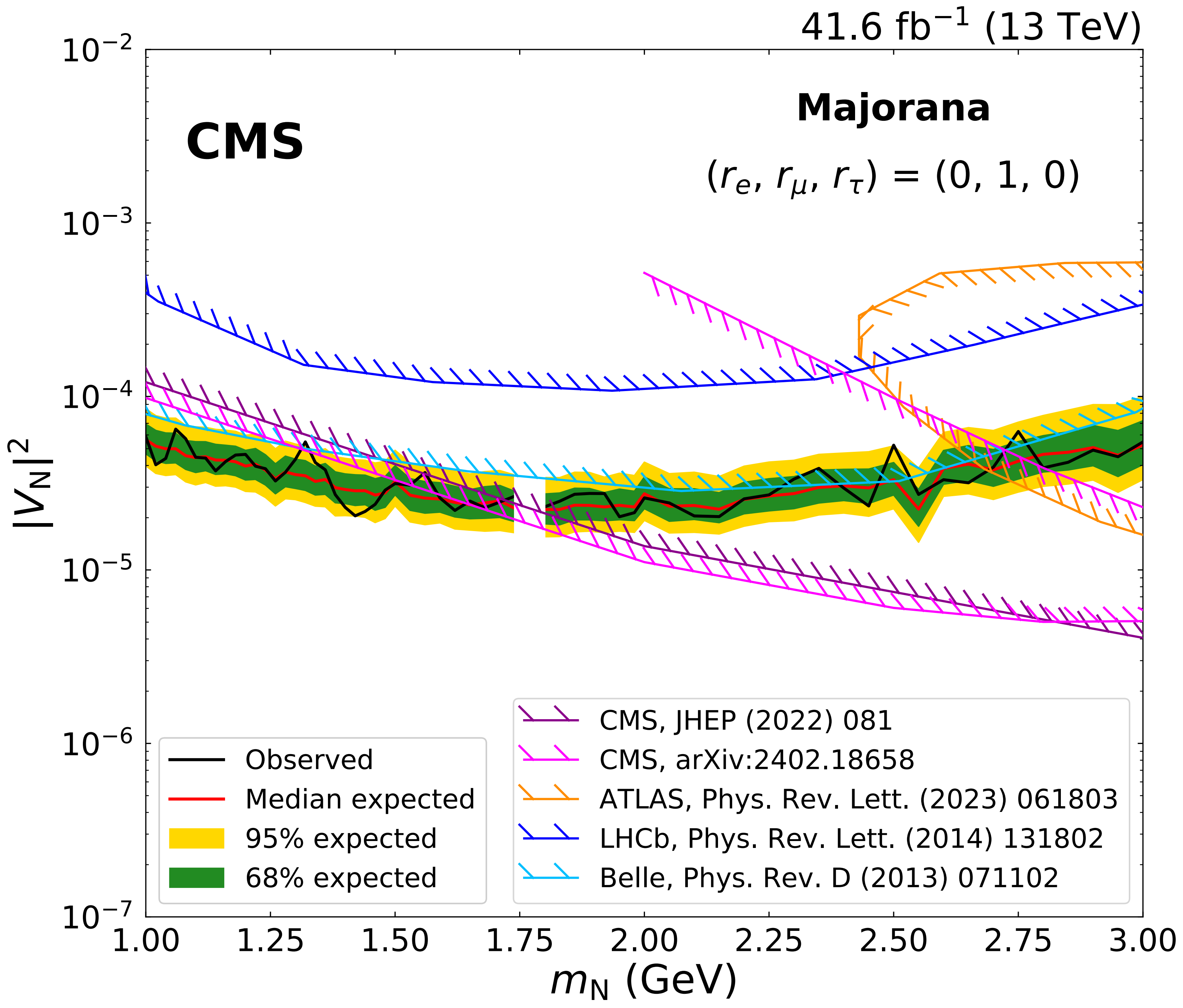

Current HNL landscape

Together these searches are considerably expanding our reach into unexplored phase space

Current HNL landscape

Together these searches are considerably expanding our reach into unexplored phase space

Run 3 prospects for HNLs

2312.14016

LHCb Run 3 projections give complementary sensitivity to ATLAS and CMS

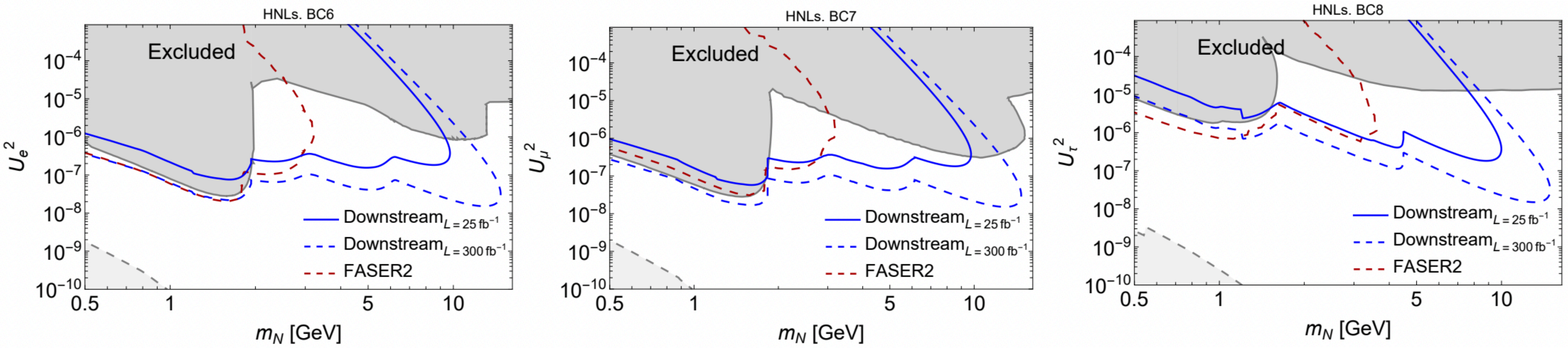

Run 3 prospects for HNLs

2312.14016

LHCb Run 3 projections give complementary sensitivity to ATLAS and CMS

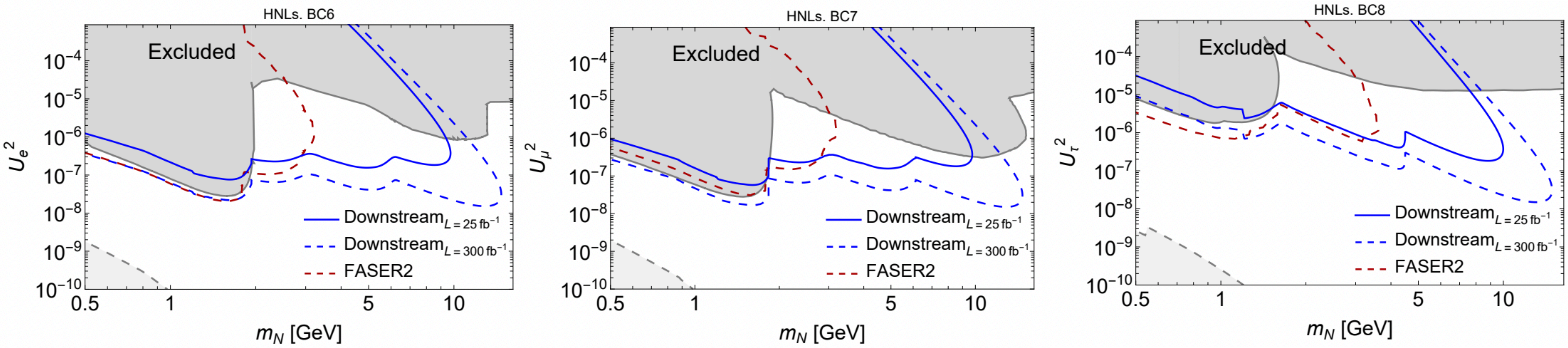

HNL models beyond the νMSM?

- e.g. "Scotogenic" models with extended $\mathbb{Z}_2$-odd scalar sector
- Potential connection to 95 GeV excess? [2306.03735]

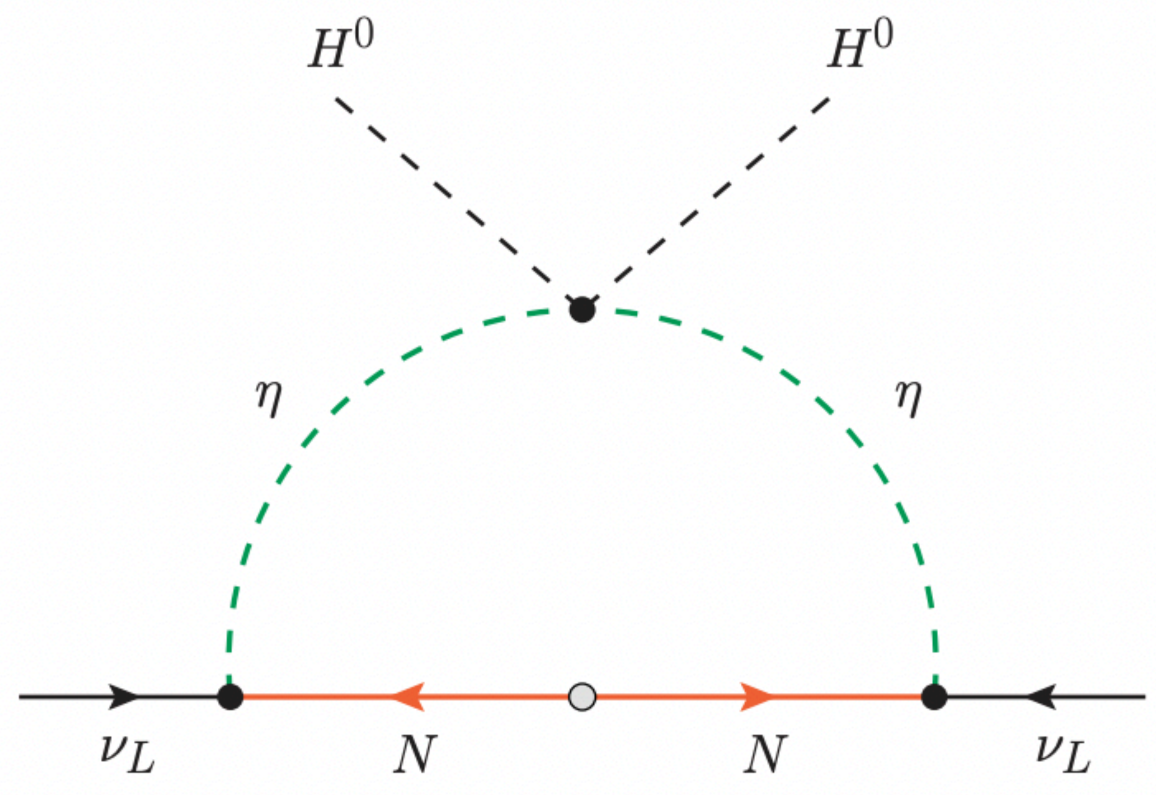

Outlook

Outlook

New techniques have significantly expanded the reach of ATLAS and CMS to Higgs portal LLP signatures

- New displaced jet triggers in CMS have enabled competitive sensitivity with only partial Run 3 dataset
- Improved displaced track reconstruction in ATLAS has revolutionized LLP search programme

Outlook

New techniques have significantly expanded the reach of ATLAS and CMS to Higgs portal LLP signatures

- New displaced jet triggers in CMS have enabled competitive sensitivity with only partial Run 3 dataset
- Improved displaced track reconstruction in ATLAS has revolutionized LLP search programme

Advancements in machine learning are enabling unprecedented sensitivity for exotic jet topologies

- e.g. graph neural networks for displaced and emerging jets

Outlook

New techniques have significantly expanded the reach of ATLAS and CMS to Higgs portal LLP signatures

- New displaced jet triggers in CMS have enabled competitive sensitivity with only partial Run 3 dataset
- Improved displaced track reconstruction in ATLAS has revolutionized LLP search programme

Advancements in machine learning are enabling unprecedented sensitivity for exotic jet topologies

- e.g. graph neural networks for displaced and emerging jets

Robust and wide-reaching HNL search program in ATLAS + CMS

- Beginning to probe channels beyond fully-leptonic final states and in new production modes

Outlook

New techniques have significantly expanded the reach of ATLAS and CMS to Higgs portal LLP signatures

- New displaced jet triggers in CMS have enabled competitive sensitivity with only partial Run 3 dataset
- Improved displaced track reconstruction in ATLAS has revolutionized LLP search programme

Advancements in machine learning are enabling unprecedented sensitivity for exotic jet topologies

- e.g. graph neural networks for displaced and emerging jets

Robust and wide-reaching HNL search program in ATLAS + CMS

- Beginning to probe channels beyond fully-leptonic final states and in new production modes

LHCb downstream tracking will add complementary sensitivity to ATLAS + CMS in Run 3

Outlook

New techniques have significantly expanded the reach of ATLAS and CMS to Higgs portal LLP signatures

- New displaced jet triggers in CMS have enabled competitive sensitivity with only partial Run 3 dataset
- Improved displaced track reconstruction in ATLAS has revolutionized LLP search programme

Advancements in machine learning are enabling unprecedented sensitivity for exotic jet topologies

- e.g. graph neural networks for displaced and emerging jets

Robust and wide-reaching HNL search program in ATLAS + CMS

- Beginning to probe channels beyond fully-leptonic final states and in new production modes

LHCb downstream tracking will add complementary sensitivity to ATLAS + CMS in Run 3

Run 3 will be an exciting time at the lifetime frontier!

Backup

Sandbox Studio/Symmetry Magazine

Hadronic vertices in ATLAS

Vertex reconstruction efficiency for different models

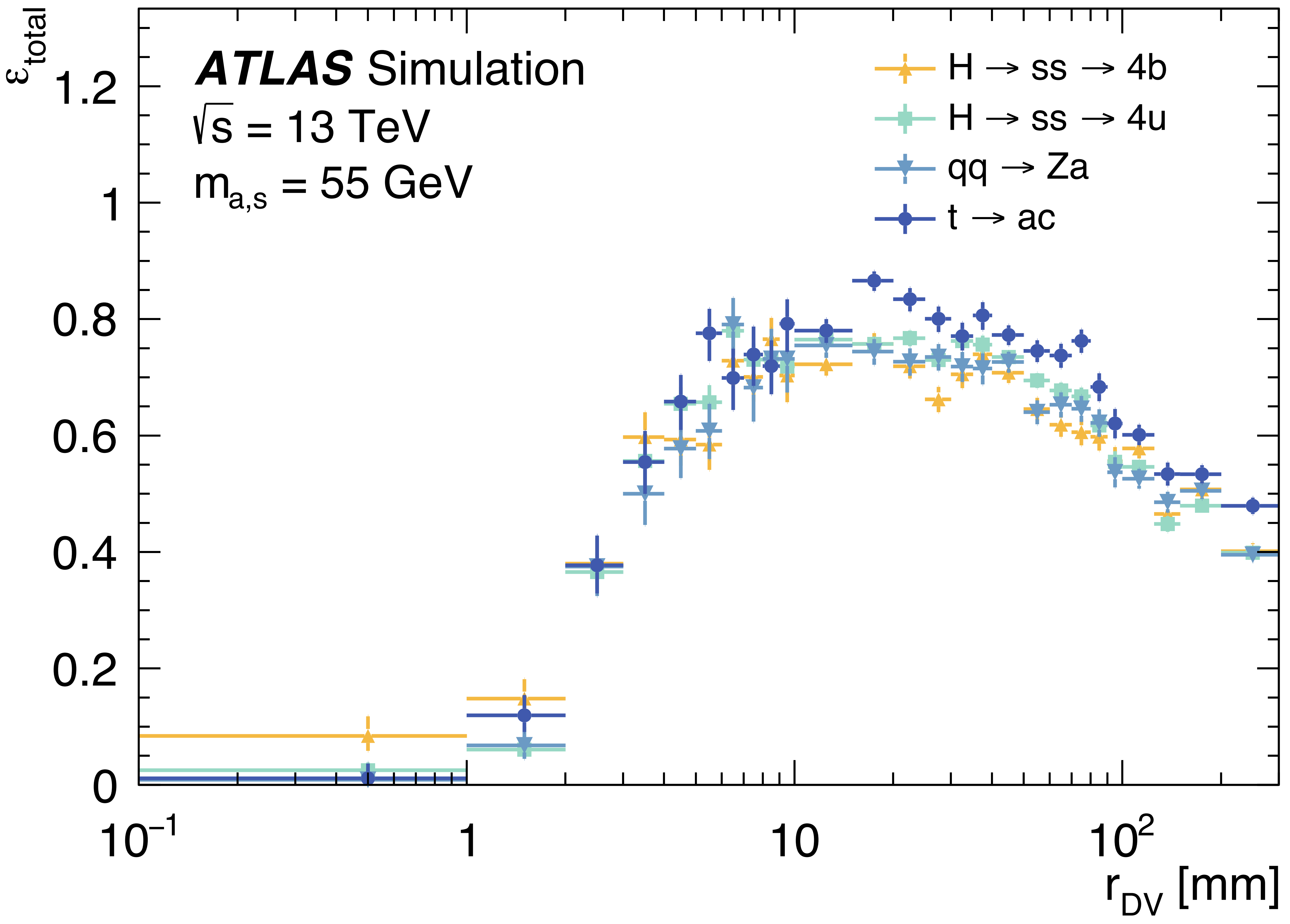

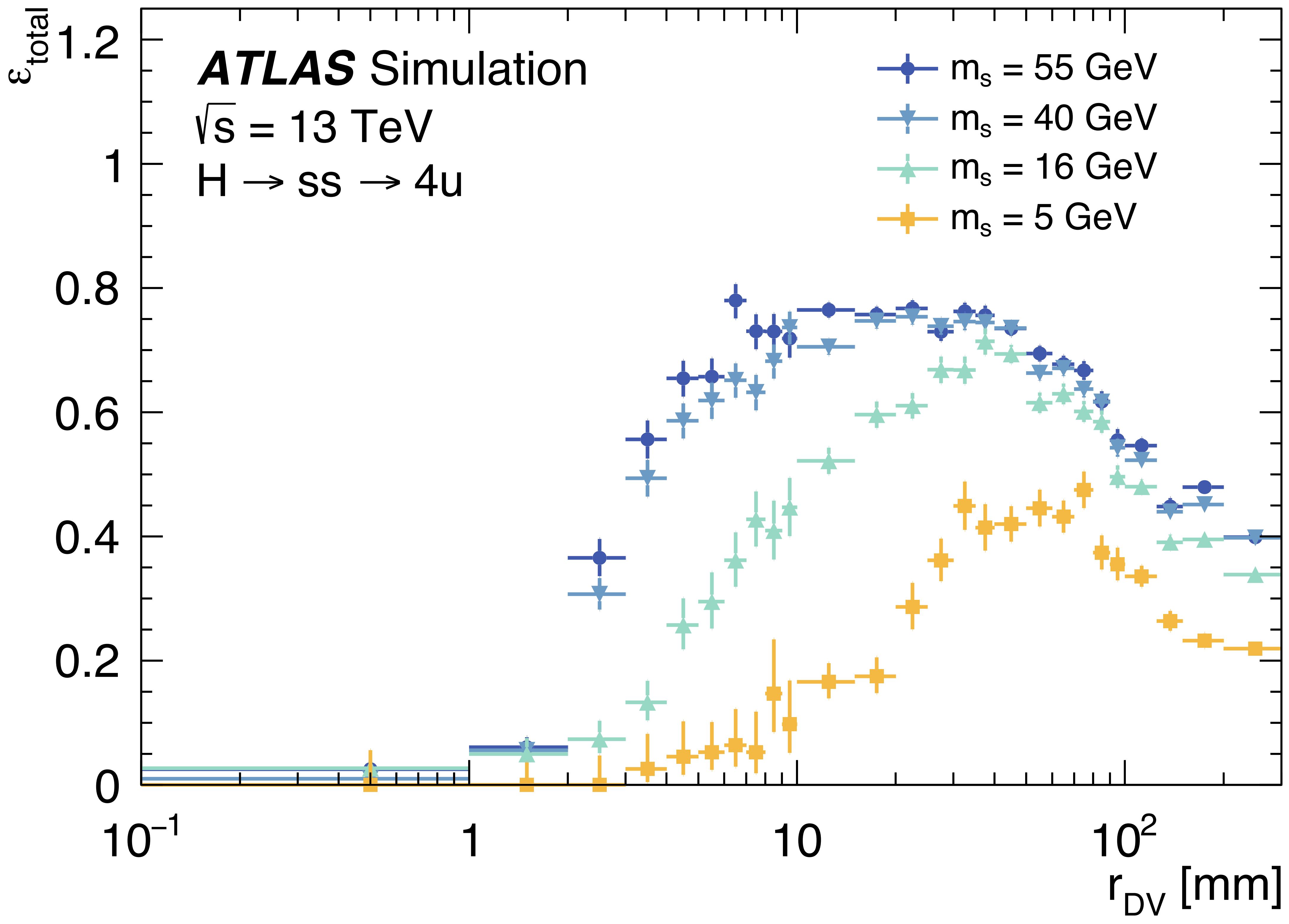

Hadronic vertices in ATLAS

Background estimate validated in CRs with intermediate event-level discriminant values and dedicated γ+jets region

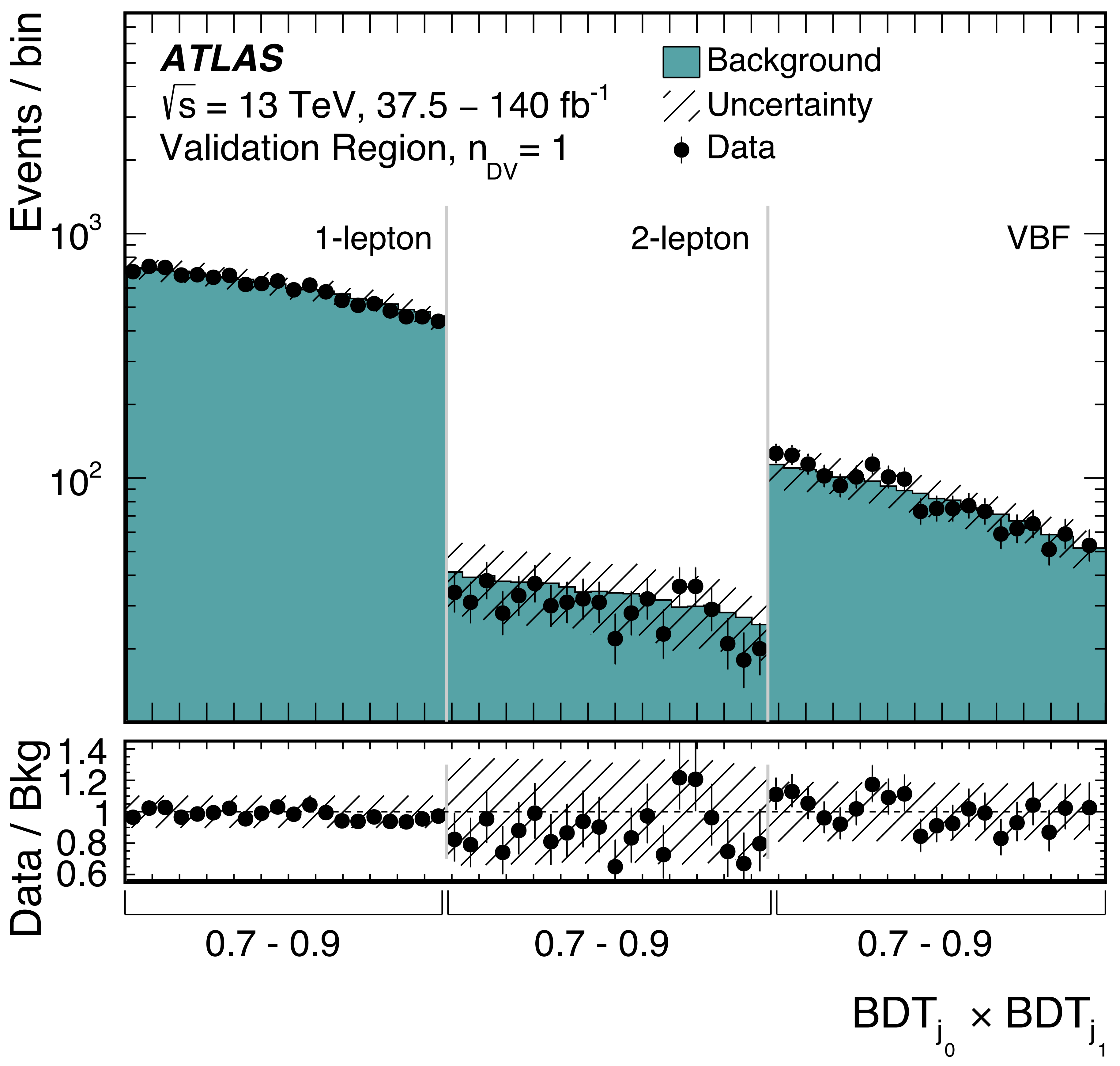

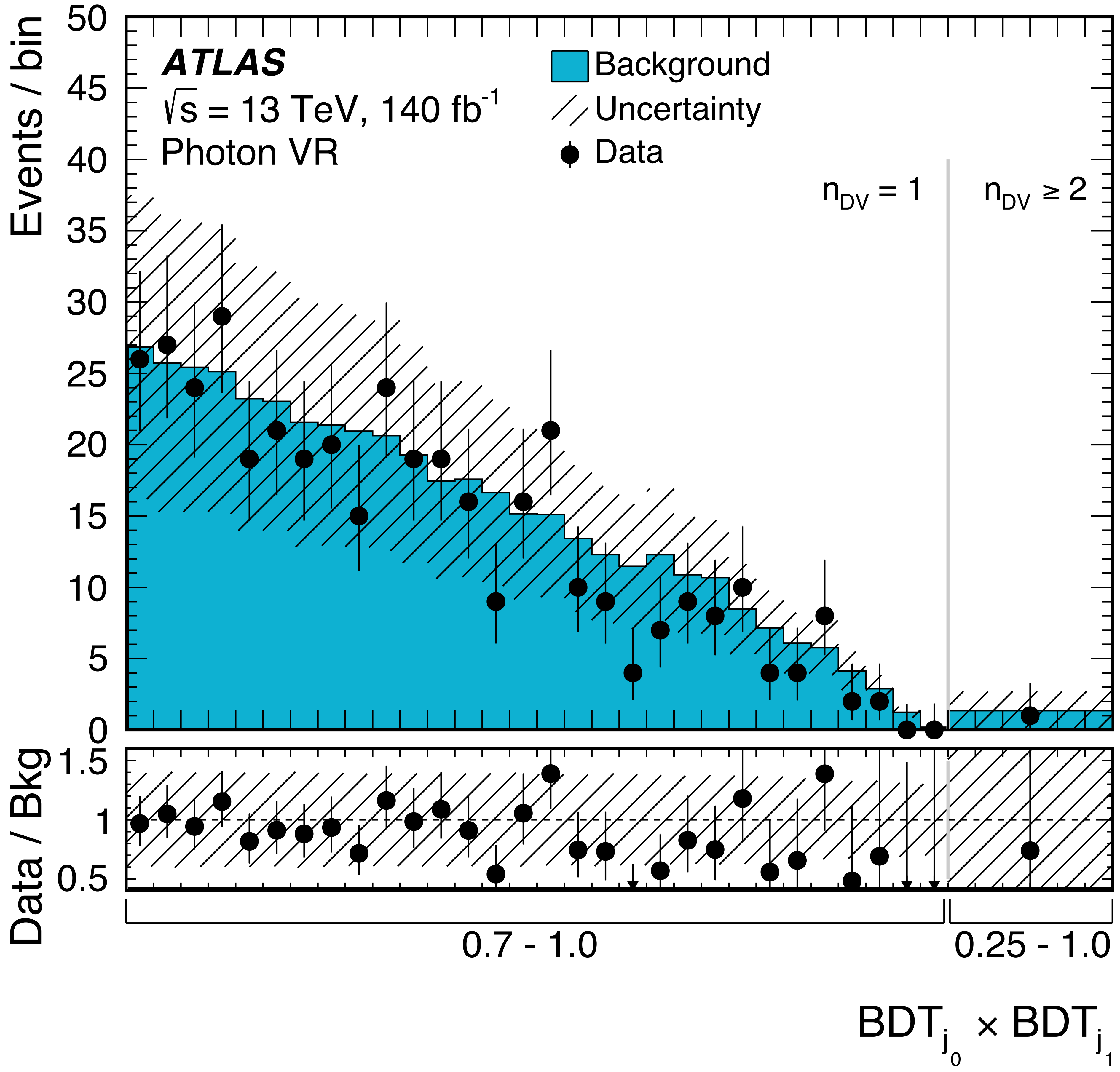

Hadronic vertices in ATLAS

Excluded regions for $\mathrm{Br}(H \to ss) = 10\,\%$

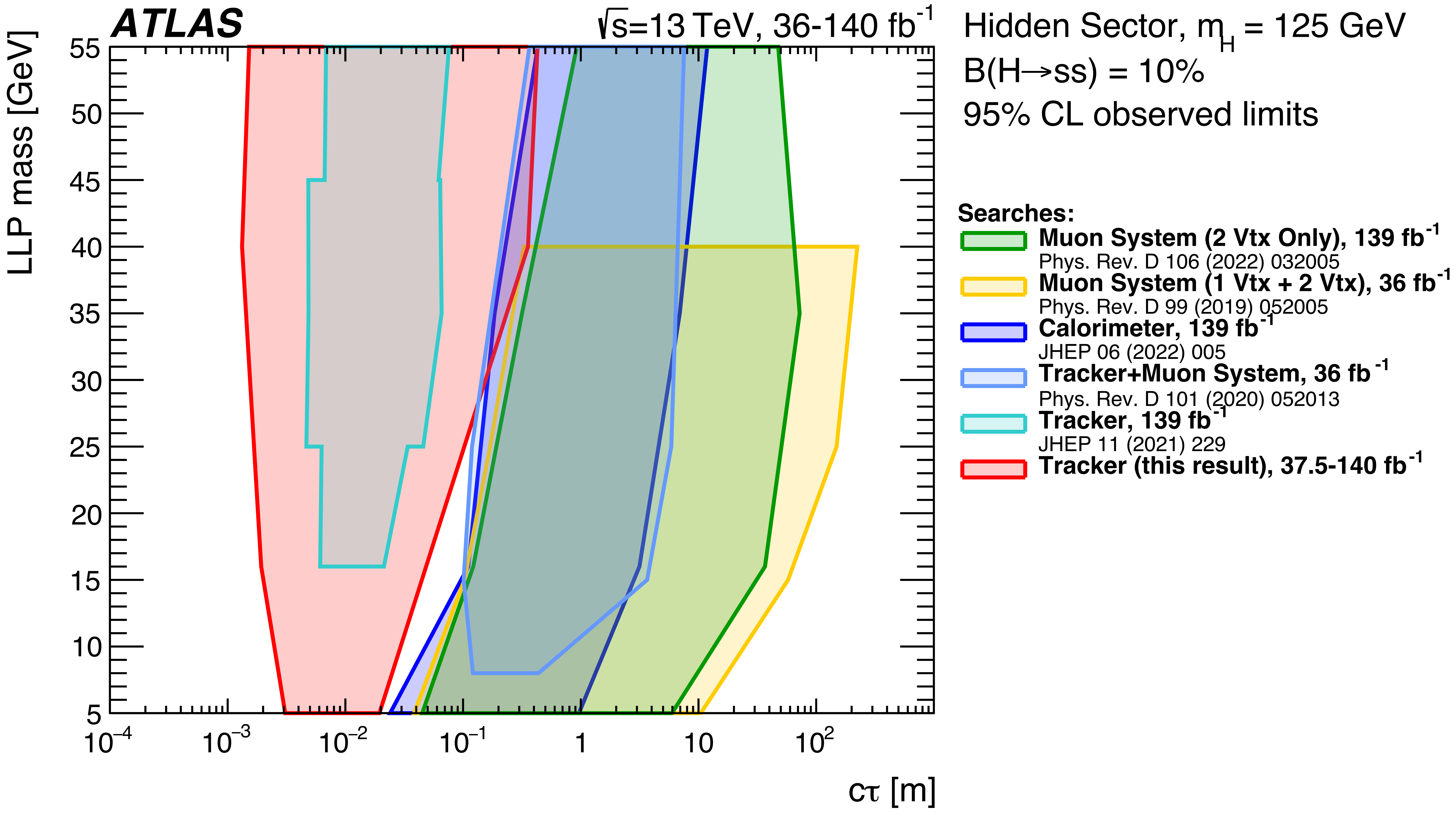

Hadronic vertices in ATLAS

Exclusion limits on $\mathrm{Br}(H \to ss)$

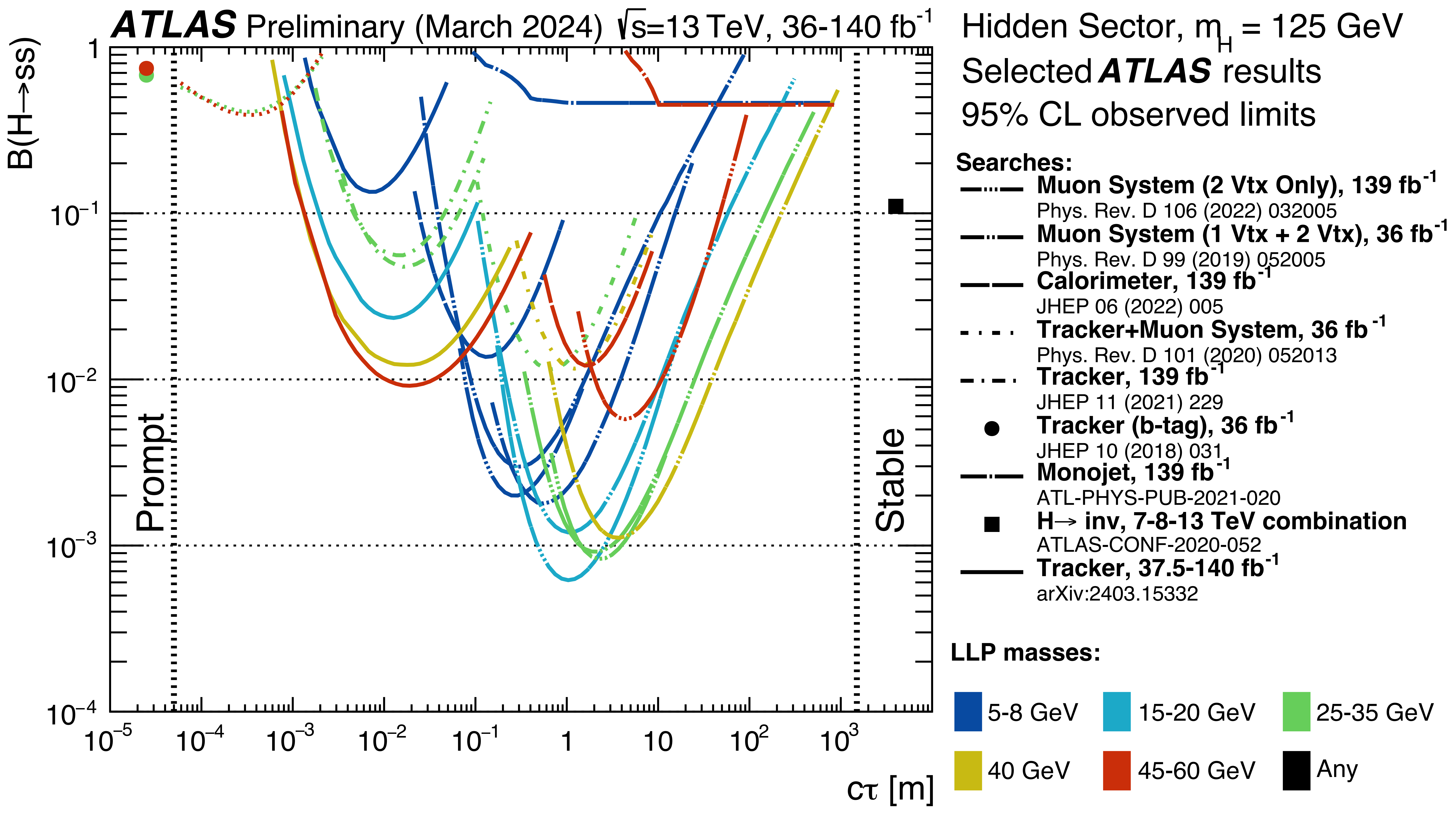

Hadronic vertices in CMS

Comparison to previous CMS results

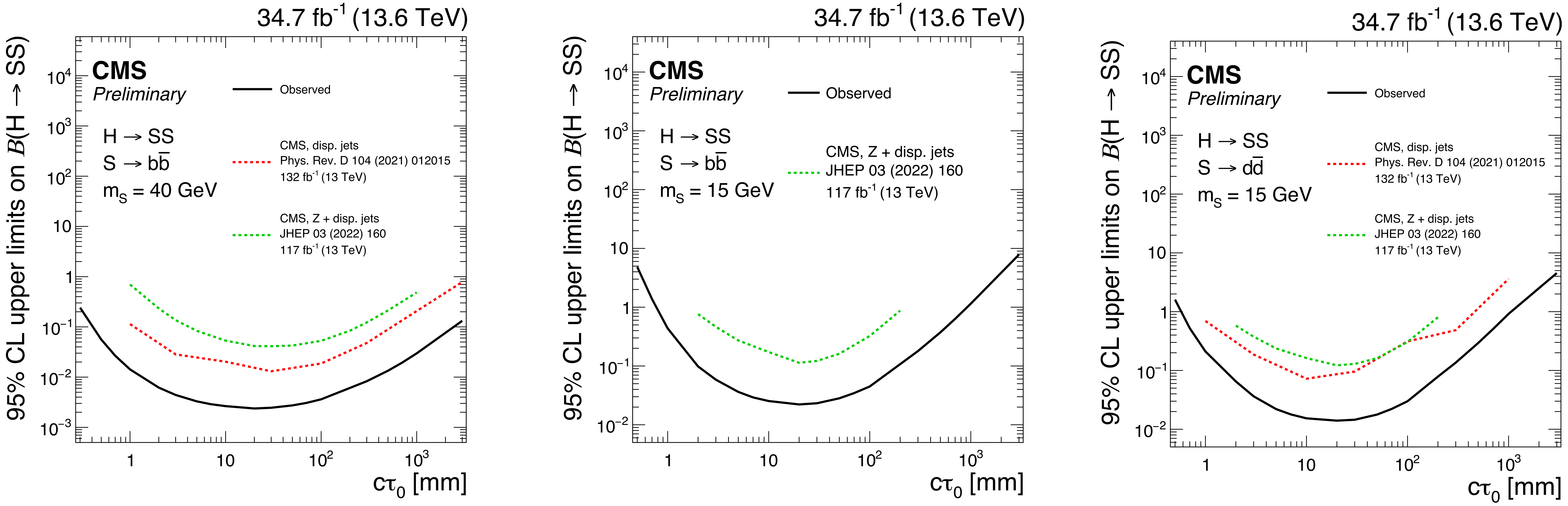

Hadronic vertices in CMS

Model independent limits on m_s and $c\tau_s$ for $\mathrm{Br}(H \to ss) = 1\,\%$

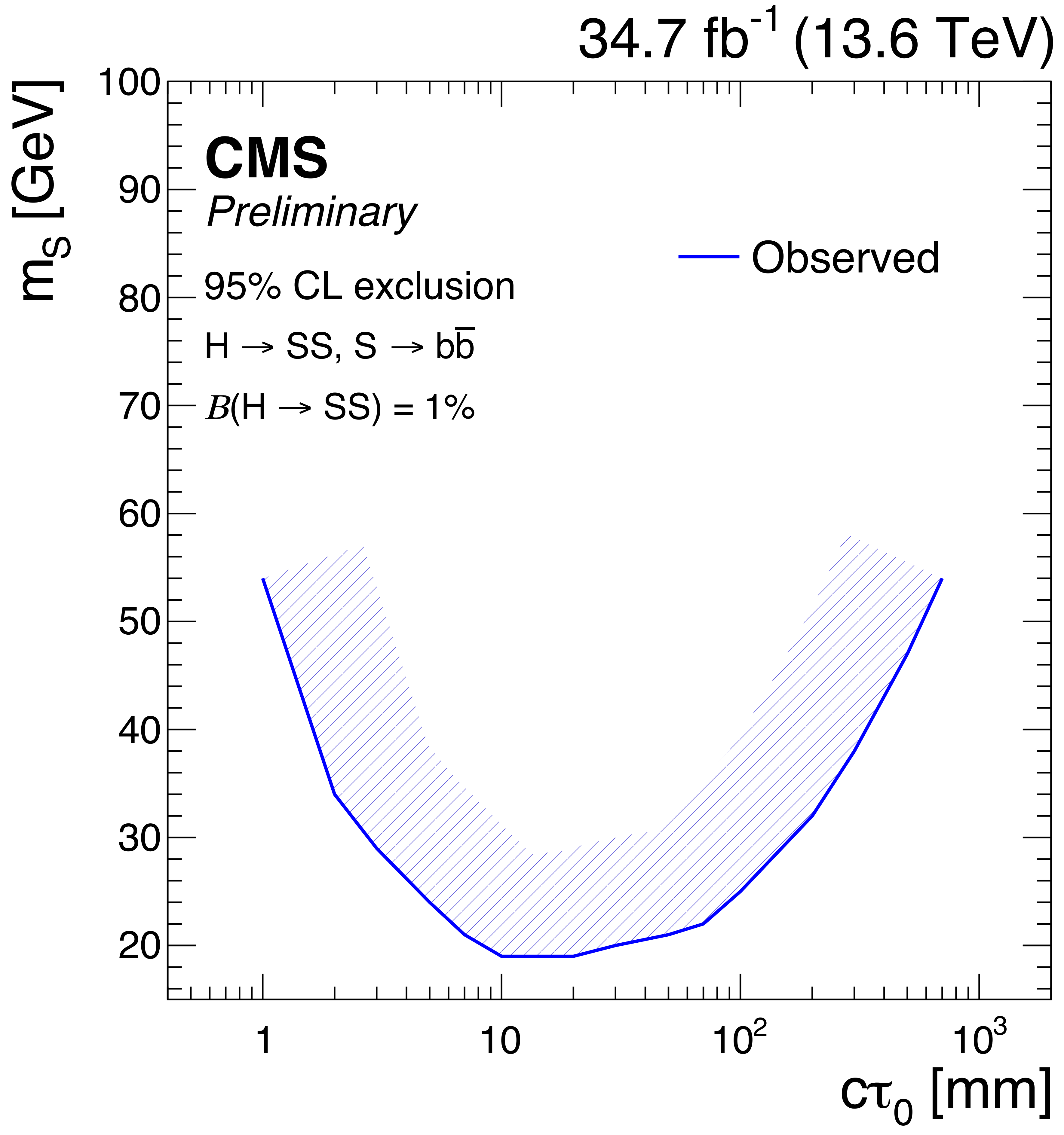

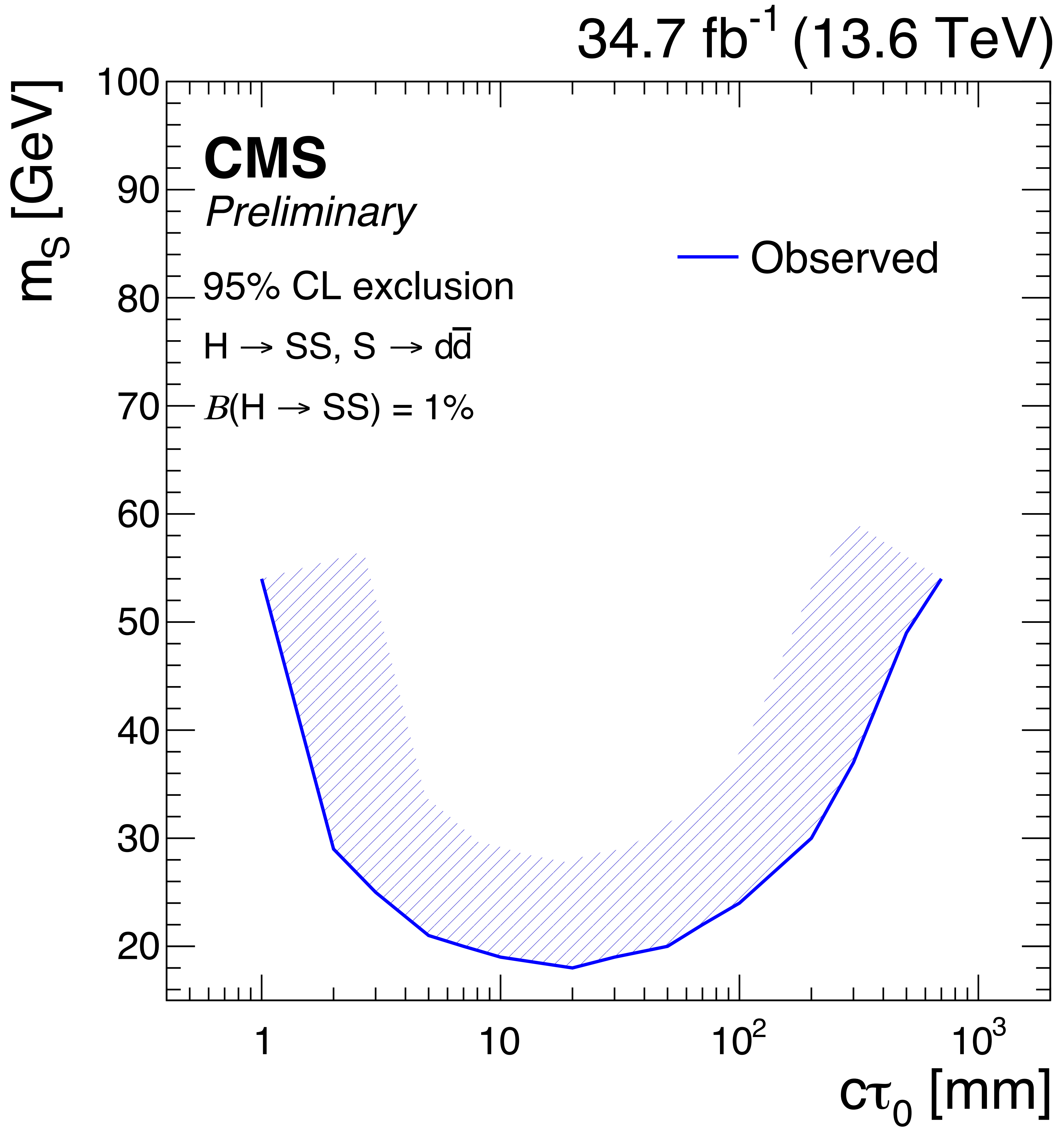

Hadronic vertices in CMS

Split SUSY and fraternal Twin Higgs limits

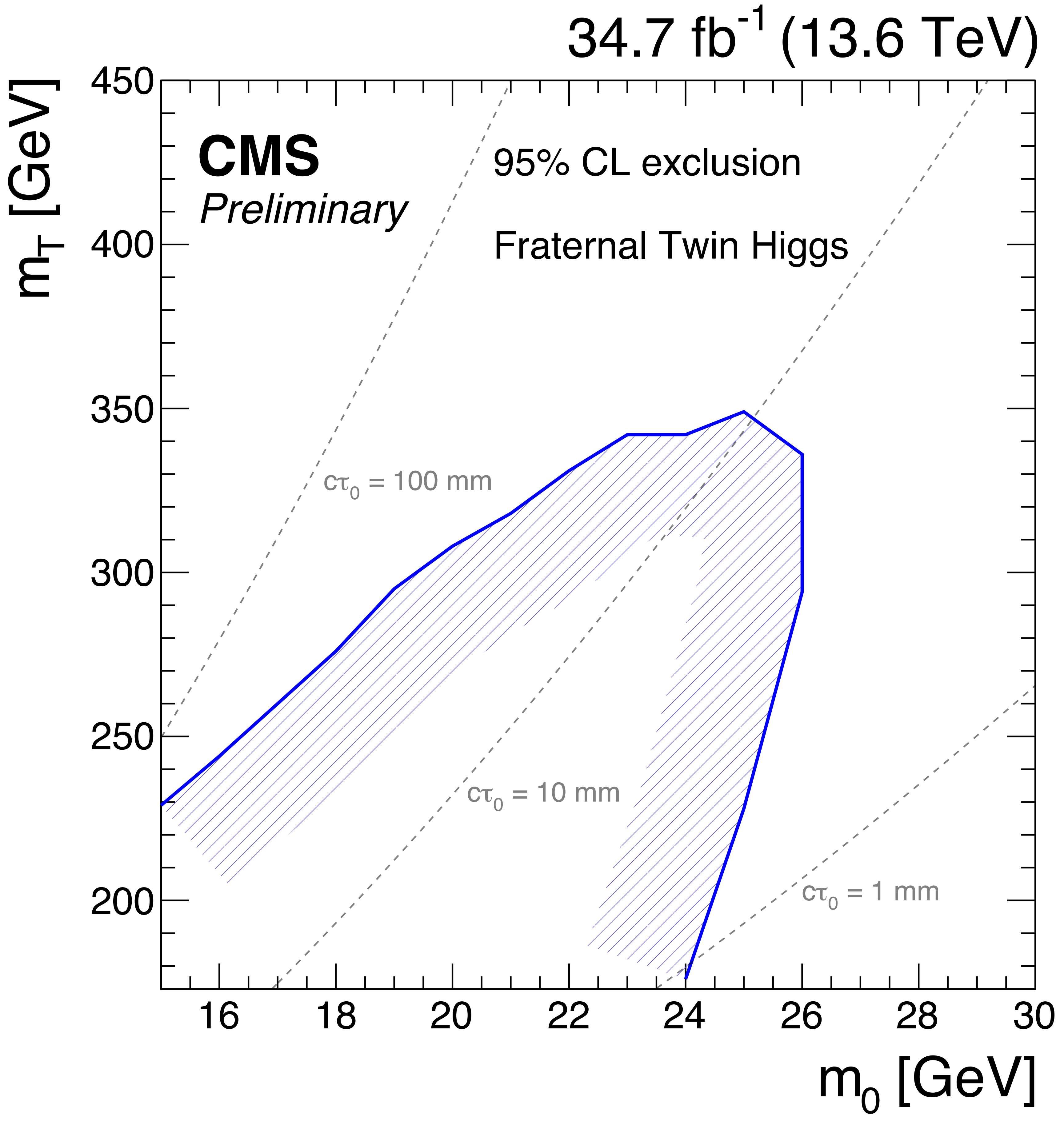

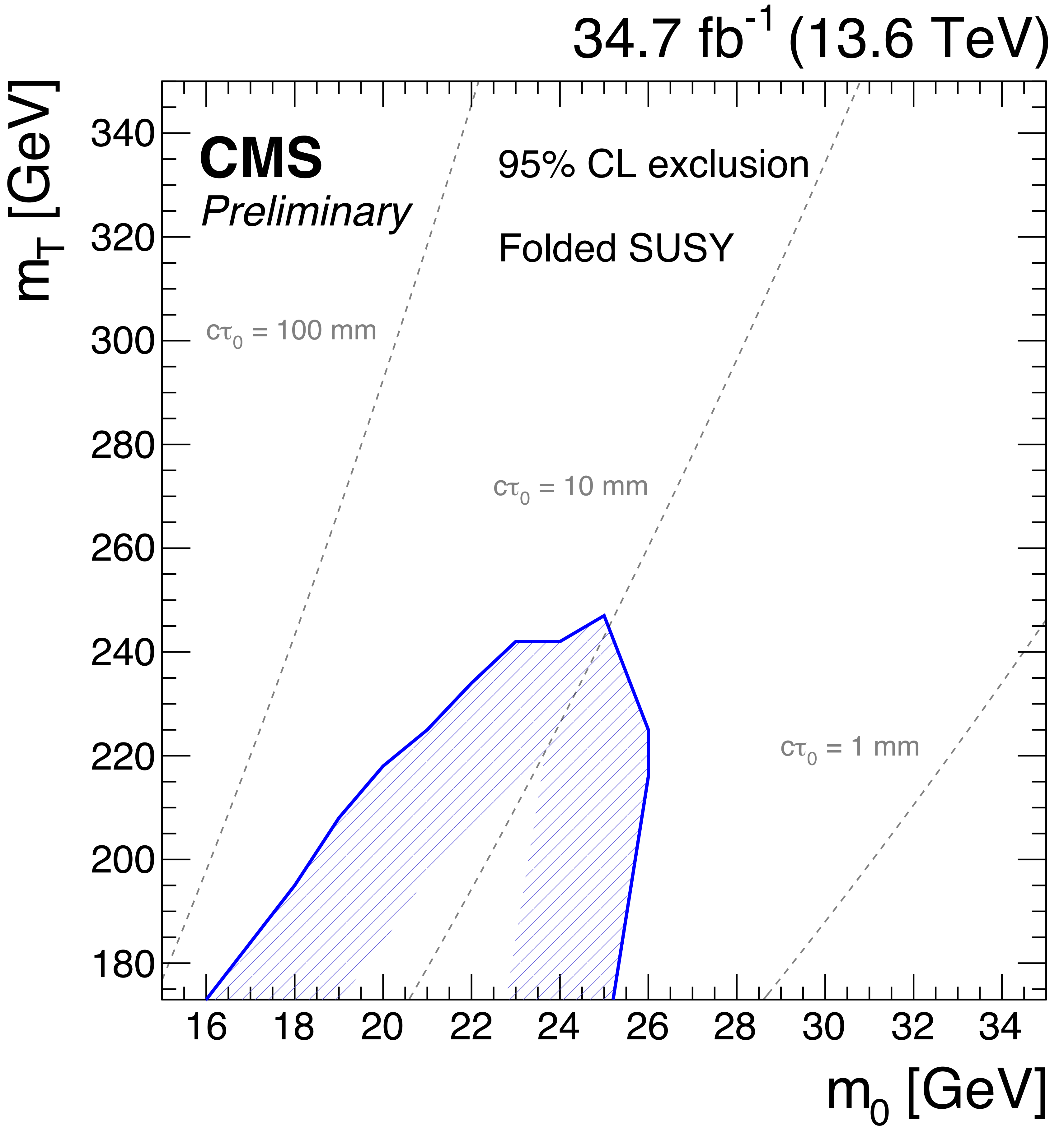

Emerging jets in CMS

Model parameters

$$c\tau_{\pi_{\rm dark}} = 80\,\text{mm} \left(\frac{1}{\kappa^4}\right)\left(\frac{2\,\text{GeV}}{f_{\pi_{\rm dark}}}\right)^2\left(\frac{100\,\text{MeV}}{m_{\rm d}}\right)^2\left(\frac{2\,\text{GeV}}{m_{\pi_{\rm dark}}}\right)\left(\frac{m_{X_{\rm dark}}}{1\,\text{TeV}}\right)^4, \quad (1)$$

$$c\tau^{\alpha\beta}_{\pi_{\rm dark}} = \frac{8\pi m^4_{X_{\rm dark}}}{N_c m_{\pi_{\rm dark}} f^2_{\pi_{\rm dark}} \sum_{i,j} |\kappa_{\alpha i}\kappa^*_{\beta j}|^2 \left(m_i^2 + m_j^2\right)\sqrt{\left(1 - \frac{(m_i+m_j)^2}{m^2_{\pi_{\rm dark}}}\right)\left(1 - \frac{(m_i-m_j)^2}{m^2_{\pi_{\rm dark}}}\right)}}, \quad (2)$$

Model parameter	List of values
$m_{X_{\rm dark}}$ [GeV]	1000, 1200, 1400, 1500, 1600, 1800, 2000, 2200, 2400, 2500
$m_{\pi_{\rm dark}}$ [GeV]	10, 20
$c\tau_{\pi_{\rm dark}}$ [mm]	1, 2, 5, 25, 45, 60, 100, 150, 225, 300, 500, 1000

$m_{X_{\rm dark}}$ [GeV]	$m_{\pi_{\rm dark}}$ [GeV]	κ_0 value				
	6	0.92	0.61	0.53	0.43	0.29
1000	10	0.62	0.42	0.36	0.30	0.20
	20	0.37	0.25	0.21	0.18	0.12
	6	1.10	0.73	0.63	0.52	0.35
1200	10	0.75	0.50	0.43	0.35	0.24
	20	0.45	0.30	0.26	0.21	0.14
	6	1.28	0.86	0.74	0.61	0.41
1400	10	0.87	0.58	0.50	0.41	0.28
	20	0.52	0.35	0.30	0.25	0.16
	6	1.47	0.98	0.85	0.69	0.46
1600	10	1.00	0.67	0.58	0.47	0.32
	20	0.59	0.40	0.34	0.28	0.19
	6	1.65	1.10	0.95	0.78	0.52
1800	10	1.12	0.75	0.65	0.53	0.36
	20	0.67	0.45	0.39	0.32	0.21
	6	1.83	1.23	1.06	0.87	0.58
2000	10	1.25	0.84	0.72	0.59	0.40
	20	0.74	0.50	0.43	0.35	0.23
	6	2.02	1.35	1.16	0.95	0.64
2200	10	1.37	0.92	0.79	0.65	0.43
	20	0.82	0.55	0.47	0.39	0.26
	6	2.20	1.47	1.27	1.04	0.70
2400	10	1.50	1.00	0.87	0.71	0.47
	20	0.89	0.60	0.51	0.42	0.28
	6	2.29	1.53	1.32	1.08	0.72
2500	10	1.56	1.04	0.90	0.74	0.49
	20	0.93	0.62	0.54	0.44	0.29

Emerging jets in CMS

Background estimated by applying EJ mistag rate to jets in CR with exactly one EJ candidate

$$N_{SR} = \sum_{\text{events} \in \text{CR}} \frac{\frac{1}{2!}\left(\sum_i \epsilon_i \prod_{j \neq i}(1-\epsilon_j)\right) + \frac{1}{3!}\left(\sum_{i \neq j} \epsilon_i \epsilon_j \prod_{k \neq i,j}(1-\epsilon_k)\right) + \frac{1}{4!}\left(\sum_{i \neq j \neq k} \epsilon_i \epsilon_j \epsilon_k\right)}{\prod_i (1-\epsilon_i)}, \quad (4)$$

$$\epsilon^{\text{avg}}(p_T) = F_b^{CR}\epsilon(b, p_T) + \left(1 - F_b^{CR}\right)\epsilon(q, p_T).$$

Mistag rate computed in γ+jets events; flavour fraction computed by fitting DeepJet output

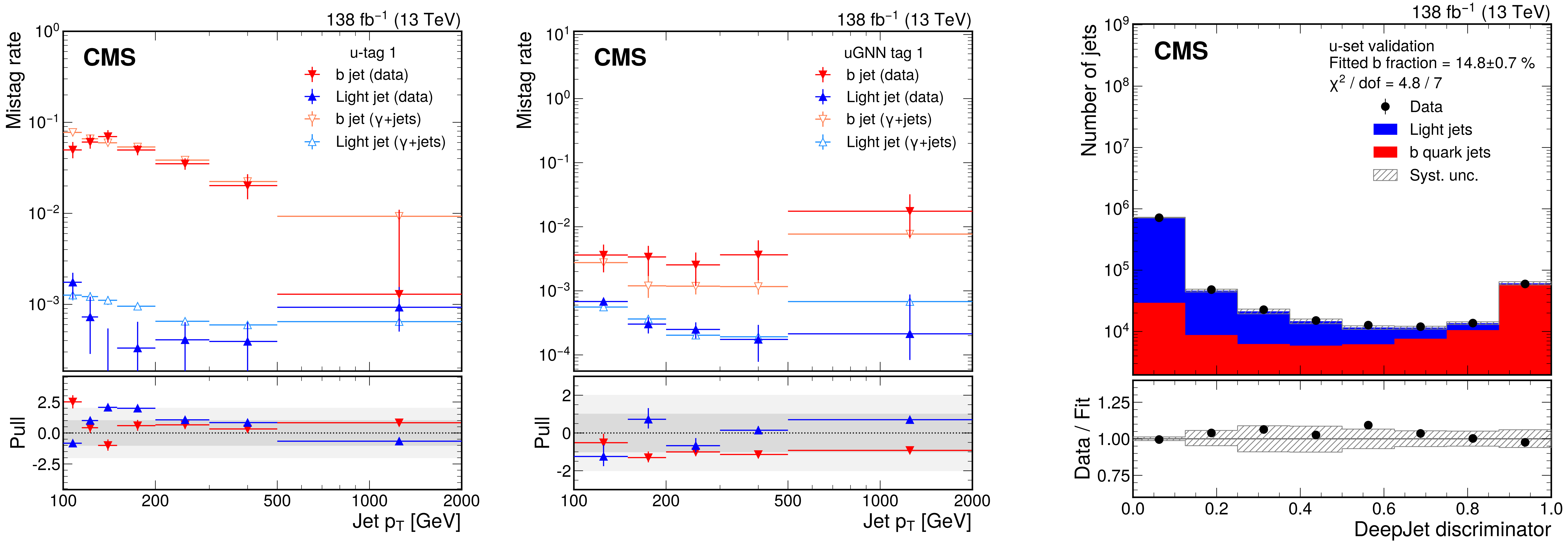

Emerging jets in CMS

Region definitions and observed yields

Selection set	H_T [GeV]	Jet p_T [GeV] (>)				EJ tagger
u-set 1	>1600	275	250	250	150	u-tag 1
u-set 2	>1600	200	200	150	150	u-tag 2
u-set 3	>1600	200	150	100	100	u-tag 3
u-set 4	>1500	200	150	100	100	u-tag 4
u-set 5	>1200	200	150	100	100	u-tag 5
u-set validation	1000–1200	100	100	100	100	validation u-tag
a-set 1	>1500	200	150	100	100	a-tag 1
a-set 2	>1800	250	250	200	200	a-tag 2
a-set 3	>1200	275	250	250	200	a-tag 2
a-set 4	>1500	275	250	250	100	a-tag 3
a-set 5	>1800	200	150	100	100	a-tag 4
a-set validation	1000–1200	100	100	100	100	validation a-tag
uGNN set 1	>1350	170	120	120	100	uGNN tag 1
uGNN set 2	>1750	300	260	250	250	uGNN tag 2
uGNN set 3	>1800	240	180	180	100	uGNN tag 3
uGNN validation	>1000	100	100	100	100	uGNN validation tag
aGNN set 1	>1300	200	140	120	100	aGNN tag 1
aGNN set 2	>1650	300	250	200	200	aGNN tag 2
aGNN set 3	>1400	270	220	220	120	aGNN tag 3
aGNN validation	>1000	100	100	100	100	aGNN validation tag

Selection set	Estimation ± stat. ± syst.	Observed yield
u-set 1	$56\ ^{+9}_{-5} \pm 20$	67
u-set 2	$20.0\ ^{+4.3}_{-2.5} \pm 7.0$	21
u-set 3	$22.9\ ^{+7.3}_{-2.1} \pm 4.9$	24
u-set 4	$7.9\ ^{+2.0}_{-1.6} \pm 2.2$	10
u-set 5	$11.3\ ^{+2.7}_{-1.9} \pm 2.0$	13
a-set 1	$8.8\ ^{+2.4}_{-1.0} \pm 2.0$	16
a-set 2	$1.67\ ^{+0.49}_{-0.23} \pm 0.38$	3
a-set 3	$1.97\ ^{+0.47}_{-0.22} \pm 0.37$	2
a-set 4	$2.30\ ^{+0.81}_{-0.30} \pm 0.39$	3
a-set 5	$10.2\ ^{+2.3}_{-1.1} \pm 3.4$	16
uGNN set 1	$15.6\ ^{+5.4}_{-1.9} \pm 3.8$	18
uGNN set 2	$0.73\ ^{+0.44}_{-0.16} \pm 0.27$	0
uGNN set 3	$7.6\ ^{+3.5}_{-1.3} \pm 2.3$	9
aGNN set 1	$45\ ^{+18}_{-8} \pm 16$	59
aGNN set 2	$0.30\ ^{+0.23}_{-0.07} \pm 0.18$	1
aGNN set 3	$3.8\ ^{+2.2}_{-0.7} \pm 2.0$	5

Emerging jets in CMS

Cut-based vs GNN tagger performance

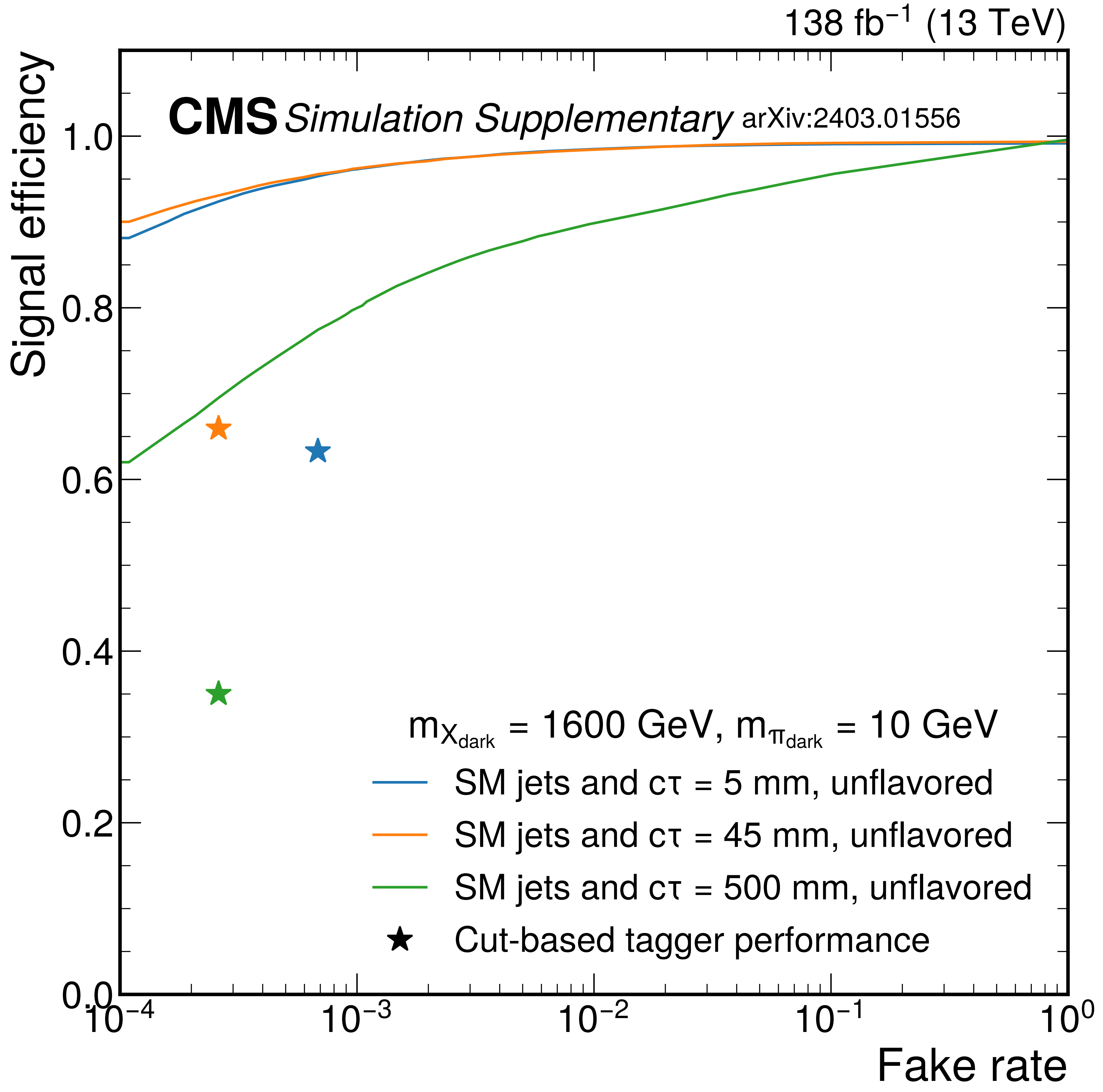

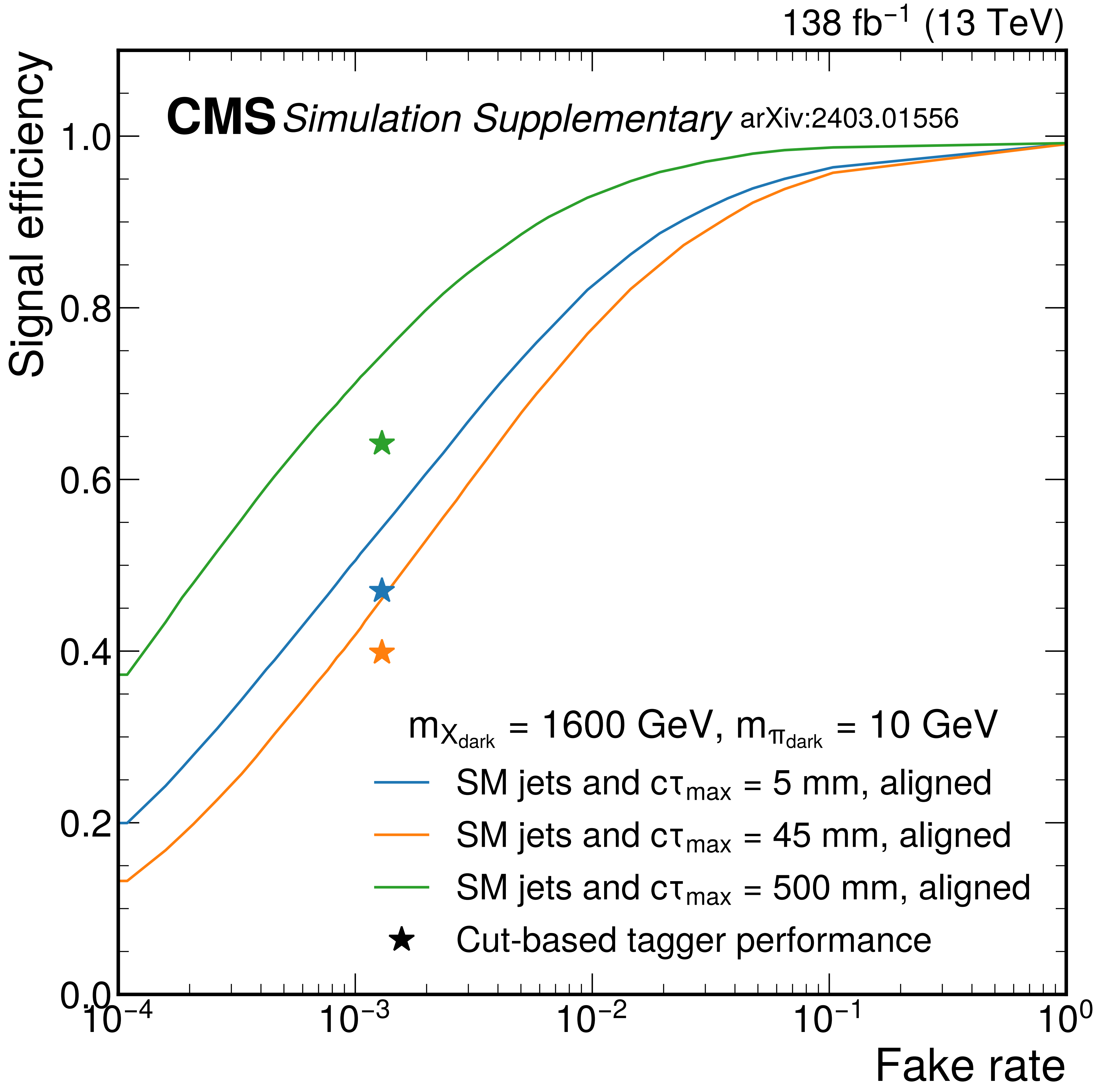

Semi-leptonic HNL decays

ABCD background estimate using displaced jet tagger score and m_{llj}

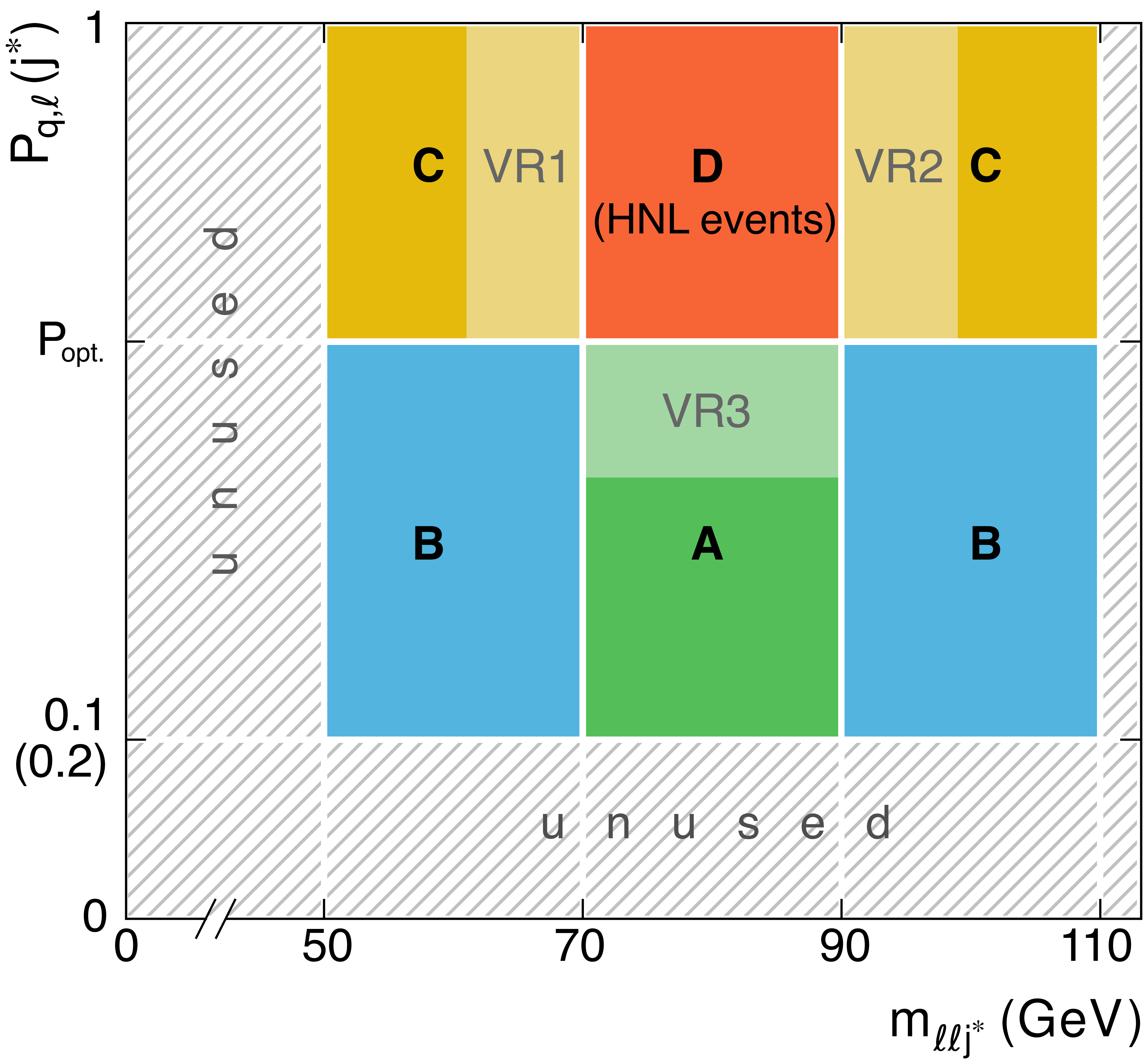

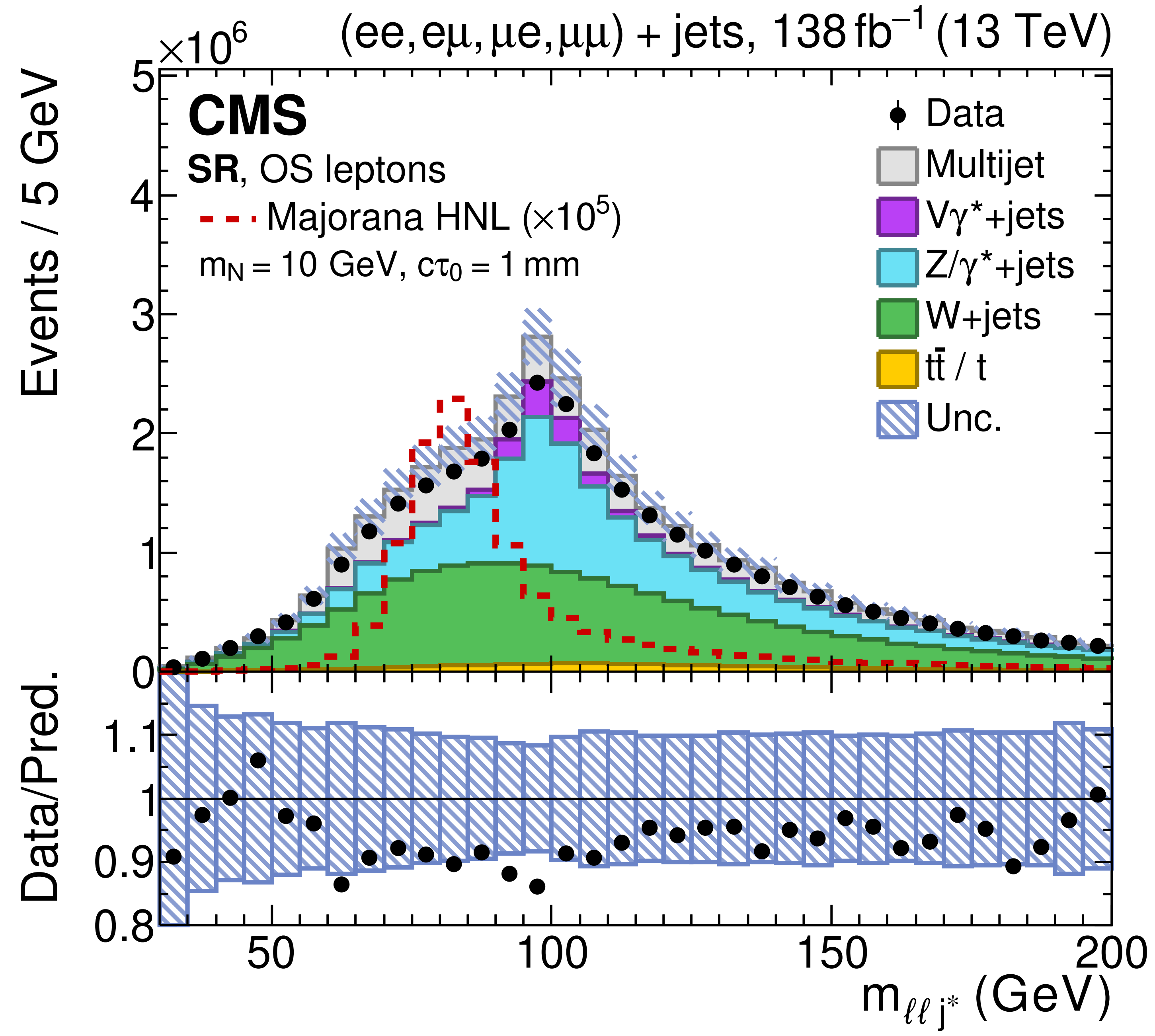

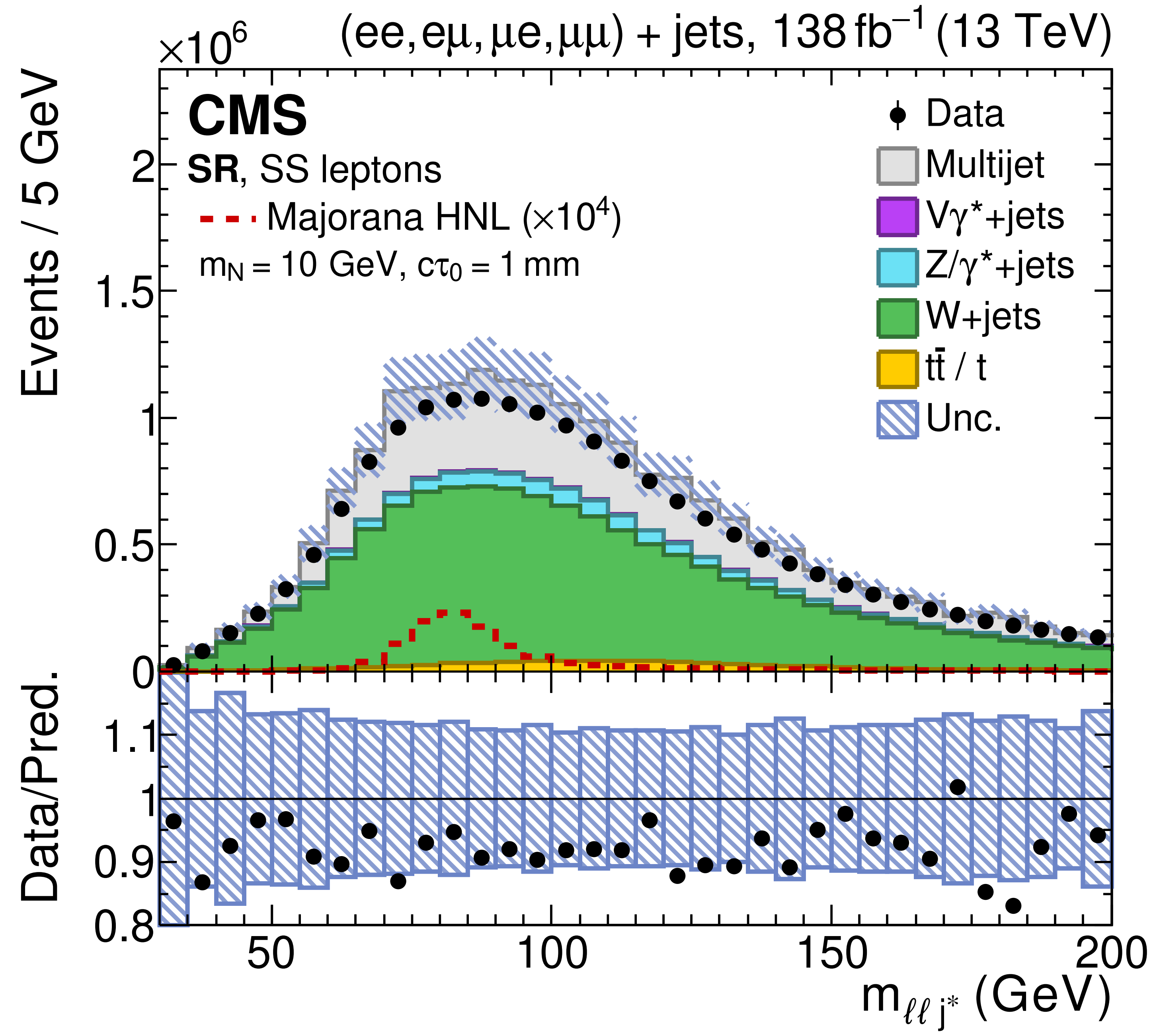

Semi-leptonic HNL decays

Observed yields are consistent with ABCD background estimate

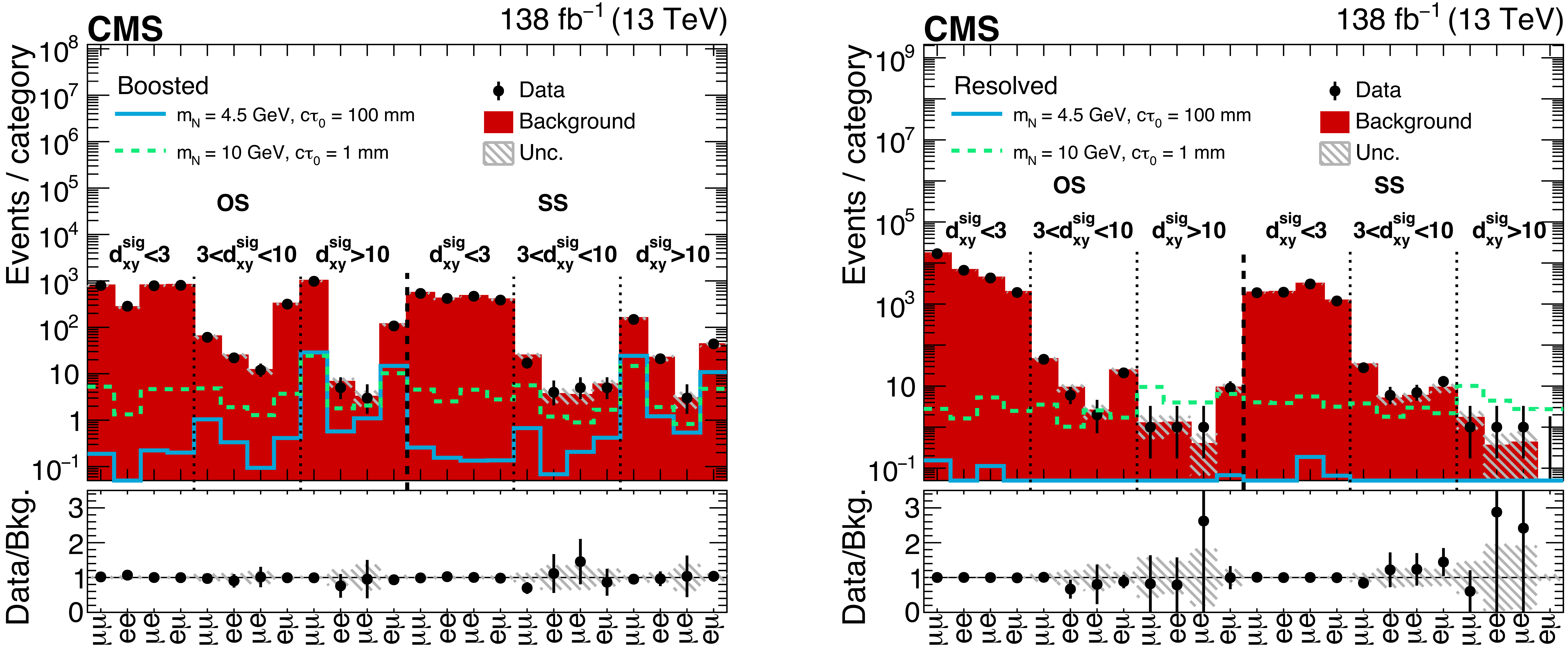

Low-mass HNLs in MS

ABCD background estimate using N_{hits} and the angle between the prompt lepton and the cluster centroid ($\Delta\phi_{\text{lep}}$)

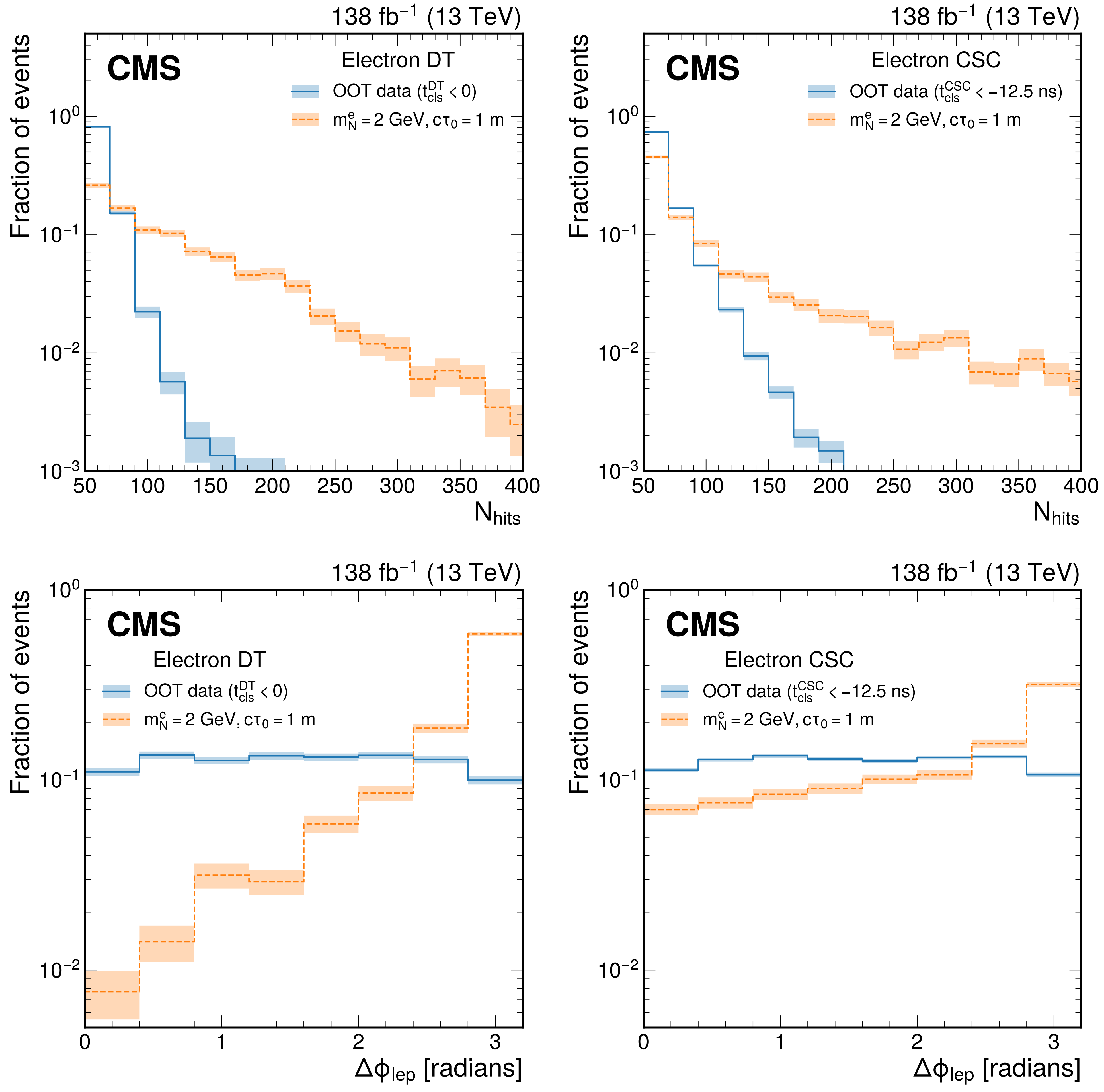

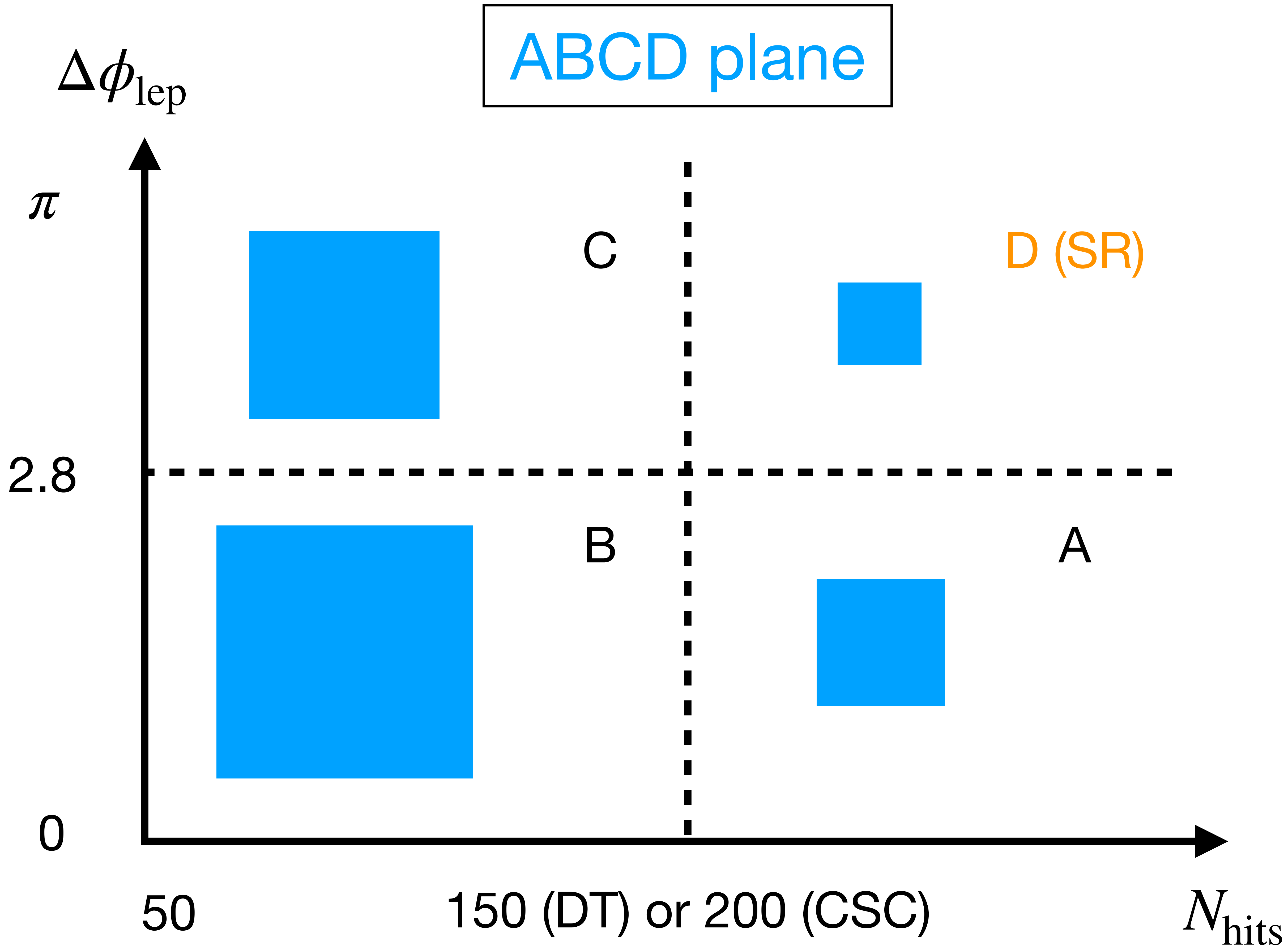

Low-mass HNLs in B-parking

Fully reconstructable final state allows for precise m_{HNL} identification

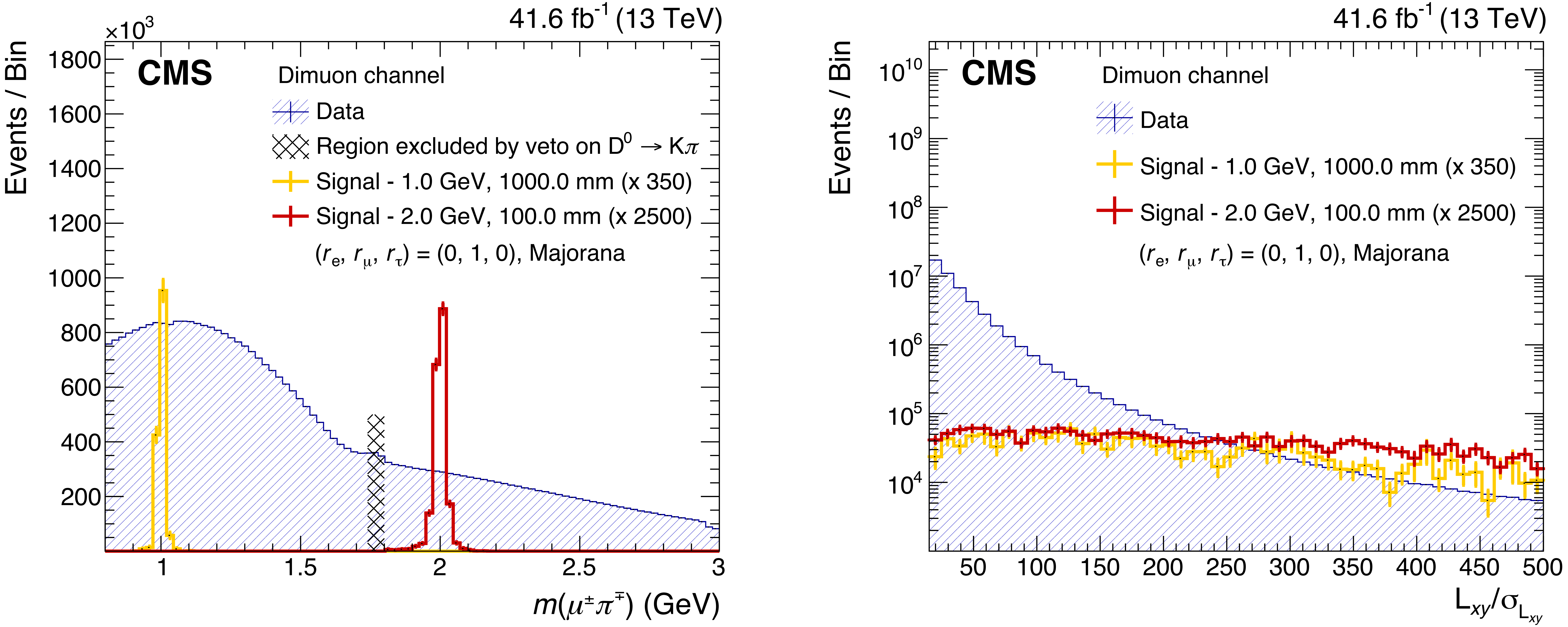

Low-mass HNLs in B-parking

Parameterized NN (pNN) used to separate signal and background

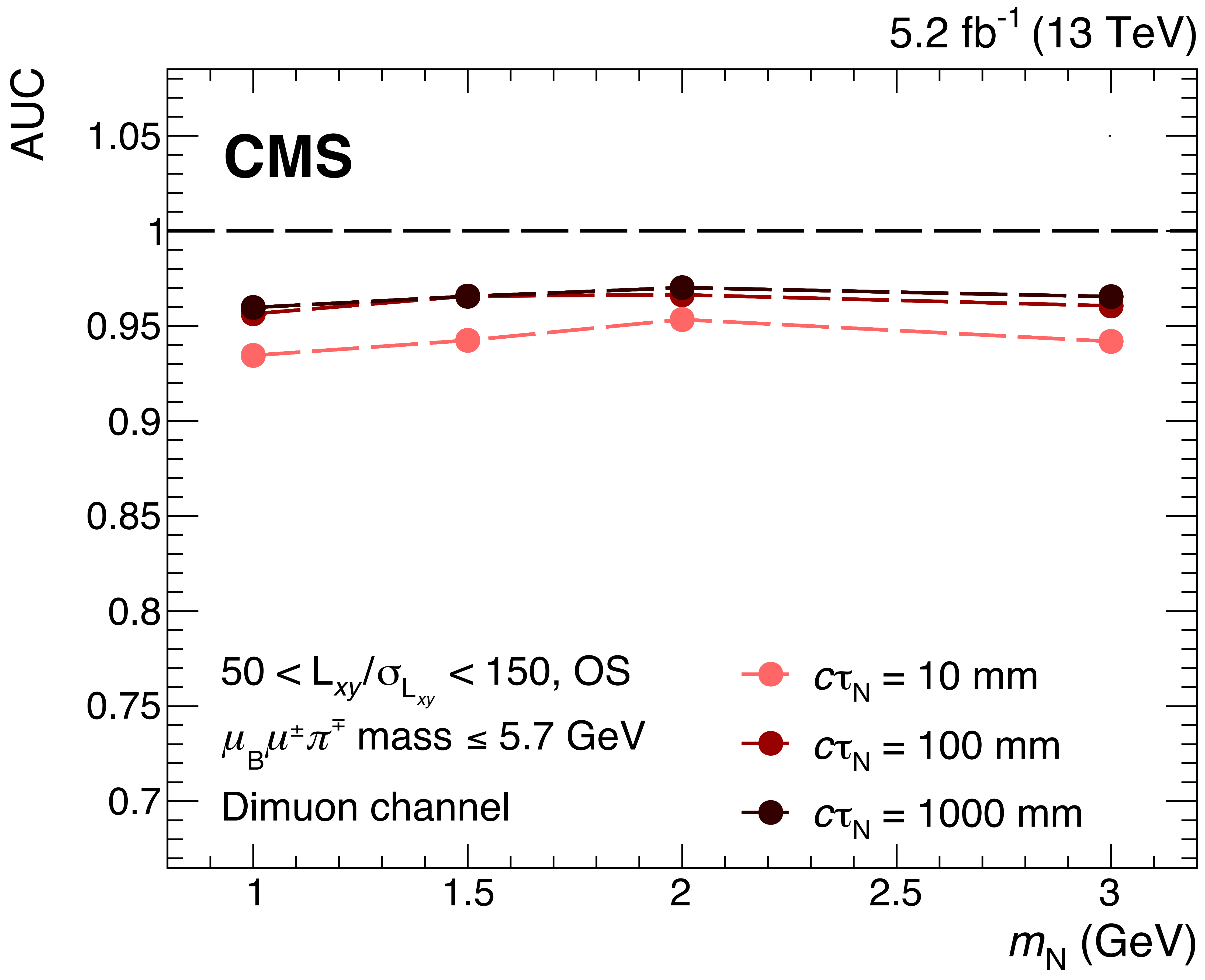

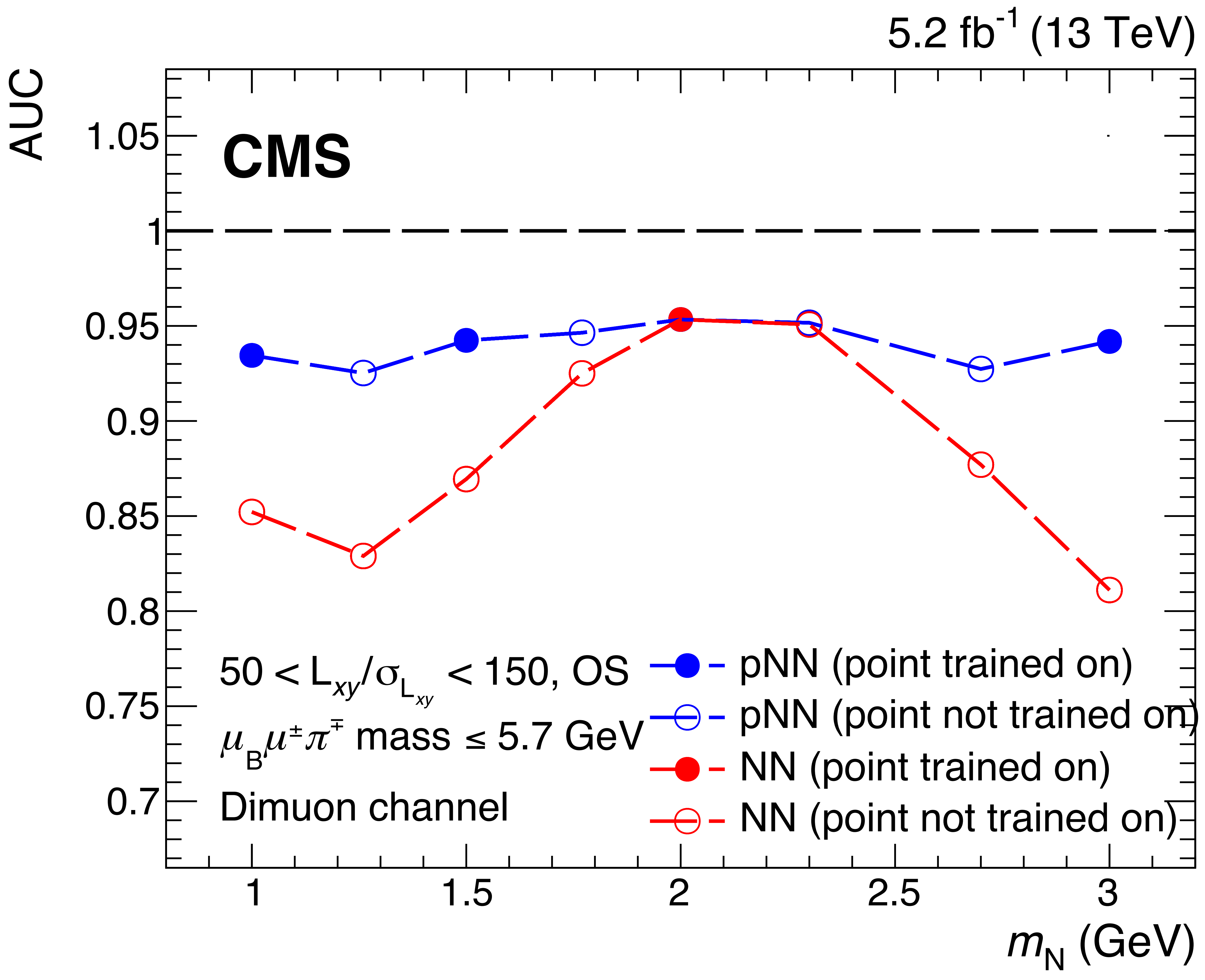

Scotogenic model

Literature review:

- Verifiable Radiative Seesaw Mechanism of Neutrino Mass and Dark Matter
- Phenomenology of the Generalised Scotogenic Model with Fermionic Dark Matter
- Generalizing the Scotogenic model
- Probing the scotogenic FIMP at the LHC
- A Scotogenic explanation for the 95 GeV excesses
- Revisiting the scotogenic model with scalar dark matter
- Shining Light on the Scotogenic Model: Interplay of Colliders and Cosmology
- Right-handed Neutrino Dark Matter with Radiative Neutrino Mass in Gauged B−L Model

Generalized Scotogenic model

Field	Generations	$SU(3)_c$	$SU(2)_L$	$U(1)_Y$	$\mathbb{Z}_2$
ℓ_L	3	$\mathbf{1}$	$\mathbf{2}$	$-1/2$	$+$
e_R	3	$\mathbf{1}$	$\mathbf{1}$	-1	$+$
H	1	$\mathbf{1}$	$\mathbf{2}$	$1/2$	$+$
η	n_η	$\mathbf{1}$	$\mathbf{2}$	$1/2$	$-$
N	n_N	$\mathbf{1}$	$\mathbf{1}$	0	$-$

Table 1: Scalar and fermion particle content of the model and representations under the gauge and global symmetries. ℓ_L and e_R are the SM left- and right-handed leptons, respectively, and H is the SM Higgs doublet.

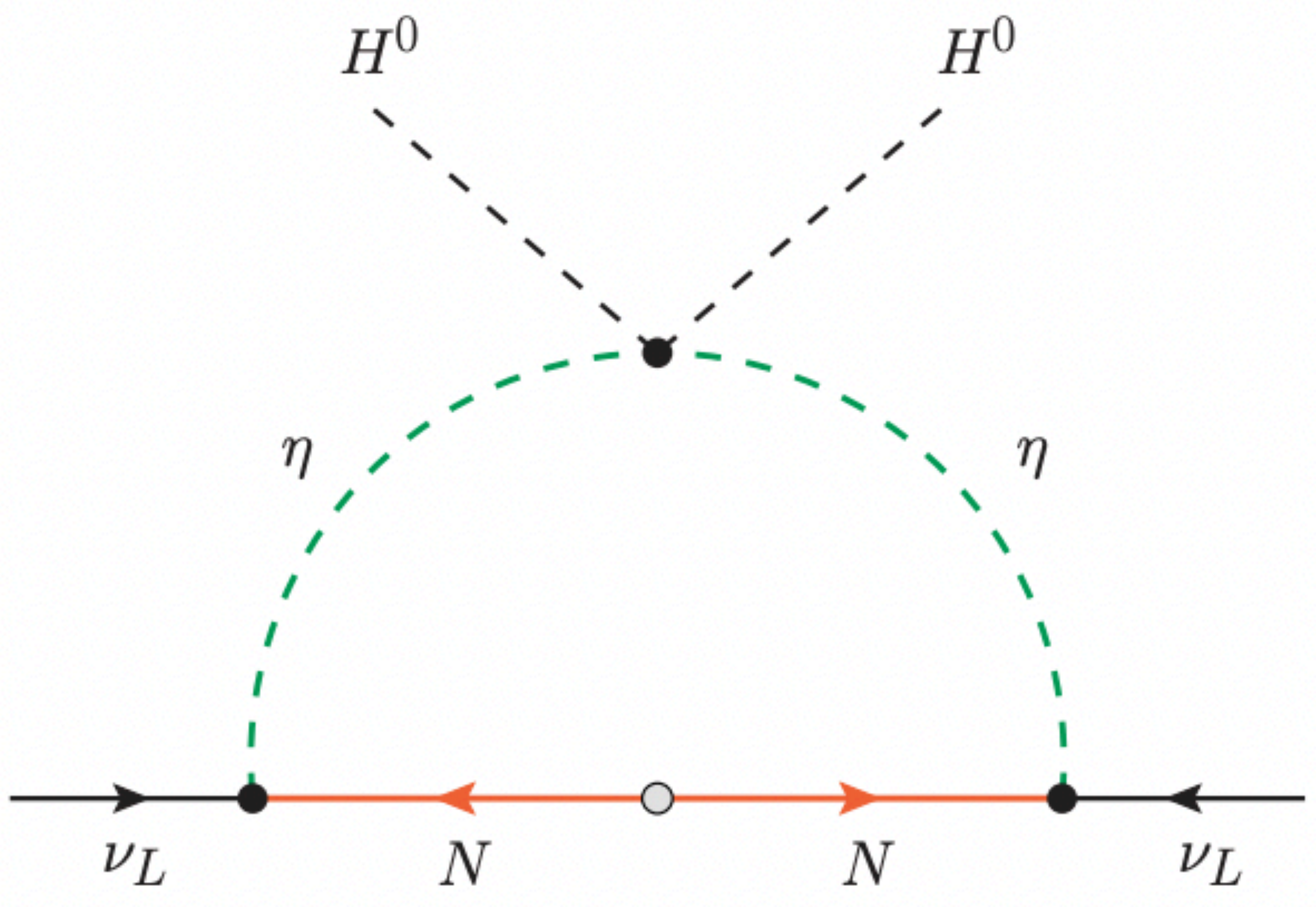

Generalized Scotogenic model

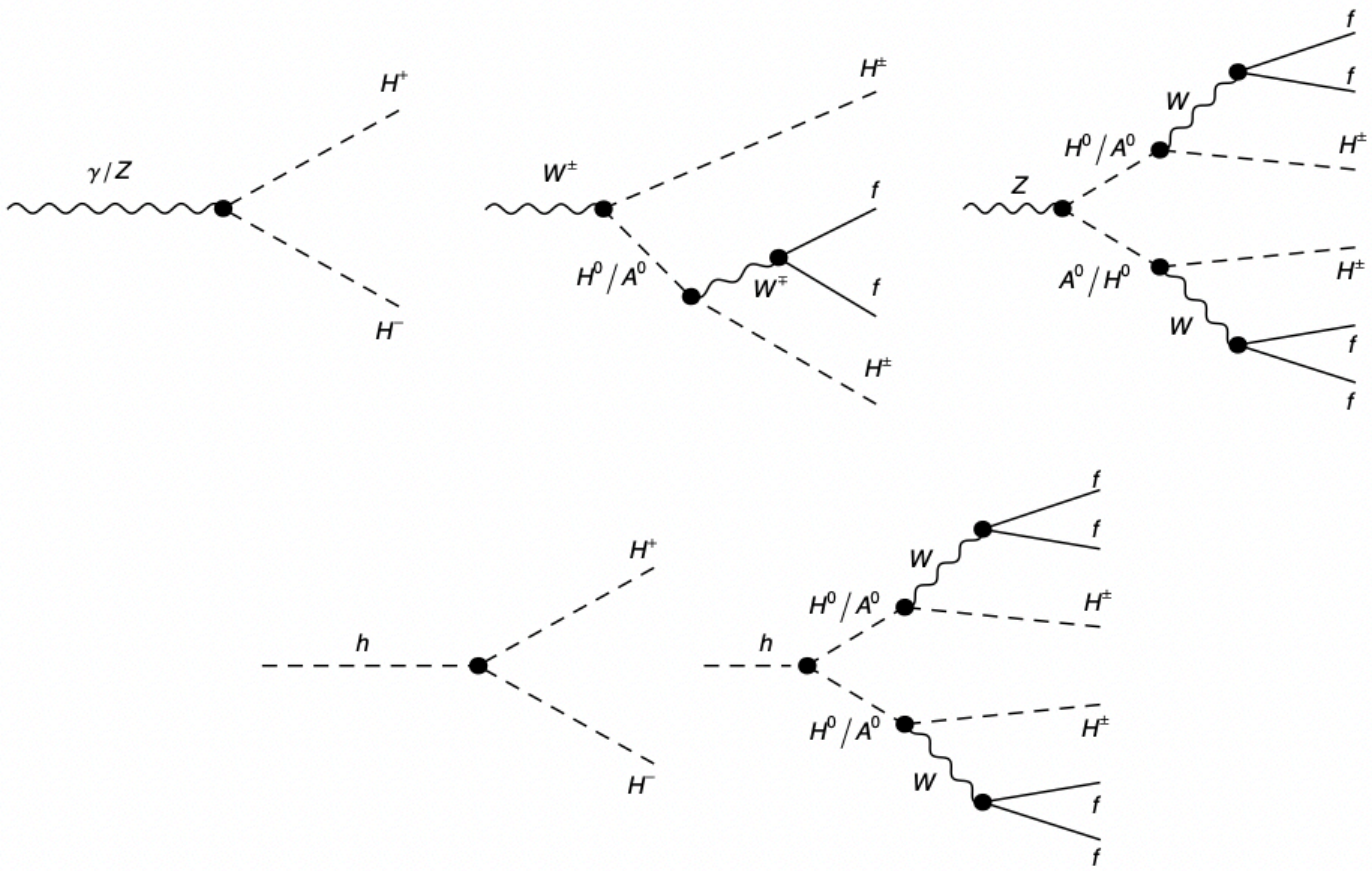

Figure 1: Drell-Yan (upper row) and gluon-gluon fusion (lower row) production channels of the Z_2-odd charged scalar.